UNIVERSITAT POLITÈCNICA DE VALÈNCIA

INSTITUTO INTERUNIVERSITARIO DE INVESTIGACIÓN DE RECONOCIMIENTO MOLECULAR Y DESARROLLO TECNOLÓGICO

UNIVERSITAT
POLITÈCNICA
DE VALÈNCIA

Novel approaches for the development of chromo fluorogenic chemosensors for detection of Cu(II) and biothiols

PhD. THESIS

Submitted by

Hazem Essam Okda

PhD. Supervisors:

Dr. Sameh El Sayed
Dr. Félix Sancenón Galarza
Prof. Ramón Martínez Máñez

Valencia, January 2020

RAMÓN MARTÍNEZ MÁÑEZ, PhD in Chemistry and Professor at the *Universitat Politècnica de València*, FÉLIX SANCENÓN GALARZA, PhD in Chemistry and Lecturer at the *Universitat Politècnica de València* and SAMEH EL SAYED, PhD in Chemistry and Postdoctoral researcher at the *University of Birmingham*.

CERTIFY:

That the work "***Novel approaches for the development of chromo fluorogenic chemosensors for detection of Cu(II) and biothiols***" has been developed by Hazem Essam Elsayed Okda under their supervision in the Instituto Interuniversitario de Investigación de Reconocimiento Molecular y Desarrollo Tecnológico (IDM) of the *Universitat Politècnica de València*, as a Thesis Project in order to obtain the international degree of PhD in Experimental and Industrial Organic Chemistry at the *Universitat Politècnica de València*.

Valencia, XXth January 2020.

Dr. Sameh El Sayed

Dr. Félix Sancenón Galarza

Prof. Ramón Martínez Máñez

بِسْمِ اللَّهِ الرَّحْمَٰنِ الرَّحِيمِ

ALMIGHT GOD SAYS:

وَمَا أُوتِيتُم مِّنَ الْعِلْمِ إِلَّا قَلِيلًا

‘‘*AND MANKIND HAVE NOT BEEN GIVEN OF KNOWLEDGE EXCEPT A LITTLE.*’’

SURAT AL-ISRA', AYAT NUMBER (85)

THE HOLY QURAN.

يَرْفَعِ اللَّهُ الَّذِينَ آمَنُوا مِنكُمْ وَالَّذِينَ أُوتُوا الْعِلْمَ دَرَجَاتٍ

‘‘*GOD ELEVATES THOSE AMONG YOU WHO BELIEVE, AND THOSE GIVEN KNOWLEDGE, MANY STEPS.*’’

SURAT Al-MUJADILAH AYAT NUMBER (11)

THE HOLY QURAN.

WHOEVER FOLLOWS A PATH TO SEEK KNOWLEDGE THEREIN, ALLAH WILL MAKE EASY FOR HIM A PATH TO PARADISE.

PROPHET MOHAMED ﷺ.

Dedication

I dedicate this work to:

My wonderful parents my father: Essam Okda and my Mother: Amal Rakha who have raised me to be the person I am today. My father, words cannot describe how much I appreciate all the hard work to make a better man of me. My mother, I am taking every step on my life due to your "Du'a" for me.

My brother and twin Mohamed, You are my backbone on my whole life. Without you, I could not continue this work.

My sister Noha, I am very grateful for your permanent encouragement and I hope you to be the next doctor.

My wife Shaimaa, You are always believe on me, you are my inspiration and soulmate. God bless you!!

My daughter Lana, "When you will get older, i hope you to be proud of your father".

My second family, uncle Mohamed Mosaad, aunt Omaima, Mostafa and Sawsan for your incredible support.

Words fail to comprehend how much i am grateful for everything thing you did for me. My extended family …. You are the whole life for me, literally.

I also dedicate this work to the soul of Prof. Dr. Ahmed H. Zewail ***"Nobel Prize Laureate in Chemistry 1999"*** *– Caltech – USA. The Egyptian-American scientist who inspired our generation to love chemistry.*

May God be with us for walking on the same path

February 26th, 1946 – August 2nd, 2016

Acknowledgements
Agradecimientos

Me tomó un tiempo publicar esto. Con esto, concluyo un largo viaje en mi vida. Ha sido la experiencia más gratificante en mi carrera profesional.

En primer lugar, me gustaría dar las gracias a mis directores de tesis, Ramón y Félix. A Ramón, por confiar en mí y darme la oportunidad de unirme a la familia del IDM. Por haber creado un grupo, un Instituto y una infraestructura de investigación en el que se han podido formar tantas personas a lo largo de los años. Sin duda, tu esfuerzo y dedicación son dignos de admirar. Gracias por tus consejos, por animarme a pensar y darme la oportunidad de desarrollar mis propias ideas.

A Félix, por estar siempre ahí, por tu ayuda y amabilidad, por tus consejos, por tus correcciones en tiempos record, y por tu buena disponibilidad para cualquier trámite o papeleo. Gracias también en lo personal, tus visitas diarias al laboratorio, por los buenos momentos fuera del laboratorio, y por la comida marroquí. ¡¡ Muchísimas gracias por todo!!

Quiero agradecer a Loles y Elena por el apoyo y hablar amablemente conmigo sobre mi familia y mi tierra. Andrea Bernardos (funny face), de verdad me siento muy agradecido por su ayuda y su encantadora sonrisa. ¡GRACIAS A TODOS!

Gracias a mis hermanos, Sameh Elsayed y Ismail Otri por vuestro gran empuje y apoyo en estos años. También a mis amigos Toni y Tania por todas ayudas, viajes y todo el tiempo que hemos pasado juntos. Aprecio vuestra amistad mucho. También mis compañeros del Máster de sensores Macarena Fabregat y Alejandro Cuenca.

Muchísimas gracias a todos mis compañeros y compañeras del laboratorio 2.6 y del IDM con los que he tenido la oportunidad de compartir estos años. Para los que ya estaban al inicio cuando entré, para los que entraron al principio, para los que fueron llegando, para

todos los que vinieron de estancia, y para los más nuevos……muchas gracias!! Para Borja, Cris M., M. Carmen, Lluís, Irene, Mar, Àngela, Edgar, Alba, Carol, Amelia, Santi, Lorena, Mónica, Luis Pla, Maria Elena, Iris, Luis Villaescusa, Gema, Bea Lozano, Adrián, Mónica, Elisa, Arianna, Cris T., Andy, Bea de Luis, Xente, Eva G., Àngels, Marta, María A., Andrea, Juanfran, Pablo, Eva B., Paula, Serena, Delphine, Alejandra, las principesas …me siento afortunado por haberos conocido y creo que es una de las mejores cosas de nuestro trabajo. Gracias por vuestra ayuda, y por los buenos momentos dentro y (mejores aún) fuera del lab. Al final, cada persona somos el resultado de las experiencias y las personas que nos encontramos en el camino, y vosotros habéis dejado huella en mí.

Took me a while to post this. With this, I conclude a long journey in my life. It has been the most gratifying experience in my professional career.

I would to thank my entire friends for their support on this work. First of all, the man who i cherish his friendship, Dr. Gerhard Mohr for his great support and our discussions in usual lunch during his frequent visits in Valencia. I owe a lot to Prof. Maria Manuela M. Raposo for her great collaboration and help to my work. How could I express my gratitude to you?

Great gratitude to my dear friend Ahmed Mehrem, Ahmed Badran's family Rahma and Sandy for their great support since my first steps in Spain. My friends in Valencia, Ahmed Fawzy, Ahmed Sherif, Ahmed Wefky, Ayman Abbas, Eslam Montaser's family Esraa and littile montaser.

Tremendous thanks to all my dears in Egypt, My Family in Egypt, my uncles, aunts, and cousins. My aunt Fatma, Dr. Samir Elshimi, My dear sisters Dr. Ola and Dr. Mona. My dear brothers Eng. Mohamed H. Rakha and Dr. Wael Osman for their push and encourgment ever. My classmates in Toukh Private Schools (TPS) Ahmed Abbas, Anas El Hadary, Adham Osama, Bahaa Osama, Ahmed Negm, Mohamed Goda, Mohamed Elmehy and Hazem Esmail. My dear friends Mohamed Yahia, Amr Kamel, Ahmed Salem Mohamed Elfaran, Mohamed Abdo, Amr Bakry and Taha Ashour. My dear brother Mohamed Abdel Monem for permeant believe on me, and great support since our first meeting.

I am in great in debt to everyone who supported me and believed me in throughout my life.

Resumen

Esta tesis doctoral, que lleva por título "*Nuevas aproximaciones para el desarrollo de sensores cromo-fluorogénicos para la detección de Cu(II) y biotioles*" aborda la síntesis, caracterización y estudio de la capacidad coordinante de nuevos sensores cromo-fluorogénicos para el reconocimiento y la detección del catión Cu(II) y de biotioles (glutatión, cisteína y homocisteína). Estos nuevos sensores, que son capaces de detectar de forma selectiva Cu(II) mediante cambios de color y/o de fluorescencia, están construidos mediante un paradigma que consiste en integrar los grupos coordinantes dentro de la estructura de la unidad indicadora. Además, los complejos de Cu(II) de los nuevos sensores se han empleado para la detección cromo-fluorogénica de biotioles mediante reacciones de desplazamiento.

El primer capítulo de esta tesis doctoral está dedicado a la introducción de los conceptos básicos de la química supramolecular, los sensores ópticos y las sondas moleculares, necesarios para entender el marco en el que se encuadran los resultados obtenidos. Por otra parte, en el segundo capítulo, se presentan los objetivos generales de esta tesis doctoral.

En el tercer capítulo se describe la síntesis y caracterización de compuesto 4-(4,5-difenil-1H-imidazol-2-il)-*N*,*N*-dimetilanilina, un sensor cromo-fluorogénico que es capaz de detectar de forma selectiva el catión Cu(II) en medios acuosos. Así, disoluciones del sensor en agua-acetonitrilo 1:1 (v/v) muestran una banda de absorción intensa centrada en 320 nm que es desplazada hacia el rojo (hasta 490 nm) desplazamiento que se ve reflejado en un cambio de color de incoloro a marón-rojizo de forma selectiva al adicionar el catión Cu(II). Este desplazamiento es debido a la formación de un complejo no fluorescente con estequiometría 1:1 donde el Cu(II) coordina con los átomos de nitrógeno del imidazol. Además, este complejo de Cu(II) se ha empleado para la detección selectiva de glutatión ya que este biotiol es capaz de inducir la desaparición de la banda de absorción a 490 nm (asociada a un cambio de color de marrón-rojizo a incoloro). En presencia de

glutatión también se produce un aumento de fluorescencia a 455 nm. Estos cambios ópticos son adscritos a un proceso de demetalación del complejo inducido de forma selectiva por el glutatión (la cisteína y la homocisteína son incapaces de producir esta respuesta). Finalmente, el complejo es capaz de detectar glutatión con una alta sensibilidad con un límite de detección de 2,0 μM.

En el capítulo cuarto de esta tesis se describe otro sensor óptico basado en el imidazol, en este caso funcionalizado con dos tiofenos, que es capaz de detectar de forma selectiva al catión Cu(II) y biotioles. En este caso disoluciones del sensor en agua-acetonitrilo 9:1 v/v están caracterizadas por la presencia de una banda de absorción a 320 nm y por una fluorescencia intensa a 475 nm. De nuevo, de todos los cationes ensayados, sílo el Cu(II) es capaz de inducir una desactivación completa de la emisión y un cambio de color en la disolución de incoloro a azul asociado con la aparición de una banda desplazada hacia el rojo a 555 nm. Estos cambios de color y de fluorescencia son debidos a la formación de complejos de estequiometría 1:1 en los que el Cu(II) coordina con los átomos de nitrógeno de imidazol. Además, también se estudió la respuesta óptica del complejo de Cu(II) en presencia de aminoácidos. En este caso, solo el glutatión, la cisteína y la homocisteína produjeron una decoloración intensa juntamente con la aparición de una banda de emisión a 475 nm. Estos cambios son debidos a un proceso de demetalación del complejo debido a la coordinación de los biotioles con el catión Cu(II). Teniendo en cuenta una posible aplicación de este sensor para detectar Cu(II) en medios biológicos se comprobó, mediante ensayos de viabilidad, que no presenta toxicidad aparente en células HeLa. Además, mediciones de microscopia confocal demuestran que el sensor puede ser empleado con éxito para detectar Cu(II) en células HeLa.

En el quinto capítulo esta tesis doctoral se abordó la síntesis y caracterización de tres sensores conteniendo grupos *N*,*N*-difenilanilino (dador de electrones) y diferentes espaciadores π (benceno y tiofeno) conectados con grupos aldehído (aceptor de electrones). Los espectros UV-visible de estos tres receptores en

acetonitrilo presentan bandas de absorción (de transferencia de carga debido a la presencia de la agrupación dadora de electrones *N*,*N*-difenilanilino conectada con puentes heteroaromáticos conteniendo grupos aldehído electrón aceptores) intensas en el intervalo que va de los 360 a los 420 nm. Se estudió el comportamiento de estos sensores en presencia de cationes y sólo el Cu(II) fue capaz de inducir la aparición de bandas en la zona infrarroja cercana en el intervalo entre 750 y 1075 nm. Además, los tres sensores son poco fluorescentes (con bandas localizadas en el intervalo entre 540 y 580 nm) y sólo el catión Cu(II) es capaz de desactivar la emisión. De nuevo, los cambios ópticos observados son debidos a la formación de complejos de estequiometría 1:1 en los que el catión Cu(II) interacciona con el átomo de oxígeno de los grupos aldehído. Estos sensores se pueden solubilizar en medios acuosos empleando dodecil sulfato. De esta forma, son capaces de detectar Cu(II) en mezclas docedil sulfato (20 mM)-acetonitrilo 9:1 v/v.

Dos sensores basados en 2,4,5-triaril imidazol (conteniendo furanos y 1,10-fenantrolina), capaces de detectar Cu(II) y biotioles, se describen en el capítulo sexto. Disoluciones de los dos sensores en acetonitrilo muestran bandas de absorción en el intervalo que va de los 320 a los 350 nm siendo además ligeramente fluorescentes. De todos los cationes empleados en el estudio, sólo el Cu(II) es capaz de inducir la aparición de nuevas bandas de absorción desplazadas hacia el rojo junto con la desactivación de la emisión de los sensores. Estos cambios son asignados a la formación de complejos de estequiometría 1:1 en los que el Cu(II) interacciona con los átomos de nitrógeno del imidazol. El sensor conteniendo furanos es capaz de detectar Cu(II) en agua-acetonitrilo 1:1 v/v y el complejo formado se ha empleado con éxito para detectar biotioles (glutatión, cisteína y homocisteína) mediante cambios de color y aparición de fluorescencia. De nuevo, la respuesta óptica obtenida en presencia de biotioles se debe a un proceso de demetalación del complejo de Cu(II).

Finalmente, el capítulo séptimo de esta tesis doctoral está dedicado a las conclusiones finales y a las perspectivas futuras que el trabajo que aquí se expone puede abrir en el campo de los sensores ópticos para la detección de cationes metálicos y biomoléculas en agua o en medios acuosos.

Resum

Aquesta tesi doctoral, que porta per títol "*Noves aproximacions per al desenvolupament de sensors cromo-fluorogènics per a la detecció de Cu(II) i biotiols*" aborda la síntesi, caracterització i estudi de la capacitat coordinant de nous sensors cromo-fluorogènics per al reconeixement i la detecció del catió Cu(II) i de biotiols (glutatió, cisteïna i homocisteïna). Aquests nous sensors, que són capaços de detectar de forma selectiva Cu(II) mitjançant canvis de color i/o de fluorescència, estan construïts mitjançant un nou paradigma que consisteix a integrar els grups coordinants dins de l'estructura de la unitat indicadora. A més, els complexos de Cu(II) dels nous sensors s'han emprat per a la detecció cromo-fluorogènica de biotiols mitjançant reaccions de desplaçament.

El primer capítol d'aquesta tesi doctoral està dedicat a la introducció dels conceptes bàsics de la química supramolecular, els sensors òptics i les sondes moleculars, necessaris per a entendre el marc en el qual s'enquadren els resultats obtinguts. D'altra banda, en el segon capítol, es presenten els objectius generals d'aquesta tesi doctoral.

En el tercer capítol es descriu la síntesi i caracterització de compost 4-(4,5-difenil-1H-imidazol-2-il)-*N,N*-dimetilanilina, un sensor cromo-fluorogènic que és capaç de detectar de forma selectiva el catió Cu(II) en medis aquosos. Així, dissolucions del sensor en aigua-acetonitril 1:1 (v/v) mostren una banda d'absorció intensa centrada en 320 nm que és desplaçada cap al roig (fins a 490 nm, desplaçament que es veu reflectit en un canvi de color d'incolor a marró-rojenc) de forma selectiva en addicionar el catió Cu(II). Aquest desplaçament és degut a la formació d'un complex no fluorescent amb estequiometria 1:1 (en aquest complex el Cu(II) coordina amb els àtoms de nitrogen del imidazol). A més, aquest complex de Cu(II) s'ha emprat per a la detecció selectiva de glutatió ja que aquest biotiol és capaç d'induir la desaparició de la banda d'absorció a 490 nm (associada a un canvi de color de marró-rojenc a incolor). En presència de glutatió també es produeix un augment de fluorescència a 455 nm. Aquests canvis òptics

són adscrits a un procés de demetal·lació del complex induït de forma selectiva pel glutatió (la cisteïna i la homocisteïna són incapaces de produir aquesta resposta). Finalment, el complex és capaç de detectar glutatió amb una alta sensibilitat ja que el límit de detecció és 2.0 μM.

En el capítol quart d'aquesta tesi es descriu un altre sensor òptic basat en el imidazol, en aquest cas funcionalitzat amb dos tiofens, que és capaç de detectar de forma selectiva al catió Cu(II) i als tres biotiols. En aquest cas dissolucions del sensor en aigua-acetonitril 9:1 v/v estan caracteritzades per la presència d'una banda d'absorció a 320 nm i per una fluorescència intensa a 475 nm. De nou, de tots els cations assajats, només el Cu(II) és capaç d'induir una desactivació completa de l'emissió i un canvi de color en la dissolució d'incolor a blau (associat amb l'aparició d'una banda desplaçada cap al roig a 555 nm). Aquests canvis de color i de fluorescència són deguts a la formació de complexos d'estequiometria 1:1 en els quals el Cu(II) coordina amb els àtoms de nitrogen d'imidazol. A més, també es va estudiar la resposta òptica del complex de Cu(II) en presència d'aminoàcids. En aquest cas, només el glutatió, la cisteïna i l'homocisteïna van produir una descoloració intensa juntament amb l'aparició d'una banda d'emissió a 475 nm. Aquests canvis són deguts a un procés de demetal·lació del complex degut a la coordinació dels biotiols amb el catió Cu(II). Tenint en compte una possible aplicació d'aquest sensor per a detectar Cu(II) en mitjans biològics es va comprovar, mitjançant assajos de viabilitat, que no presenta toxicitat aparent en cèl·lules HeLa. A més, mesures de microscòpia confocal demostren que el sensor pot ser emprat amb èxit per a detectar Cu(II) en cèl·lules HeLa.

En el cinquè capítol d'aquesta tesi doctoral, es va abordar la síntesi i caracterització de tres sensors contenint grups *N,N*-difenilanilino (donador d'electrons) i diferents espaiadors π (benzè i tiofè) connectats amb grups aldehid (acceptor d'electrons). Els espectres UV-visible d'aquests tres receptors en acetonitril presenten bandes d'absorció (de transferència de càrrega a causa de la presència de l'agrupació donadora d'electrons *N,N*-difenilanilino connectada amb

ponts heteroaromàtics contenint grups aldehid electró acceptors) intenses en l'interval que va dels 360 als 420 nm. Es va estudiar el comportament d'aquests sensors en presència de cations i sols el Cu(II) va ser capaç d'induir l'aparició de bandes en la zona infraroja pròxima en l'interval entre 750 i 1075 nm. A més, els tres sensors són poc fluorescents (amb bandes localitzades en l'interval entre 540 i 580 nm) i només el catió Cu(II) és capaç de desactivar l'emissió. De nou, els canvis òptics observats són deguts a la formació de complexos d'estequiometria 1:1 en els quals el catió Cu(II) interacciona amb l'àtom d'oxigen dels grups aldehid. Aquests sensors es poden solubilitzar en medis aquosos emprant dodecil sulfat. D'aquesta forma, són capaços de detectar Cu(II) en mescles docedil sulfat (20 mM)-acetonitril 9:1 v/v.

Dos sensors basats en 2,4,5-triaril imidazol (contenint furans i 1,10-fenantrolina), capaços de detectar Cu(II) i biotiols, es descriuen en el capítol sisè. Dissolucions dels dos sensors en acetonitril mostren bandes d'absorció en l'interval que va dels 320 als 350 nm sent a més lleugerament fluorescents. De tots els cations emprats en l'estudi, només el Cu(II) és capaç d'induir l'aparició de noves bandes d'absorció desplaçades cap al roig juntament amb la desactivació de l'emissió dels sensors. Aquests canvis són assignats a la formació de complexos d'estequiometria 1:1 en els quals el Cu(II) interacciona amb els àtoms de nitrogen de l'imidazol. El sensor contenint furans és capaç de detectar Cu(II) en aigua-acetonitril 1:1 v/v i el complex format s'ha emprat amb èxit per a detectar biotiols (glutatió, cisteïna i homocisteïna) mitjançant canvis de color i aparició de fluorescència. De nou, la resposta òptica obtinguda en presència de biotiols es deu a un procés de demetal·lació del complex de Cu(II).

Finalment, el capítol setè d'aquesta tesi doctoral està dedicat a les conclusions finals i a les perspectives futures que el treball que ací s'exposa pot obrir en el camp dels sensors òptics per a la detecció de cations metàl·lics i biomolècules en aigua o en medis aquosos.

Abstract

This PhD thesis entitled *"Novel approaches for the development of chromo-fluorogenic chemosensors for detection of Cu(II) and biothiols"* is devoted to the synthesis, characterization and coordination behaviour of new chromo-fluorogenic probes for the recognition and detection of Cu(II) cations and biothiols (glutathione, cysteine and homocysteine). These new probes, which selectively detect Cu(II) cation through colour and/or emission changes, are constructed using a paradigm in which the binding units are included into the signalling unit structure. Besides, some of the Cu(II) complexes of these new probes are used for the chromo-fluorogenic detection of biothiols using displacement reactions.

The first chapter of this PhD thesis gives an overview about the conceptual framework in which are located the studies presented in this thesis, which combine concepts related with supramolecular chemistry, optical sensors and molecular probes. In the second chapter, the general objectives of this PhD thesis are presented.

The third chapter is devoted to the synthesis and characterization of 4-(4,5-diphenyl-1H-imidazole-2-yl)-*N*,*N*-dimethylaniline, a chromo-fluorogenic probe for selective Cu(II) detection in aqueous environment. Water-acetonitrile 1:1 (v/v) solutions of this probe presented a marked absorption band at ca. 320 nm that is selectively red-shifted (to 490 nm reflected in a colour change from colourless to reddish-brown) upon addition of Cu(II) cation. This shift was ascribed to the formation of a non-emissive 1:1 stoichiometry complex in which Cu(II) coordinated with the nitrogen atoms of the imidazole ring. Besides, this Cu(II) complex was used for the selective and sensitive detection of glutathione, which induced the disappearance of the 490 nm absorption with a marked colour change from reddish-brown to colourless. Also a marked emission at 455 nm was observed after glutathione addition. These optical changes were ascribed to a glutathione-induced demetallation process which generated the free probe. In

addition, the Cu(II) complex detected glutathione with a remarkable limit of detection as low as 2.0 μM.

The fourth chapter presented an imidazole-based probe functionalized with two thiophene subunits for the selective detection of Cu(II) cation and biothiols. Water-acetonitrile 9:1 (v/v) solutions of the free probe showed an absorption band at 320 and a marked emission at 475 nm. Of all the cations tested, only Cu(II) induced an emission quenching with a significant colour change from colourless to deep blue (appearance of a new absorption band centred at 555 nm). These remarkable optical changes were ascribed to the formation of 1:1 stoichiometry complexes in which the metal cation coordinated with the nitrogen atoms of the imidazole heterocycle. Besides, the optical response of the Cu(II) complex was tested in the presence of selected amino acids. Of all the amino acids tested, only glutathione, cysteine and homocysteine induced a marked bleaching of the complex solution with a remarkable growing of an emission band centred at 475 nm. These optical changes were ascribed to a demetallation process induced by the coordination of biothiols with Cu(II). Furthermore, viability assays indicated the non-toxicity of the probe for HeLa cells. Also, the probe was successfully employed to detect Cu(II) in HeLa cells using confocal microscopy.

The fifth chapter presented the synthesis and characterization of three probes containing *N,N*-diphenylanilino (as a donor group) and different π-spacers (benzene and thiophene) connected with aldehyde moieties. Absorption spectra of the three probes in acetonitrile showed an intense absorption band in the UV-visible region (360-420 nm range) which can be attributed to an intramolecular charge-transfer transition as consequence of the presence of *N,N*-diphenylanilino electron donor moiety directly linked to (hetero)aromatic bridges functionalized with the aldehyde electron acceptor group. Of all the cations tested, only Cu(II) induced the appearance of marked near infrared absorption bands in the 750-1075 nm interval. Besides, the three probes are moderately emissive (with bands in the 540-580 nm interval) and only Cu(II) cation was able to induce a

fluorescence quenching. The optical changes were ascribed to the formation of 1:1 stoichiometry complexes in the which Cu(II) cation probably interacted with the oxygen atom of the aldehyde functional group. Finally, using sodium dodecyl sulfate (20 mM)-acetonitrile 9:1 v/v mixtures, these probes were solubilized and were successfully used for the detection of Cu(II) in aqueous environments.

Two 2,4,5-triaryl imidazole probes for the selective recognition of Cu(II) and biothiols were presented in the sixth chapter. Both probes presented marked absorption bands in the UV zone (320-350 nm range) and were moderately emissive in acetonitrile. Of all the cations tested, only Cu(II) induced the appearance of red shifted absorptions and the quenching of the emission bands. Job's plots indicated the formation of 1:1 stoichiometry complexes in which Cu(II) cation interacted with the nitrogen atoms of the imidazole heterocycle located in the core of both probes. The probe containing furan rings was able to detect Cu(II) in water-acetonitrile 1:1 v/v solutions and the complex formed was also used to detect biothiols in aqueous environment (by marked colour changes and the appearance of a moderate emission). Again, the optical response obtained in the presence of biothiols was ascribed to a demetallation process.

Finally, the seventh chapter of this PhD thesis is devoted to the final conclusions and future perspectives that the results presented in this work could open in the field of optical probes for the detection of metal cations and biomolecules in aqueous environments.

Publications

Results of this PhD Thesis and other contributions have resulted in the following scientific publications:

- **Hazem Essam Okda**, Sameh El Sayed, Rosa C.M. Ferreira, Susana P.G. Costa, M. Manuela M. Raposo, Ramón Martínez-Máñez, Félix Sancenón, *''4-(4,5-Diphenyl-1H-imidazole-2-yl)-N,N-dimethylaniline-Cu(II) complex, a highly selective probe for glutathione sensing in water-acetonitrile mixtures'' Dyes and Pigments,* **2018***, 159, 45–48.*

- **Hazem Essam Okda**, Sameh El Sayed, Ismael Otri, Rosa C.M. Ferreira, Susana P.G. Costa, M. Manuela M. Raposo, Ramón Martínez-Máñez, Félix Sancenón, *''A simple and easy-to-prepare imidazole-based probe for the selective chromo-fluorogenic recognition of biothiols and Cu(II) in aqueous environments'' Dyes and Pigments,* **2019***, 162, 303–308.*

- **Hazem Essam Okda**, Sameh El Sayed, Rosa C. M. Ferreira, Susana P. G. Costa, M. Manuela M. Raposo, Ramón Martínez-Máñez, Félix Sancenón, *''N,N-Diphenylanilino-heterocyclic aldehyde-based chemosensors for UV-vis/NIR and fluorescence Cu(II) detection'' New J. Chem.*, **2019**, *43, 7393-7402.*

- **Hazem Essam Okda**, Sameh El Sayed, Ismael Otri, R. Cristina M. Ferreira, Susana P. G. Costa, M. Manuela M. Raposo, Ramón Martínez-Máñez, Félix Sancenón, *''2,4,5-triaryl imidazole probes for the selective chromo-fluorogenic detection of Cu(II). Prospective use of the Cu(II) complexes for the optical recognition of biothiols'' Polyhedron,* ***2019****, 170, 388-394.*

- **Hazem Essam Okda**, Rosa Cristina M. Ferreira, Susana P. G. Costa, Hugo Gonçalves, Michael Belsley, M. Manuela M. Raposo, Ramón Martínez-Máñez, Félix Sancenón, *''Synthesis, optical properties and chemosensory ability of novel push-pull imidazoles bearing a phenanthrene moiety''* **2019**, *submitted*.

Abbreviations and Acronyms

UV/VIS and UV-Vis	Ultraviolet–visible
UPV	Universidad Politécnica de Valencia
Ex and ex	Excitation
K_a	Association Constant
ACN	Acetonitrile
ACS	American Chemical Society
BODIPY	Boron-dipyrromethene
Bu_4N	Tetra-*n*-butylammonium
CD_3CN	Deuterated Acetonitrile
$CDCl_3$	Deuterated Chloroform
CHEF	Chelation Enhanced Fluorescence
CHEQ	Chelation Enhancement Quenching
CIBER-BBN	Centro de Investigación Biomédica en Red en Bioingeniería, Biomateriales y Nanomedicina
CTAB	*n*-cetyltrimethylammonium bromide
CyS	Cysteine
Hcy	Homocysteine
GSH	Glutathione
SDS	Sodium dodecyl sulfate
DMEM	Dulbecco's Modified Eagle's Medium
DMF	Dimethyl Formamide
DMSO	Dimethylsulfoxide
EM	Electron Microscopy
Em and em	Emission
ESIPIT	Excited-State Intramolecular Proton Transfer
EtOH	Ethanol
Fl	Fluorescence
FRET	Fluorescence Resonance Energy Transfer
HeLa	Henrietta Lacks (human cell line)
HEPES	[4-(2-hydroxyethyl)-1-piperazineethanesulfonic acid
HOMO	Highest Occupied Molecular Orbital
HRMS	High Resolution Mass Spectra
ICT	Internal Charge Transfer
IDM	Instituto de Reconocimiento Molecular y Desarrollo Tecnológico

IR	Infrared
IUPAC	International Union of Pure and Applied Chemistry
LOD	Limit of Detection
LUMO	Lowest Unoccupied Molecular Orbital
MCR	Molecular Chemical Receptor
MeCN	Methyl Cyanide (Acetonitrile)
MeOH	Methanol
MLCT	Metal-to-Ligand Charge Transfer
Mp	Melting Point
MscL	Mechanosensitive Channel of Large Conductance
MS-EI	Mass Spectrometry by Electron Impact Ionization
NMR	Nuclear Magnetic Resonance
PBS	Phosphate Buffered Saline
PET	Photoinduced Electron Transfer
Ph	Phenyl Groups
PhD	Doctor of Philosophy of Philosophy Doctorate
H_3BO_3	Boric acid
^{13}***C-NMR***	Carbon-13 nuclear magnetic resonance
ESIPT	Excited State Intramolecular Proton Transfer
FTIR	Fourier-transform infrared spectroscopy
WHO	World Health Organization
IR	Infrared
NIR	Near-infrared
PD	Parkinson's disease
λ_{exc}	Excitation wavelength
RT	Room Temperature

Table of contens

Chapter 1: General introduction

1. General Introduction

1.1 Supramolecuar Chemistry

In the last decades supramolecular chemistry became a well stablished field in chemistry. One of the most relevant subjects of supramolecular chemistry is the study of host-guest interactions and its application for the development of molecular chemosensors for the detection of chemical species. Taking into account these facts, this PhD thesis is devoted to the synthesis and characterization of new chemical sensors based on supramolecular and coordination chemistry principles. For this reason, main concepts related with supramolecular chemistry and certain applications will be briefly explained on the following pages.

1.1.1 Supramolecular chemistry and molecular recognition.

Supramolecular chemistry is a relatively new chemistry field and its first bases can be traced by the late nineteenth century. At this respect, intermolecular forces were discovered in 1873 by Dr Johannes Van der Waals Diderik, Nobel Prize in physics in 1910.[1] Then, another important early contribution was the synthesis and study of cyclodextrins by Dr Villiers in 1891.[2] These studies were followed by the seminal works of Dr. Alfred Werner (Nobel Prize in chemistry in 1913) about the theory of coordination and study of metal complexes presented in 1893.[3] Moreover, an important landmark in the field of supramolecular chemistry was the introduction of the "lock and key" principle, proposed by Emil Fischer in 1894,

[1] a) J. D. Van der Waals, *Nobel Lecture: Physics 1901-1921*, **1967**, 255-265. b) J. D. Van der Waals, *"On the continuity of the gaseous and liquid state"*, PhD Dissertation. Leiden University, **1873**.

[2] A. C. R. Villiers, *Hebd. Seances. Acad. Sci*., **1891**, *112*, 536-538.

[3] a) A. Werner, *Nobel Lecture: Chemistry 1901-1921*, **1966**, 256-269. b) K. Bowman-James, *Acc. Chem. Res.*, **2005**, *38*, 671–678.

which was the origin of "molecular recognition".[4] This concept proposed that the mechanism by which an enzyme recognizes and interacts with a substrate could be similar to a lock and a key system.

After these first contributions, the study of the interactions between molecules in chemical and biological processes became of importance for the whole scientific community. The first synthetic receptors, able to present molecular recognition features, were prepared by Pedersen (crown ethers) and Cram (cryptands).[5,6] These seminal works introduced the host-guest chemistry concept in which molecular recognition plays a fundamental role. From the late 1970s, Jean-Marie Lehn was the first chemist who described the concept of complex intermolecular interactions as ''supramolecular'' – literally 'beyond, or transcending, the molecule'.[7] Moreover, Lehn stated that just as there is a field of molecular chemistry based on the covalent bond, there is a field of supramolecular chemistry, the chemistry of molecular assemblies and of the intermolecular bond.[8]

As Lehn acknowledges, the applications of this terminology to the chemical species has much to do with K. L. Wolf who introduced the term "übermoleküle" to describe the self-association of carboxylic acids to form a 'supermolecule' through hydrogen bonding.[9] In this sense, a 'supermolecule' can be defined as a large entity composed of molecular subunits, which could be applied equally to a

[4] a) H. E. Fischer, *Nobel Lecture: Chemistry 1901-1921*, **1966**, 21-35. b) E. Fischer, *Ber. Dtsch. Chem. Ges*., **1895**, *28*, 1429-1438.

[5] a) C. J. Pedersen, *J. Am. Chem. Soc.* **1957**, *79*, 2295-2299. b) C. J. Pedersen, *J. Am. Chem. Soc.* **1967**, *89*, 7017-7036.

[6] a) D. J. Cram, *J. Am. Chem. Soc.* **1978**, *100*, 8190-8202. b) D. J. Cram, J. M. Cram, *Science*, **1974**, *183*, 803-809.

[7] J. M. Lehn, *Angew. Chem*., **1988**, *100*, 91-116.

[8] J. M. Lehn, Cryptates: inclusion complexes of macropolycyclic receptor molecules. *Pure Appl Chem.,* **1978**, 50, 871–892.

[9] K. L. Wolf, H. Frahm, H. Harms, *Z Phys. Chem., Abt. B*, **1937**, *36*, 237–287.

covalently linked polymer as to an assembly held together by weaker interactions. Supermolecule structures are the result of not only additive but also cooperative interactions through non-covalent interactions as hydrogen bonding, metal coordination, hydrophobic forces, van der Waals forces, π-π interactions and electrostatic effects, to generate unique nanostructured supermolecules that present different properties (often better) than the sum of the properties of each individual component.[10] As a result of all these contributions, on the discovery and study of the specific interactions of crown ethers and cryptands, Jean M. Lehn, Donald J. Cram[11] and Charles J. Pedersen[12] awarded the Nobel Prize of chemistry in 1987.

Nowadays, supramolecular chemistry is a well stablished field in chemistry and its fundamental concepts have been used for the development of a large number of applications (ca. synthesis and characterization of chemical sensors for specific recognition of compounds, design of new types of materials, development of molecular machinery and the synthesis of highly complex self-assembled structures). Besides, supramolecular chemistry has also influenced in the emerging science of nanotechnology and in the development of catalysts.[13]

1.1.2 From molecular to supramolecular chemistry.

Molecular chemistry studies the structure, reactivity and properties of simple molecules, formed by the union of atoms by covalent bonds. On the other hand, supramolecular chemistry provides us the tools to understand how the molecules

[10] D. K. Smith, *J. Chem. Edu.,* **2005**, *82*, 393-400.

[11] D. J. Cram, *Nobel Lecture: Chemistry 1981-1990*, **1992**, 419-437.

[12] C. J. Pedersen, *Nobel Lecture: Chemistry 1981-1990*, **1992**, 495-511.

[13] S. Carmelo, M. S. Jeffrey, P. D. Michael, Z. Valeria, A. Giuseppe, R. N. Kenneth, *Chem. Eur. J*, **2017**, *23*, 16813-16818.

organize themselves by intermolecular forces to build up more complex units, which are referred to as supra or supermolecules. Thus, the main purpose of the supramolecular chemistry is to gain control over the intermolecular bond.

According to Prof. Lehn supramolecular chemistry may be defined as "chemistry beyond the molecules" or "chemistry of non-covalent bond" and deals with organized complex entities that resulted from the association of two or more chemical species through non-covalent interaction.[14] Prof. Lehn indicated that the nature of relationship between molecular and supramolecular chemistries resembles that of the individual families and the whole society.[15] Molecules are like individual families that are formed by persons (atoms). In addition, each family has its special features and the interaction between the members is controlled by molecular chemistry. However, the interaction between one family and others in the whole society to form bigger associations and alliances with different characteristics (supermolecule) are controlled by supramolecular chemistry.[16]

In 1953, James Watson and Francis Crick proved the importance of intermolecular forces in the molecular structure of nucleic acids (DNA) and its significance for information transfer in living organisms.[17] Due to its well defined and stable structure, allowing replication and recombination processes, DNA became one of the best examples to understand the nature of the molecular recognition and to illustrate the differences between molecular and supramolecular chemistry. DNA helix consists of two polynucleotide strands with arrays of complementary nitrogenated bases joined by non-covalent hydrogen

[14] K. Ariga, T. Kunitake, *Supramolecular Chemistry-Fundamentals and application © Springer Verlag Berlin Heidelberg Edition,* **2006**.

[15] J. M. Lehn*, "Supramolecular chemistry can help to understand better how to make efficient drugs"*. Universitat Autònoma de Barcelona, Spain. October **2012**. Lecture.

[16] J. M. Lehn, Supramolecular chemistry, Ed. VCH, **1995**.

[17] J. Watson, F. Crick, *Nobel Lecture: Physiology or Medicine,* **1962**.

bonds. Moreover, this helix conformation is obtained by combining two different types of supramolecular interactions namely: (i) hydrogen bonds formed between proton-donor groups (NH) of the bases and proton-acceptor groups (C=O and C-N) of cytosine and guanine; (ii) π-π stacking interactions among aromatic rings of nucleobases (Figure 1.1).

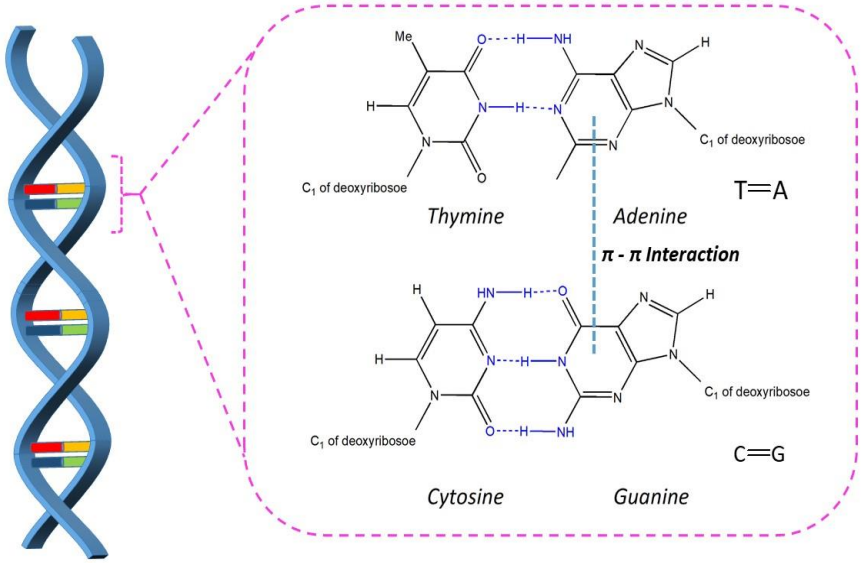

Figure 1.1. Hydrogen bonded complementary A-T and G-C base pairs in DNA helix. Sandwich π-staking interaction between aromatic rings and primary and secondary hydrogen bond interactions.

Cellulose is a natural polymeric macromolecule whose structure is closely related with the nature of intermolecular forces. At this respect, each hydroxyl group of one saccharide unit can form hydrogen bonds with other -OH moieties in neighbour sugar molecules in the same polysaccharide chain (Figure 1.2).[18] In addition, hydrogen bonds between two saccharides in parallel polysaccharide chains can be formed. Moreover, these hydrogen bonds reduce the distance between polysaccharide chains forming a coherent mono horizontal layer of

[18] T. Donglin, L. Tao, Z. Rongchun, W. Qiang, C. Tiehong, S. Pingchuan, R. Ayyalusamy*, J. Phys. Chem. B*, **2017**, 121, 6108-6116.

polysaccharides like a sheet. Besides that, there is another type of non-covalent interaction in cellulose where the formed sheets stacked tightly into layers held together by Van der Waals forces to form a micro fibril.

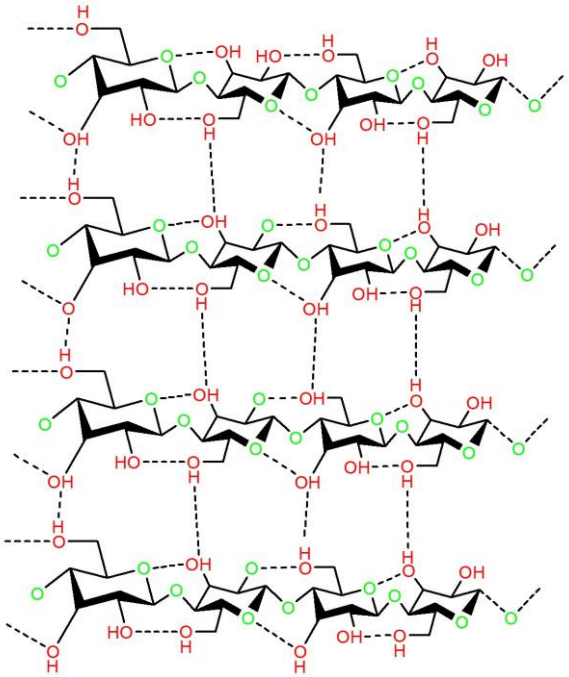

Figure 1.2. Intermolecular interactions in cellulose: side-to-side hydrogen bonds between hydroxyl groups of the polysaccharide chains in the same horizontal layer.

Bearing in mind the infinite number of possibilities given by the noncovalent bond chemistry an organization of this new discipline should be useful. For this reason, supramolecular chemistry can be divided into three main areas:

- ***Molecular recognition chemistry***: Chemistry associated with a molecule recognizing another molecule, also defined as host-guest chemistry.
- ***Molecular self-assembly***: Chemistry process of spontaneous formation of supermolecules without guidance from an outside source.
- ***Preparation of functional systems***: Interdisciplinar applications of supramolecular chemistry to prepare functional systems such as chemical

templated capsules, control release systems, nano superstructures or mechanically interlocked switchable scaffolds (molecular machines).

1.1.3 Molecular recognition (Host-Guest chemistry).

From a color change in a flask to highly sophisticated biological mechanisms, every action that occurs around us is the result of chemical reactions or physicochemical interactions occurring in various combinations. These reactions and interactions often seem to occur randomly, but this is rarely true. They often occur between selected partners, especially when the reactions and interactions occur in a highly organized system such as those found in biological settings – as the molecule recognizes the best (or better) partner. This mechanism is called "molecular recognition".

In molecular recognition processes a guest molecule selectively recognizes its host partner through several molecular interactions forming a host-guest complex (supramolecule). In order to form a stable complex, the host molecule must possess a high degree of complementarity (in terms of geometric and electronic features) with the guest (Figure 1.3). Usually, the interactions between both partners are of non-covalent nature (hydrogen bonding, metal coordination, hydrophobic forces, Van der Waals forces and π - π interactions).[19]

[19] a) F. P. Schmidtchen, *Chem. Soc. Rev.,* **2010**, *39*, 3916-3935. b) D. W. Smith, *J. Chem. Edu.,* **2005**, *82*, 393-400.

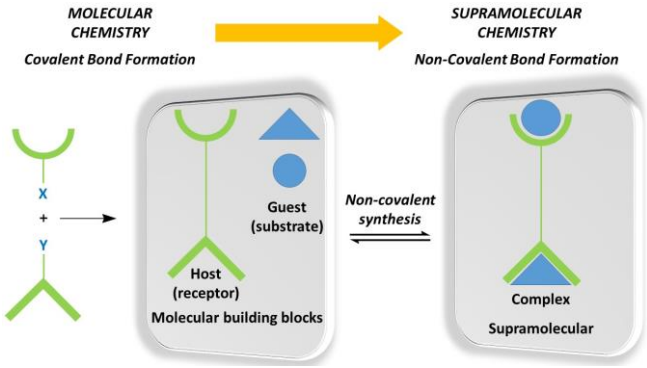

Figure 1.3. Scheme of host-guest interaction in supramolecular chemistry.

Historically, the first model of molecular recognition is the lock-key principle suggested by Emil Fischer in 1894.[20] In this model, an enzyme (host) can discriminate among different substrates (guests) through the specific geometric complementarity between host and guest (Figure 1.4). At this respect, only one guest fit exactly into one host like only a key enter in a specific lock. Knowledge of this simple principle allowed explaining the enzymatic catalysis, the compression of many complex biological processes and setting up the foundation for the preparation and optimization of new synthetic hosts (receptors).[21]

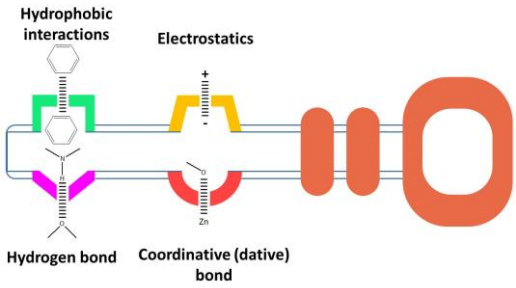

Figure 1.4. The lock and key principle: receptor sites in the host (lock) are complementary to the guest (key).

[20] E. Fischer, *Ber. Dtsch. Chem. Ges.*, **1895**, *28*, 1429-1438.

[21] a) F. W. Lichtenthaler, *Angew. Chem.*, **1992**, *104*, 1577-1593. b) D. E. Koshland, *Angew. Chem.*, **1995**, *33*, 2375-2378.

The first crown ether synthesis was described by Pedersen in 1967. These artificial hosts were accidentally found as a by-product of an organic reaction. Figure 1.5 showed the synthetic procedure used by Pedersen which yielded accidentaly the first crown ether. Pedersern used tetrahydropyranyl monoprotected catechol (**D_1**) in order to prepare bisphenol acyclic ether **1** (see Figure 1.5). However, compound **D_1** contained impurities of catechol and, as a consequence, crown ether **2** was obtained in 0.4 % yield. Besides, Pedersen observed that compound **2** was able to entrap a K^+ cation in the cavity of the cyclic ether. Pedersen called the cyclic compound "crown ether" because the cyclic host "wears" the ion guest like a crown.[22]

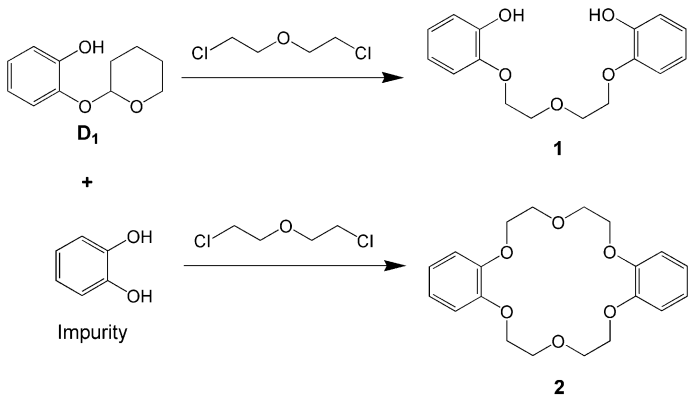

Figure 1.5. Scheme of the unexpected synthesis of crown ethers carried out by Pedersen in 1967.

Taking into account the first pioneering work of Pedersen, many reserachers started to work in the synthesis and characterization of abiotic receptors for metal cations. At this respect, the first podands and crown ethers (structures **3** and **4** in Figure 1.6) and cryptands (structures **5** and **6** in Figure 1.6) were prepared by Pedersen and Cram respectively.[23,24] Besides, at the end of the same decade, the

[22] C. J. Pedersen, *J. Am. Chem. Soc.*, **1967**, *89*, 7017-7036

[23] a) D. J. Cram, *J. Am. Chem. Soc.* **1978**, *100*, 8190-8202. b) D. J. Cram, J. M. Cram, *Science*, **1974**, *183*, 803-809.

first synthetic receptors for anion coordination were prepared by Biallas and Simmons (see Figure 1.7).[25]

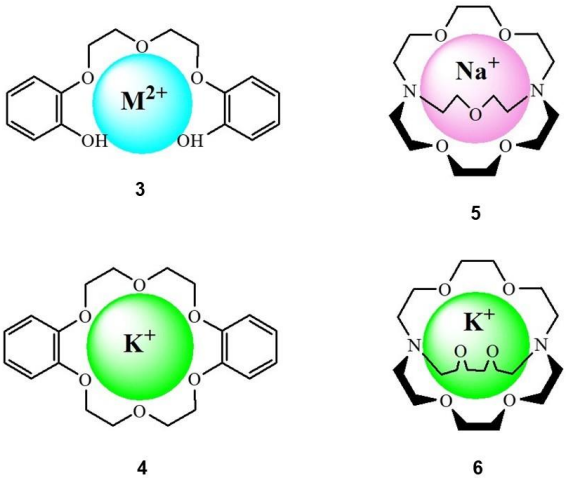

Figure 1.6. Metal complex based on crown ethers and cryptands. Left: Pedersen´s complexes of divalent cations (**3**) and K^+ (**4**) with crown ethers. Right: Complex of Na^+ (**5**) and K^+ (**6**) with two of the first synthetic cryptands.

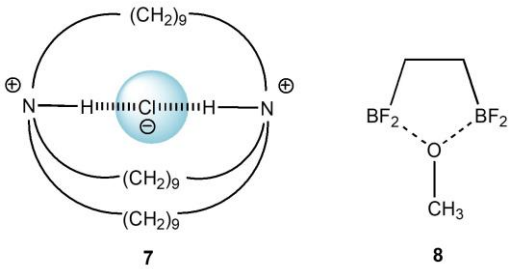

Figure 1.7. Representation of the first anion receptors. Left: chelated complex (**7**) formed between macrobicyclic amines and Cl^- anion, reported by Park and Simmons. Right: chelated complex (**8**) formed between bidentade 1,2-bis(difluoroboryl)ethane and methoxide anion, reported by Shriver and Biallas.

[24] C. J. Pedersen, *J. Am. Chem. Soc.* **1957**, *79*, 2295-2299.

[25] a) D. F. Shriver, M. J. Biallas, *J. Am. Chem. Soc.*, **1967**, *89*, 1078. b) C. H. Park, H. E. Simmons, *J. Am. Chem. Soc.*, **1968**, *90*, 2429-2431.

During the design of a molecular receptor, it is necessary an extensive evaluation of the size, shape, geometry, charge, hydrophilic/lipophilic character and other physico-chemical characteristics of guest-analyte interaction to provide the required amount of intermolecular forces between the host and the guest in order to assure coordination. In addition, an assessment of the environment in which molecular recognition takes places is very important when designing the receptor due to the influence of intermolecular processes such as solvation and electrostatic interactions between molecular chemical receptor, medium and analyte.[26] The main parameter of host-guest interaction is the selectivity, which is defined as the ability of the host to distinguish among different guests. In order to understand the nature of this selectivity, a number of different factors should be overviewed such as complementarity between the guest and the host binding sites, cooperativity of the binding groups and preorganization of the host.[27]

- ***Complementarity*****:** Both the host and guest must have mutual spatially and electronically complementary binding sites to form the supermolecule.
- ***Cooperativity*****:** A host molecule with multiple binding sites that are covalently connected (i.e. acting as a 'team') forms a more stable host–guest complex than a similar system with sites that are not covalently connected (therefore acting separately from each other).
- ***Preorganization*****:** A pre-organized host has a series of binding sites in a well-defined geometry within its structure and does not require a significant conformational change in order to bind to a specific guest in the most stable possible way.

[26] a) G. V. Oshovsky, D. N. Reinhoudt, W. Verboom, *Angew. Chem. Int. Ed*. **2007**, *46*, 2366 -2393. b) S. Kubik, *Chem. Soc. Rev.,* **2010**, *39*, 3648-3663.

[27] J. W. Steed, J. L. Atwood, *Supramolecular Chemistry*, © **2009**, John Wiley & Sons, Ltd.

Moreover, the complex formed from the host-guest interatction of two or more molecules by non-covalent bonds is an equilibrium process defined by a binding constant. In recent years, the synthesis of new molecular receptors with enhanced selectivities toward selected guests is a field of research that deserved much attention. Desing of selective molecular receptors is especially appealing for industrial, biomedical or environmental applications.[28]

1.1.4 Chemical sensors (chemosensors).

The IUPAC definition of chemosensor is ‘‘a device that transforms chemical information ranging from the concentration of a specific sample component to total composition analysis into an analytically useful signal”. All chemosensors are designed to contain two subunits that can interact selectively with an analyte (guest) displaying a measurable signal. The two subunits are:

1. ***Binding Site***: is the unit responsible of the recognition of the analyte. The process of recognition depends on the host molecule characteristics. The binding subunit is designed in order to achieve a selective coordination via a suitable receptor-guest complementarity.
2. ***Signalling Subunit:*** it acts as a signal transducer and informs of the recognition process that occurs at molecular level through changes in a measurable macroscopic signal.

As previously mentioned, the receptor subunit is the main part responsible for displaying a selective molecular recognition with one specific guest. This selective recognition can be achieved by an accurate design of the binding site in order to introduce a high degree of complementarity (matching size, shape, charge, etc.)

[28] a) D. N. Reinhoudt, J. F. Stoddart, R. Ungaro, *Chem. Eur. J.*, **1998**, *4*, 1349-1351. b) P. J. Lusby, *Annu. Rep. Prog. Chem.*, *Sect. A: Inorg. Chem.*, **2013**, *109*, 254-276.

with the target analyte. As a consequence of the molecular recognition, and the high complementary between host and guest, the chemical information is transformed by the signaling subunit into a macroscopic measurable signal as an alarm signal or output response.[29]

On the other hand, the signaling subunit is a molecular entity able to transduce the interaction of the target analyte with the binding site into a detectable and easy-to measure signal, revealing the presence of the guest. Signals widely used to detect the presence of certain guest molecules are changes in color,[30] fluorescence[31] or modulations in electrochemical properties (redox potential).[32] Chemosensor sensitivity is the result of both the receptor ability to carry out the molecular recognition at low concentrations of guest and of the signaling subunit ability to report the event. Both selectivity and sensitivity are strongly influenced by several conditions and physico-chemical characteristics of the enviroment in which the molecular recognition takes place.

According to the sensing approach princiciple of the signal subunit chemical sensors could be classified as:

- ***Optical sensors***: If the molecular recognition is transduced in optical phenomena as changes in absorbance, transmittance, fluorescence, luminescence, light scattering or optothermal effect.
- ***Electrochemical sensors***: When the final signal result in a modulation of electrical current condition by redox process.

[29] Q. D. Tuan, K. J. Seung, *Chem. Rev.*, **2010**, *110*, 6280-6301.

[30] a) H. G. Löhr, F. Vögtle, *Acc. Chem. Res.*, **1985**, *18*, 65-72. b) M. Takagi, K. Ueno, *Top. Curr. Chem.*, **1984**, *121*, 39-65. c) B. Kaur, K. Navneet, S. Kumar, *Coord. Chem. Rev.*, **2018**, *358*, 13–69.

[31] D. Wua, L. Chen, W. Lee, G. D. Wua, L. Chen, W. Lee, K. Gyeongju, J. Yin, J. Yoon, J. Yin, J, Yoon, *Chem. Rev.*, **2012**, *112*, 1910–1956.

[32] a) P. D. Beer, *Chem. Commun*., **1996**, 689-696. b) P. D. Beer, *Coord. Chem. Rev.*, **2000**, *205*, 131-155.

- ***Mass sensitive sensors***: When the recognition process is reported as the mass change at a specially modified surface that resulting into a change of a property of the support material.
- ***Magnetic sensors***: When the analitical signal is a change of paramagnetic properties.
- ***Thermometric sensors***: When the signal is based in the measurement of the heat effects of a specific chemical reaction or adsorption molecules, which involve the analyte.
- ***Radiation sensors***: If non-optical radiation as α-, β-, γ- or X-rays is the basis for the signaling.

The important advantages, with respect to other analytical methods, offered by the optical (chromo-fluorogenic) chemosensors are related to the possibility of use cheap and simple instrumentation, the need of very small quantity of sample and in some cases, the possibility of "in situ" and "on time" measurements. Moreover, colorimetric sensors induced noticeable color changes observable to the naked eye and can be used for rapid qualitative determinations. On the other hand, fluorogenic chemosensors have a high degree of sensitivity and normally allow the achievement of lower detection limits when compared with colorimetric techniques. In this PhD thesis we focused our attention toward the development of optical chemosensors for the detection of cations, anions and chemical species of industrial, biomedical or environmental interest.

1.2 Optical chemosensors.

As cited above, optical chemosensors are those abiotic probes in which coordination with a target analyte induced rearrangements in their electronic structure that are reflected in colour or emission changes. One interesting goal in

the development of optical chemosensors deals with the synthesis of highly selective systems.[33] Reversibility and fast response will be also appealing features for an applicable sensor to be taken into account in its design. In addition, these kinds of chemosensors are extensively used for the detection of anions, cations or neutral molecules in biological and environmental samples. In the next section the three main approaches used for the design of optical chemosensors are described.

1.2.1 Optical chemosensors, design fundaments.

Although the binding site plays a crucial role in the selective detection of the target analyte, the signalling subunit is a very significant part of the optical chemosensor. Both components, binding and signaling subunits, can be arranged in diferent fashion to construct chromo-fluorogenic chemical sensors. Three main approaches are used in the design of chromo-fluorogenic chemosensors: **(i)** the ‘‘binding site-signaling subunit’’ protocol, **(ii)** the ‘‘displacement’’ approach and **(iii)** the ‘‘chemodosimeter’’ paradigm (see Figure 1.8). Selection of one of the three approaches for the synthesis of a new optical chemosensor depens on some parameters such as analyte affinity, binding selectivity and the medium in which the sensing is performed.

[33] a) R. Martínez-Máñez, F. Sancenón, *Chem. Rev.*, **2003**, *103*, 4419-4476. b) M. E. Moragues, R. Martínez-Máñez, F. Sancenón, *Chem. Soc. Rev.*, **2011**, *40*, 2593-2643. c) L. E. Santos-Figueroa, M. E. Moragues, E. Climent, A. Agostini, R. Martínez-Máñez, F. Sancenón, *Chem. Soc. Rev.* **2013**, *42*, 3489-3613.

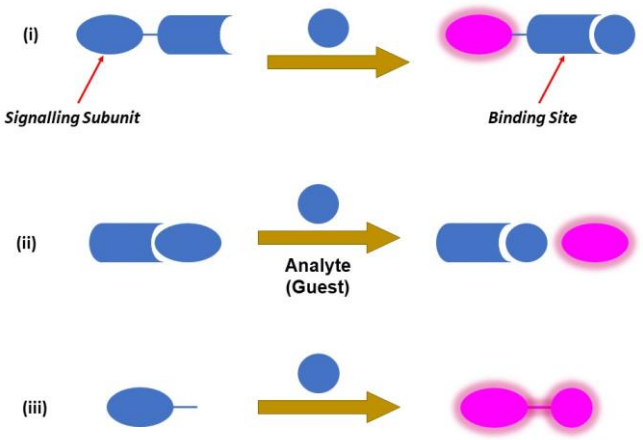

Figure 1.8. Scheme of the three main approaches used in the development of optical chemosesors: **(i)** binding site-signaling subunit; **(ii)** displacment protocol; and **(iii)** chemodosimeter approach.

1.2.1.1 ''Binding site – signaling subunit'' approach.

The binding site-signaling subunit protocol is the most common design for the development of optical chemosensors. On this approach, the chemosensor consists of two covalently bonded parts; i.e. the ''binding site'' (which is responsible of the selective analyte binding) and the ''signaling subunit'' (a chromophore or a fluorophore). Moreover, in some cases, an additional part called the spacer, which is able to modify the geometry of the system and tune the electronic interaction between the receptor and photoactive unit, is included (see Figure 1.8). In general, the binding site subunit is designed to have effective non-covalent interactions with a specific analyte. According to the coordination of the target analyte (via hydrogen bonding, proton transfer processes, etc.) with the binding site, the physical properties of the signaling subunit results in a

measurable modulations either in the colour (chromogenic chemosensor) or in its emission (fluorogenic chemosensor).[34]

This approach has been extensively used for the synthesis of optical probes for charged and neutral species. Colorimetric detection of cations have been achieved using several photoactive molecules conjugated to an appropriate binding unit through a number of different linkages.[35]

One of the first examples of chromogenic chemosensors constructed using the signaling subunit-bindind site approach was reported by Vögtle and co-workers in 1978. The prepared probe (**9** in Figure 1.9) consisted in a crown ether binding site electronically connected with an azo dye.[36] In addition, the key point in the chemosensor design is the incorporation of one of the nitrogen atoms of the azo dye inside the structure of the crown ether. Acetonitrile solutions of receptor **9** showed an absorption band centered at 477 nm that is the responsible of the orange color. Of all the cations tested, only Ba^{2+} was able to induce a remarkable bathochromic shift of the visible band (from 477 to 357 nm) that was reflected in a color change from orange to yellow. The observed bathochromic shift was ascribed to a coordination of Ba^{2+} cation with the crown ether. The interaction of this cation with the nitrogen atom of the azo dye located in the crown ether induced an increase in the HOMO/LUMO energy gap that was reflected in the observed colour change.

[34] B. Kaur, K. Navneet, K. Subodh, *Coord. Chem. Rev.*, **2018**, *358*, 13–69.

[35] a) K. Ghosh, T. S. Beilstein, *J. Org. Chem.*, **2010**, *6*, 44. b) D. Udhayakumari, S. Velmathi, P. Venkatesan, S. P. Wu, *Anal. Methods*, **2015**, *7*, 1161. c) L. Tang, P. Zhou, Q. Zhang, Z. Huang, J. Zhao, M. Cai, *Inorg. Chem. Commun.*, **2013**, *36*, 100. d) T. Anand, G. Sivaraman, D. Chellappa, *J. Photochem. Photobiol. A: Chem.*, **2014**, *281*, 147. e) X. Zhao, Q. Ma, X. Zhang, B. Huang, R.Q. Yu, *Anal. Sci.*, **2010**, *26*, 585. f) F. A. Abebe, E. Sinn, *Tetrahedron Lett.*, **2011**, *52*, 5234. g) C. Y. Chou, S. R. Liu, S. P. Wu, *Analyst*, **2013**, *138*, 3264.

[36] J. P. Dix, F. Vögtle, *Angew. Chem. Int. Ed.*, **1978**, *17*, 857.

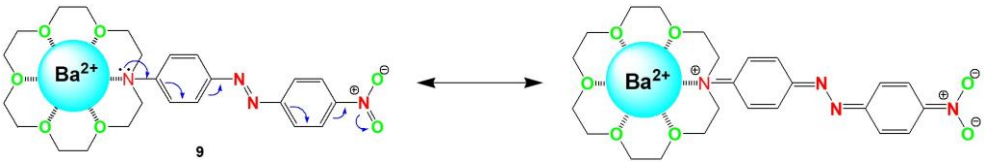

Figure 1.9. Chromogenic probe based on a crown ether linked with an azo dye for the selective recognition of Ba^{2+} cation.

Tian *et al*. developed a highly selective intracellular red-fluorescent sensor **10**, which was suitable for K^+ detection (Figure 1.10).[37] HEPES solutions of probe **10** showed a very weak emission due to a photoinduced electron transfer (PET) process. Of all the cations tested, only K^+ induced a marked emission enhancement at 650 nm due to the fact that its preferential coordination with probe **10** inhibited the PET process. According to the high selectivity, receptor **10** became useful for intracellular K^+ sensing over a wide range of biological conditions.

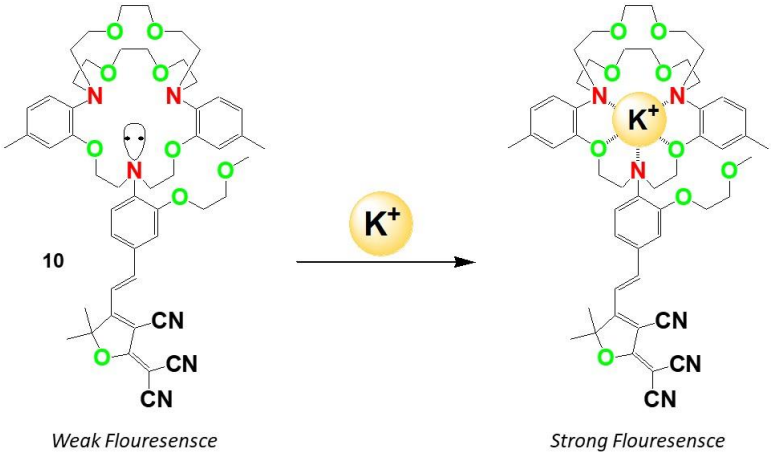

Figure 1.10. Fluorogenic probe **10** for the selective recognition of K^+ in biological settings.

[37] X. Zhou, S. Fengyu, Y. Tian, C. Youngbull, R. H. Johnson, D. R. Meldrum, *J. Am. Chem. Soc.*, **2011**, *133*, 18530–18533.

On the the same context, many anion chemosensors have been developed using the binding site-signaling subunit approach. For example, Amitava et al synthesized a new anthraquinone derivative as a fluoride chemosensor (Figure 1.11).[38] At this respect, DMSO/CH_3CN (1:9, v/v) solution of chemosensor **11** presented an absorption band at 459 nm that was bathochromically shifted (to 561 nm) only in the presence of fluoride anion. These variations were reflected in a colour change from yellow to purple upon fluoride coordination with chemosensor **11**. The chromogenic response was ascribed to a charge-transfer interaction between the electron rich urea/thiourea bound fluoride ion and the electron deficient anthraquinone moieties.

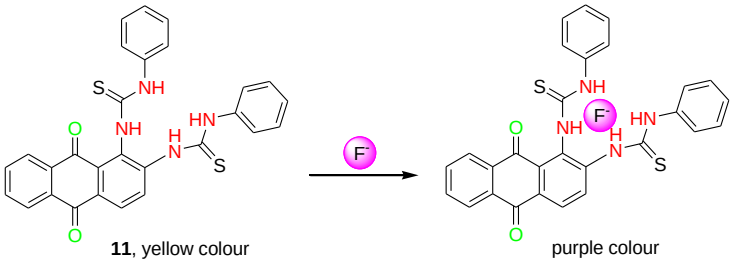

Figure 1.11. Chemosensor **11** for the chromogenic recognition of fluoride anion.

1.2.1.2 "Displacement" approach.

Displacement assays have also been widely used to develop chromo-fluorogenic chemosensors since the pioneering work of the research groups of Anslyn[39] and Fabbrizzi,[40] who were inspired in displacement reactions in

[38] D. A. Jose, D. K. Kumar, B. Ganguly, D. Amitava, *Org. Lett.*, **2004**, *6*, 3445–3448.

[39] a) J. J. Lavigne, E. V. Anslyn, *Angew. Chem., Int. Ed.*, **1999**, *38*, 3666–3669. b) A. Metzger, E. V. Anslyn, *Angew. Chem., Int. Ed.*, **1998**, *37*, 649–652. c) K. Niikura, A. Metzger, E. V. Anslyn, *J. Am. Chem. Soc.*, **1998**, *120*, 8533–8534. d) H. A. Haddou, S. L. Wiskur, V. M. Lynch, E. V. Anslyn, *J. Am. Chem. Soc.*, **2001**, *123*, 11296–11297. e) S. L. Wiskur, E. V. Anslyn, *J. Am. Chem. Soc.*, **2001**, *123*, 10109–10110. f) Z. Zong, E. V. Anslyn, *J. Am. Chem. Soc.*, **2002**, *124*, 9014–9015. g) S. L. Wiskur, P. N. Floriano, E. V. Anslyn, J. T. McDevitt, *Angew. Chem., Int. Ed.*, **2003**, *42*, 2070–2072.

immunoassay protocols. In this paradigm, the binding site (as receptor) forms an inclusion complex with the signaling subunit (either a dye or a fluorophore). However, upon addition of the target analyte, for which the receptor has a high affinity, a displacement reaction occurs; i.e. the receptor binds to the analyte and releases the signaling subunit to the medium.[41] Finally, the difference in optical properties between the free signaling subunit and the complexed indicator leads to the detection of the corresponding analyte. This approach has two remarkable advantages: (i) it allows testing a large number of binding site/signalling subunit combinations in order to obtain tuned sensing probes; (ii) most of the designed ensembles usually display sensing features in either aqueous solutions or organic–aqueous mixed solutions allowing the design of realistic sensing protocols.

As an example of using this approach, a novel fluorescent chemosrensor based on gold nanoparticles appended with a fluorophore was synthesised by Paul D. Beer *et al.* for the selective detection of 2-chloroethyl methyl sulfide (Figure 1.12).[42] In this work, upon excitation at 345 nm in chloroform, the probe showed a weak emission band. However, upon addation of 2-chloroethyl methyl sulfide, a significant enhancement in emission intensity was observed due to the displacement of the fluorophore from the surface of the nanoparticles resulting in a switching 'ON' of the fluorescence.

[40] a) L. Fabbrizzi, N. Marcotte, F. Stomeo, A. Taglietti, *Angew. Chem., Int. Ed*., **2002**, *41*, 3811–3814. b) M. A. Hortala, L. Fabbrizzi, N. Marcotte, F. Stomeo, A. Taglietti, *J. Am. Chem. Soc*., **2003**, *125*, 20–21. c) L. Fabbrizzi, A. Leone, A. Taglietti, *Angew. Chem., Int. Ed*., **2001**, *40*, 3066–3069.

[41] K. S. Kyung, L. D. Hoon, H. J. In, J. Yoon, *Acc. Chem. Res.*, **2009**, *42*, 23-31.

[42] R. C. Knighton, M. R. Sambrook, J. C. Vincent, S. A. Smith, C. J. Serpell, J. Cookson, M. S. Vickersa, P. D. Beer, Chem. Commun., **2013**, *49*, 2293-2295.

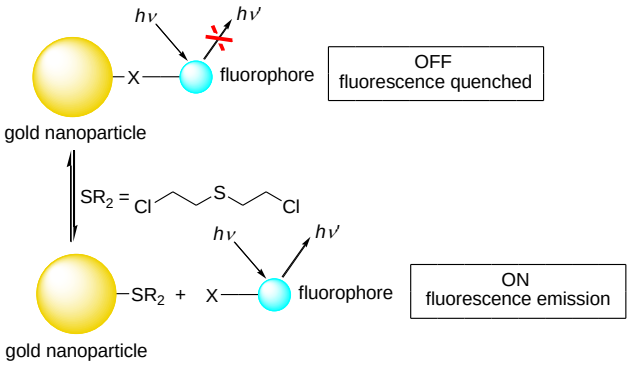

Figure 1.12. Schematic representation of sensing of 2-chloroethyl methyl sulfide by displacement assay.

In another example, Wilton-Ely, Martínez-Máñez and co-workers developed a chromo-fluorogenic sensor for CO detection (Figure 1.13).[43] The authors prepared probe **12** that showed an absorption band at 390 nm in methanol solution. However, when CO was bubbled into dichloromethane or methanol solutions of **12** an instantaneous and remarkable color change from red to yellow was observed. Moreover, the displacement of the BTD ligand by CO also results in the recovery of the fluorescence emission of the pyrene group. Thus, whereas probe **12** is very weakly fluorescent in methanol (λ_{ex} 355 nm, λ_{em} 458 nm), formation of the complex [Ru(CH=CHPyr-1)Cl(CO)$_2$(PPh$_3$)$_2$] (**13**) resulted in a remarkable 36-fold increase in emission.

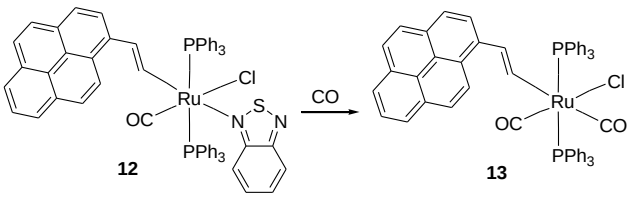

Figure 1.13. Representation scheme of reactivity of probe **12** with CO to give dicarbonyl complex.

[43] M. E. Moragues, A. Toscani, F. Sancenon, R. M. Mañez, A. J. P. White, J. D. E. T. Wilton-Ely, *J. Am. Chem. Soc.*, **2014**, *136*, 11930−11933.

1.2.1.3 "Chemodosimeter" paradigm.

The chemodosimeter paradigm became a well-established approach for the chromo-fluorogenic recognition of anions and neutral molecules.[44] Chemodosimeters are molecular probes designed in such a way that changed their optical properties upon reaction with selected analytes. The underlying idea of this paradigm is to take advantage of the selective reactivity that certain chemical species may display. Hence, the use of anion-induced reactions has advantages as the high selectivity usually reached even in aqueous solutions or in mixed organic-aqueous solutions and an accumulative effect that is related directly with the anion concentration.[45]

For example, the use of urea or thiourea derivatives for desing of chromogenic chemodosimeters for anions was extensively explored by Fabbrizzi and co-workers. One of the prepared chemosensors in depicted in Figure 1.14.[46] Chemodosimeter **14** consists of urea polarized N-H fragments which behaves as H-bond donors toward anions. The chromogenic response of chemodosometer **14** was studied in the presence of fluoride, acetate, benzoate, dihydrogen phosphate, nitrite, hydrogen sulfate, and nitrate anions. Of all the anions tested only fluoride was able to induce remarkable shifts in the UV-visible bands that were reflected in colour changes. At this respect, upon addition of the first equivalent of F^- to the acetonitrile solution of **14**, the visible charge transfer band underwent a red shift from 325 to 375 nm, while the solution bacame yellow-orange. Then, after addition of the second anion equivalent, a new band developed at 475 nm and

[44] a) Y. Yuming, Z. Qiang, F. Wei, L. Fuyou, *Chem. Rev.*, **2013**, *113*, 192-270. b) Q. D. Tuan, K. J. Seung Chem. Rev., **2010**, *110*, 6280-6301.

[45] a) Y. Lun, W. Shuailiang, H. Kunzhu, L. Zhiguo, G. Feng, Z. Wenbin, *Tetrahedron*, **2015**, *71*, 4679-4706. b) P. A. Gale, C. Caltagirone, *Chem. Soc. Rev.*, **2015**, *44*, 4212-4227.

[46] V. Amendola, D. Esteban-Gómez, L. Fabbrizzi, M. Licchelli, *Acc. Chem. Res.*, **2006**, *39*, 343-353.

the solution changed to red. The new absorption band at 475 nm was ascribed to the deprotonated receptor **14**.

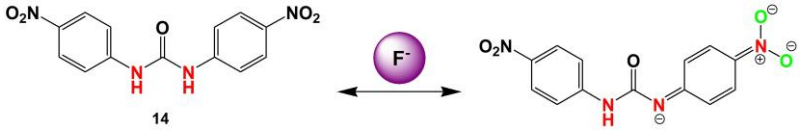

Figure 1.14. Resonance representation of the deprotonated form of **14**.

Another reaction that is extensively used for the development of optical chemodosimeters for fluoride anion is the hydrolysis of Si-O bonds.[47] One recent example was described by El Sayed and co-workers in 2013. The authors prepared chemodosimeter **15** which was used as a chromo-fluorogenic chemodosimeter for F^- anion (Figure 1.15).[48] CTABr solutions of probe **15** (which was included inside micelles formed by surfactant molecules) were colourless (absorption band centered at 325 nm). Of all the anions tested, only fluoride induced a marked colour change from colourless to yellow (appearance of a new absorption band at 425 nm) due to the hydrolysis of the silyl ether moiety, which generated an electronically delocalized stilbene-pyridine anion.

[47] Y. Zhou, J. F. Zhang, J. Yoon, *Chem. Rev.*, **2014**, *114*, 5511−5571.

[48] S. Elsayed, A. Alessandro, L. E. S. Figueroa, R. M. Mañez, F. Sancenon, *ChemistryOpen*, **2013**, *2*, 58-62.

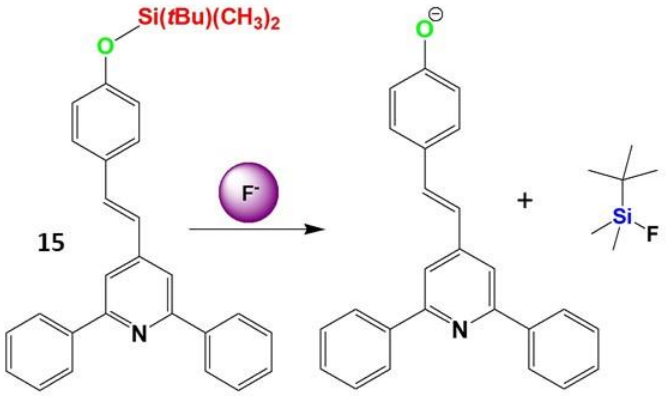

Figure 1.15. F^- anion induced the cleavage of the Si-O bond in receptor **15** that gives a highly fluorescent stilbene-pyridine derivative.

Hua and co-workers prepared a new chemodosimeter for cyanide detection (Figure 1.16).[49] In this case, chemodosimeter **16** utilized an unreactive formyl group as the electron-withdrawing component. Due to cyanide recognition process the internal charge transfer (ICT) of **16** was redirected and lead to a remarkably colorimetric response. At this respect, receptor **16** exhibit four absorption bands at 570, 452, 360, and 293 nm. Addition of cyanide induced a marked decrease in the absorbance of the bands centered at 570 and 452 nm and, at the same time, a remarkable increase in the intensity of absorption at 293 nm occured. As a result, a remarkable colour change from dark brown to light yellow, which can be observed by the naked eye, was produced.

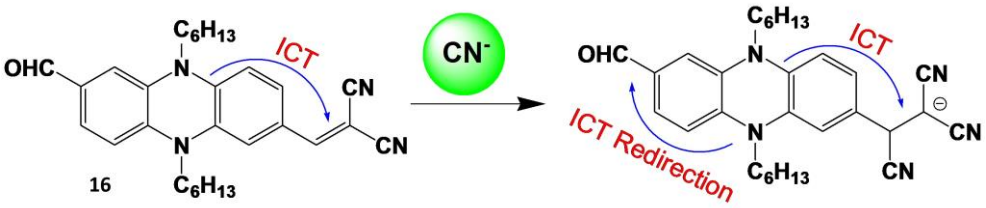

Figure 1.16. Chemical structure of chemodosimeter **16** and the mechanism of CN^- recogntion.

[49] L. Y. Xin, L. J. Yang, Y. Qu, H. Jianli, *ACS Appl. Mater. Interfaces*, **2013**, *5*, 1317−1326.

The chemodosimer approach is also widley used for the detection of cations. At this respect, Zhao and co-workers developed a new NIR rhodamine derivative as a chemodosimeter for Hg^{2+} detection (Figure 1.17).[50] Chemodosimeter **17** in HEPES buffer/ethanol (1:1 v:v) solution displayed weak luminescence upon excitation at 630 nm. Nevertheless, upon addition of Hg^{2+}, there was a thiolactone ring-opening process leading to a fluoresence turn-on emission at 745 nm.

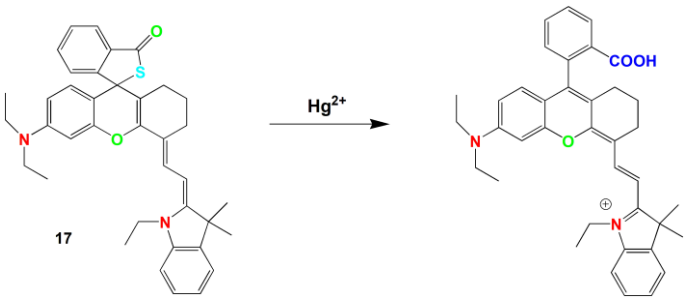

Figure 1.17. The proposed recognition mechanism of chemodosimeter **17** towards Hg^{2+}.

1.2.2 Optical signaling mechanisms.

In order to properly desing optical chemosensors, the selection of the signaling unit is a crucial issue. For this reason the most important feautres of an optical reporter (a chromophore or a fluorophore) such as light absorption behavior, stability, reactivity, etc. must be taken into account. Moreover, the binding site and the optical reporter should be structurally integrated as much as possible in order to maximize their communication and the optical effects observed upon guest binding.[51]

[50] Y. Huiran, H. Chunmiao, Z. Xingjun, L. Yi, Z. K. Yin, L. Shujuan, Z. Qiang, L. Fuyou, H. Wei, *Adv. Funct. Mater.*, **2016**, *26*, 1945 - 1953.

[51] a) P.J. Hung, J.L. Chir, W. Ting, A.T. Wu, *J. Lumin.*,**2015**, *158*, 371–375. b) M. Orojloo, S. Amani, *Aust. J. Chem.*, **2016**, *69*, 911–918. c) D. H. Wang, Y. Zhang, R. Sun, D. Z. Zhao, *RSC Adv.,* **2016**, *6*, 4640–4646. d) S. A. Lee, J. J. Lee, G. R. You, Y. W. Choi, C. Kim, *RSC Adv.*, **2015**, *5*, 95618–95630.

Furthermore, it should be taken into account that sometimes the integration of an optical reporter into a molecular receptor can modify the optical properties of the chromophore or fluorophore used.[52] For instance, the latter effect is directly utilized in the design of probes based in the displacement approach. In addition, there is an important distinction between the guest binding effects on chromophores and fluorophores. At this respect, the chromophores display useful absorbance changes generally as a result of variations in the molecular structure, including proton transfer, charge transfer and isomerization. Moreover, the effects exhibited by the fluorophores are much more sensitive to delicate changes in the geometry and electronic structure of the ground state, as well as the electronic excited state.[53] Due to the above mentioned reasons, the optical signaling mechanisms become an important field to study.

1.2.2.1 Colorimetric sensors.

These chemosensors are normaly constructed in such a way that coordination with selected analytes induced changes in their electronic features in the form of intra/intermolecular charge transfer (ICT) transitions (including LMCT and MLCT).[54] For instance, to achieve colorimetric detection of metal cations chemosensor with a D-π-A structure have been developed. D-π-A systems can be obtained by introduction of electron donating (ED) groups and electron acceptor (EA) groups in the receptor molecule at appropriate positions. Moreover, in these

[52] a) Y. W. Choi, G. J. Park, Y. J. Na, H. Y. Jo, S. A. Lee, G. R. You, C. Kim, *Sens. Actuators B*, **2014**, *194*, 343–352. b) G. J. Park, J. J. Lee, G. R. You, L. T. Nguyen, I. Noh, C. Kim, *Sens. Actuators B*, **2016**, *223*, 509–519. c) D. P. Domínguez, M. Rodríguez, G. R. Ortíz, J. L. Maldonado, M. A. M. Nava, O. B. García, R. Santillan, N. Farfán, *Sens. Actuators B*, **2015**, *207*, 511–517. d) S. Malkondu, S. Erdemir, *Tetrahedron*, **2014**, *70*, 5494–5498.

[53] S. Malkondu, D. Turhan, A. Kocak, *Tetrahedron Lett.*, **2015**, *56*, 162-167.

[54] a) D. Maity, T. Govindaraju, *Inorg. Chem.*, **2011**, *50*, 11282–11284. b) Q. Zhao, F.Y. Li, C.H. Huang, *Chem. Soc. Rev.*, **2010**, *39*, 3007–3030. c) Y.J. Na, W.Y. Choi, G.R. You, C. Kim, *Sens. Actuators B,* **2016**, *223*, 234–240.

systems, the deciding factor is whether a particular metal ion will bind ED or EA group depending upon the HSAB concept (Pearson acid-base concept) of the hardness and softness of the binding sites and analyte.[55]

Generally, the binding of cations with the EA group strengthens the D-π-A system with increased push-pull ICT effect and results in red shift along with increased chances of occurrence of LMCT transitions.[56] On the other hand, the binding of the metal ion with ED group decreases its donating ability, which virtually converts the D-π-A system to an A-π-A system reducing the conjugation. Consequently, it results in a blue shift in the absorption band and increases the chances of MLCT transitions (Figure 1.18).[57]

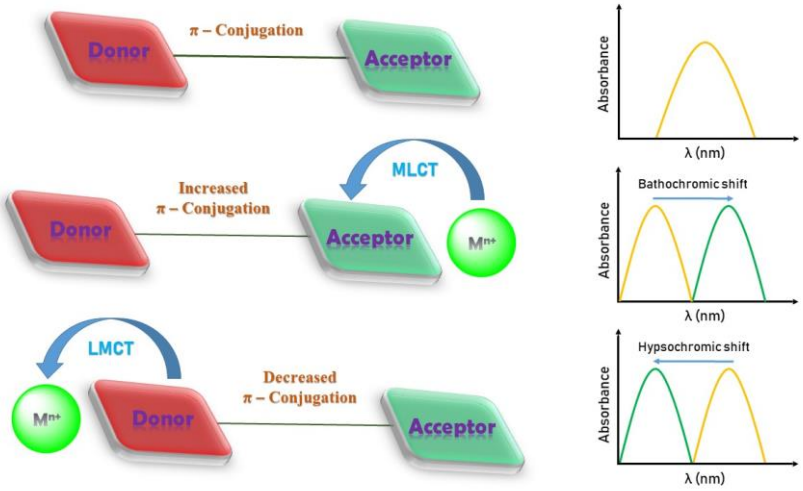

Figure 1.18. Pictorial representation of the effect of cation binding on D-π-A system and on absorption spectrum.

[55] R. G. Pearson, "Hard and soft acids and bases, HSAB, part 1: Fundamental principles". *J. Chem. Educ.,* **1968**, *45*, 581–586.

[56] R. Rani, K. Paul, V. Luxami, *New J. Chem.*, **2016**, *40*, 2418–2422.

[57] a) M. Caricato, C. Coluccini, D.A.V. Griend, A. Fornic, D. Pasini, *New J. Chem.*, **2013**, *37*, 2792–2799. b) E. Hrishikesan, P. Kannan, Inorg. *Chem. Commun.*, **2013**, *37*, 21–25. c) E.M. Lee, S.Y. Gwon, S.H. Kim, *Spectrochim. Acta Part A*, **2014**, *120*, 646–649.

More precisely, the increased conjugation/electron density in the sensor molecule results in the red shift of the absorption band and decreased conjugation/electron density results in blue shift with relevant changes in the colour enabling chromogenic detection.[58] Optical modulations are generally observed in organic solvents or organic solvents-aqueous solution mixtures. One of the most remarkable drawbacks to this approach, especially for anion recognition is that, the interaction of the analyte with the binding sites usually relies on relatively weak interactions.[59]

1.2.2.2 Fluorogenic sensors.

The use of fluorescent molecules as signaling subunits for the design and development of molecular sensors is a field that has been investigated extensively. In fluorogenic sensors binding of the analyte often alters the fluorescence features of the signaling unit. Fluorescent sensors based on a variety of platforms have been developed for a number of metal ions.[60] Taking into account the relevance of the fluorogenic sensors, the most common photophysical mechanisms, which promote fluorescence changes upon analyte binding, are described below.

[58] a) P. V. S. Ajay, J. Printo, D. S. Kiruba, L. Susithra, K. Takatoshi, M. Sivakumar, *Mater Sci Eng C Mater Biol Appl.*, **2017**, *78*, 1231-1245. b) I. Noorhayati, C. Daping, *ACS Sens.*, **2018**, *3*, 1756-1764.

[59] a) G. D. Smith, I. L. Topolnicki, V. E. Zwicker, K. A. Jolliffe, N. J. Elizabeth, *Analyst*, **2017**, *142*, 3549-3563. b) P. Alreja, K. Navneet, *RSC Adv.*, **2016**, *6*, 23169-23217. c) A. Ghosh, J. D. Amilan, R. Kaushik*, Sens. Actuators, B*, **2016**, *229*, 545-560.

[60] a) H. Ziyang, Z. Rongfeng, C. R. Peng, *Curr Opin Chem Biol.*, **2018**, *43*, 87-96. b) J. L. Kolanowski, L. Fei, J. N. Elizabeth, *Chem. Soc. Rev.*, **2018**, *47*, 195-208.

1.2.2.2.1 Excited state intramolecular proton transfer (ESIPT).

Grotthuss mechanism, which is also known as proton jumping mechanism, can be used to modulate the optical signal in some chromo-fluorgenic chemosensors. In this process the photoexcited molecules relax their energy through tautomerization by transfer of protons. The tautomerization often takes the form of keto-enol tautomerism (Figure 1.19).[61]

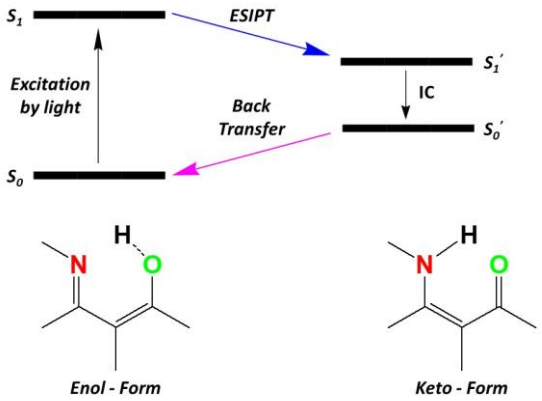

Figure 1.19. Schematic representation of the excited-state intramolecular proton transfer (ESIPT) process.

1.2.2.2.2 Photo-induced electron transfer (PET)

In a PET mechanism, the excitation of a fluorophore by light induces an electron transfer from HOMO to LUMO that results in an excited state of the fluorophore. This new state of higher energy content can be a strong reducing or oxidizing system. In this context when another species able to donate or to accept an electron interacts with the excited fluorophore a deactivation by a redox reaction occurs and the emision is quenched. Coordination of target analytes with

[61] M. Y. Berezin, S. Achilefu, *Chem. Rev.*, **2010**, *110*, 2641–2684.

the binding site can change this procces resulting in a modulation in the emission that is used as optical output (Figure 1.20).[62]

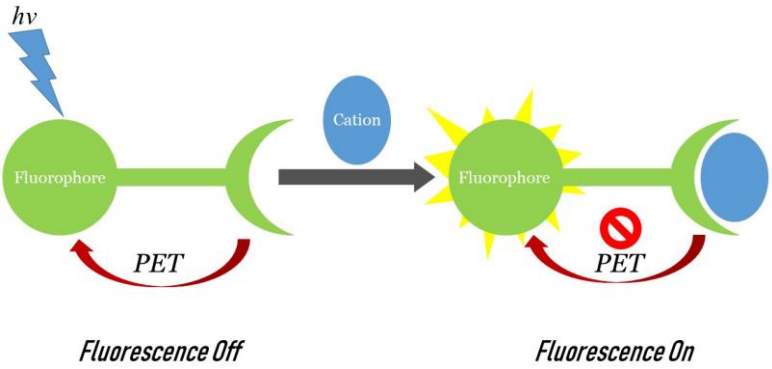

Figure 1.20. Schematic representation of a photoinduced electron transfer process (PET) in a fluorgenic sensor.

1.2.2.2.3 Fluorescence resonance energy transfer (FRET).

In FRET chemosensor design, normally two fluorophores are joined by a flexible binding-site spacer. The presence of an external target analyte forces the two fluorophores to move close (turn-on FRET) or far (turn-off FRET) each other. A donor fluorophore, initially in its electronic excited state, may transfer energy to an acceptor fluorophore through nonradiative dipole–dipole coupling.[63] When the FRET is turn-on the excitation of a fluorophore is transferred to the second fluorophore and the emission of the latter is shown. On the other hand, in turn-off FRET, the emission from the electronic excited state of the former is detected.

[62] a) Q. Zhao, F.Y. Li, C.H. Huang, *Chem. Soc. Rev.*, **2010**, *39*, 3007–3030. b) Y.J. Na, W.Y. Choi, G.R. You, C. Kim, *Sens. Actuators B*, **2016**, *223*, 234–240. c) T. Gunnlaugsson, H.D.P. Ali, M. Glynn, P.E. Kruger, G.M. Hussey, F.M. Pfeffer, C.M.D. dos Santos, J. Tierney, *J. Fluoresc.*, **2005**, *15*, 287–299.

[63] a) Z.-X. Han, X.-B. Zhang, Z. Li, Y.-J. Gong, X.-Y. Wu, Z. Jin, C.-M. He, L.-X. Jian, J. Zhang, G.-L. Shen, R. Q. Yu, *Anal. Chem.*, **2010**, *82*, 3108–3113. b) C.Y. Li, Y. Zhou, Y.F. Li, C.X. Zou, X.F. Kong, *Sens. Actuators B*, **2013**, *186*, 360 – 366.

The efficiency of this energy transfer is inversely proportional to the sixth power of the distance between donor and acceptor, making FRET extremely sensitive to small changes in distance (Figure 1.21).

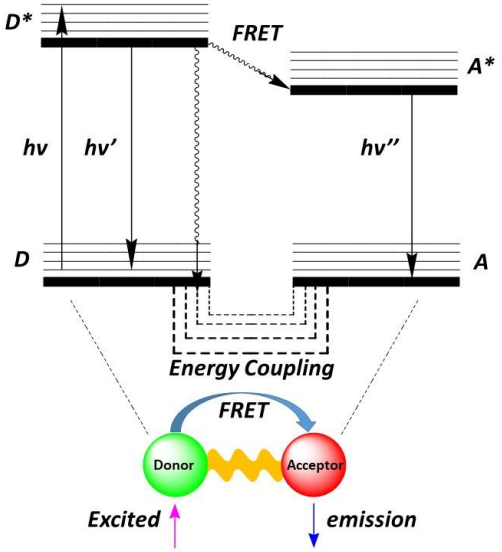

Figure 1.21. Schematic representation of the energy transfer process based on FRET.

1.2.2.2.4 Excimer – exciplex formation (EF).

As in FRET, the EF process is a distance-dependent interaction between the excited state and the ground state of two fluorophores. In chemosensor designing by EF, the distance between both fluorophores is modulated by complexation with chemical species, which can favor or hinder excimer/exciplex formation (Figure 1.22). In addition, the ratio between the emission intensity of the monomer and the excimer can be used to quantitative measures. In this case, "ratiometric sensors" can be developed.[64]

[64] Y. Zhang, Y. Fang, N.Z. Xu, M.Q. Zhang, G.Z. Wu, C. Yao, *Chin. Chem. Lett.*, **2016**, *27*, 1673–1678.

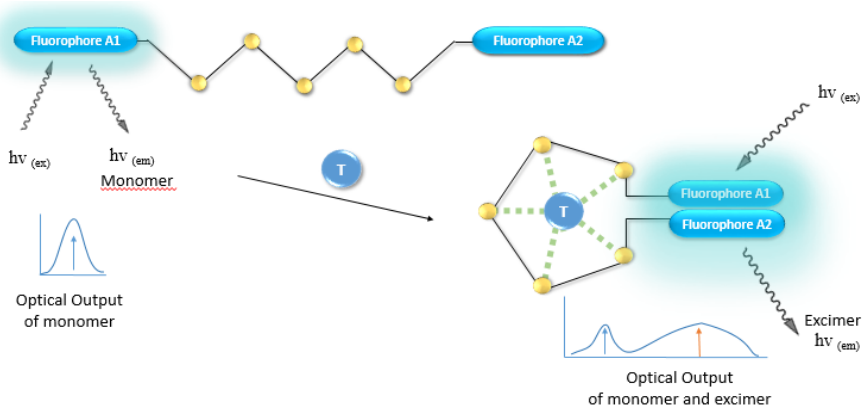

Figure 1.22. Schematic representation or excimer or exciplex formation

Chapter 2: Objectives

2. Objectives

The main objective of this Ph D thesis is the synthesis and characterization of a new family of optical chemosensors, in which the binding sites are included into the structre of the signalling unit, for the chromo-fluorogenic recognition of metal cations and biomolecules (ca. amino acids).

The specific objectives are:

- To develop a family of optical chemosensors containing imidazole heterocycle and other electron donor or electron acceptor rings in their structure.

- To test the chromo-fluorogenic response of the imidazole-containing chemosensors in the presence of metal cations and biomolecules.

- To develop a family of optical chemosensors containing *N*,*N*-diphenylanilino units and different aromatic rings (benzene and thiophene) in their structure.

- To test the chromo-fluorogenic response of the *N*,*N*-diphenylanilino-containing chemosensors in the presence of metal cations and biomolecules.

Chapter 3.

4-(4,5-Diphenyl-1H-imidazole-2-yl)-N,N-dimethylaniline-Cu(II) complex, a highly selective probe for glutathione sensing in water-acetonitrile mixtures

*4-(4,5-Diphenyl-1*H*-imidazole-2-yl)*-N,N-*dimethylaniline-Cu(II) complex, a highly selective probe for glutathione sensing in water-acetonitrile mixtures*

Hazem Essam Okda,[a,b,c] Sameh El Sayed,[a,b,c] Rosa C.M. Ferreira,[d] Susana P.G. Costa,[d] M. Manuela M. Raposo,[d] Ramón Martínez-Máñez,[a,b,c]* and Félix Sancenón,[a,b,c]*

[a] *Instituto Interuniversitario de Investigación de Reconocimiento Molecular y Desarrollo Tecnológico (IDM), Universitat Politècnica de València, Universitat de València, Spain.*

[b] *Departamento de Química, Universitat Politècnica de València, Camino de Vera s/n, 46022, València, Spain.*

[c] *CIBER de Bioingeniería, Biomateriales y Nanomedicina (CIBER-BBN), Spain.*

[d] *Centro de Química, Universidade do Minho, Campus de Gualtar, 4710-057, Braga, Portugal.*

Received: April 26, 2018
Published online: May 30, 2018

Dyes and Pigments, **2018**, 159, 45–48

3.1 Abstract

The imidazole derivative 4-(4,5-diphenyl-1*H*-imidazol-2-yl)-*N,N*-dimethylaniline (probe **1**) formed a highly coloured and non-emissive 1:1 stoichiometry complex with Cu(II) in water-acetonitrile 1:1 (v/v) solutions. Among all the amino acids (Lys, Val, Gln, Leu, His, Thr, Trp, Gly, Phe, Arg, Ile, Met, Ser, Ala, Pro, Tyr, Gly, Asn, Asp, Glu, Cys and Hcy) and tripeptides (GSH) tested, only GSH induced the bleaching of the **1**·Cu(II) solution together with a marked emission enhancement at 411 nm (excitation at 320 nm). These chromo-fluorogenic changes were ascribed to a selective GSH-induced demetallation of the **1**·Cu(II) complex that resulted in a recovery of the spectroscopic features of probe **1**. In addition to the remarkable selectivity of **1**·Cu(II) complex toward GSH a competitive limit of detection as low as 2 μM was determined using fluorescence measurements.

3.2 Introduction

Biothiols, such as glutathione (GSH), cysteine (Cys), and homocysteine (Hcy), are biomolecules containing thiol groups.[1] Cys and Hcy are components of many peptides that have a wide range of cellular biological functions. Besides, the three biothiols play important roles in the body's biochemical defence system because they are involved in reversible redox homeostasis processes which maintain the equilibrium of reduced free thiol and oxidized disulphide forms.[2] As the most abundant reductive biothiol (with concentrations in the millimolar range in living systems), GSH mediates many cellular functions such as maintenance of intracellular redox activities, xenobiotic metabolism, intracellular signal transduction and gene regulation.[3] Moreover, abnormal levels of biothiols affect the normal physiological and pathological functions and are related with a number of diseases such as cancer, AIDS, liver damage, Alzheimer, osteoporosis, inflammatory bowel diseases and cardiovascular diseases.[4-9]

In this context, several studies have been devoted to the development of efficient methods for the detection of the concentration of GSH in physiological media. Several strategies such as mass spectrometry,[10] high-performance liquid chromatography,[11,12] enzymatic methods,[13] electrochemical assays,[14] surface-enhanced Raman scattering,[15–17] and combinatorial library-based sensors[18,19] have been described for the detection and quantification of GSH.

However, these methods require expensive equipment, are time-consuming and the selectivity achieved is, in some cases, low. Bearing in mind the above-mentioned facts, the development of probes able to display colour and/or fluorescence changes in water or mixed aqueous solutions in the presence of target bio-relevant thiols is a timely research area.[20] Within different approaches described for the preparation of chromo-fluorogenic sensors of biothiols, the use of displacement processes involving non-emissive fluorophore-Cu(II) complexes has attracted great attention in the last years.[21] In spite of the fact that most of the reported fluorophore-Cu(II) complexes allowed GSH detection in aqueous environments their response is in general unselective and Cys and Hcy also induced emission modulations.[21] Only three recently published examples, based on the use of a coumarin derivative,[22] graphitic carbon nitride,[23] and a displacement assay with an iminophenol-Cu(II) complex,[24] allowed GSH selective detection in the presence of Cys and Hcy in aqueous environments.

Given our interest in the design of optical chemosensors for the detection of anions and cations of biological and environmental significance[25] herein we report the selective chromo-fluorogenic detection of GSH using a complex formed by 4-(4,5-diphenyl-1*H*-imidazol-2-yl)-*N,N*-dimethylaniline (**1** in Scheme 1) and Cu(II). The emission of probe **1** was selectively quenched in the presence of Cu(II) due to the formation of 1:1 stoichiometry complex. In the presence of GSH the emission of probe **1** was fully restored due to a demetallation reaction.

3.3 Experimental section

- ***Chemicals***

Commercially available reagents 4-(dimethylamino)benzaldehyde (**1a**), 1,2-diphenylethane-1,2-dione (**1b**), and ammonium acetate were purchased from Sigma-Aldrich and Acros and used as received. TLC analyses were carried out on 0.25 mm thick pre-coated silica plates (Merck Fertigplatten Kieselgel $60F_{254}$) and spots were visualized under UV light. Chromatography on silica gel was carried out on Merck Kieselgel (230–240 mesh).

- ***Materials and methods***

All melting points were measured on a Stuart SMP3 melting point apparatus. IR spectra were determined on a BOMEM MB 104 spectrophotometer using KBr discs. NMR spectra were obtained on a Bruker Avance III 400 at an operating frequency of 400 MHz for ^{1}H and 100.6 MHz for ^{13}C using the solvent peak as internal reference at 25 ^{o}C. All chemical shifts are given in ppm using δH Me_4Si=0 ppm as reference. Assignments were supported by spin decoupling-double resonance and bi-dimensional heteronuclear correlation techniques. UV/visible titration profiles were carried out with JASCO V-650 spectrophotometer (Easton, MD, USA). Fluorescence measurements were recorded with a JASCO FP-8500 spectrophotometer.

- ***Synthesis of probe 1***

4-(Dimethylamino) benzaldehyde (**1a**) (0.15 g, 1 mmol), 1,2-diphenylethane-1,2-dione (**1b**) (0.33 g, 1 mmol) and NH_4OAc (1.54 g, 20 mmol) were dissolved in glacial acetic acid (5 mL), followed by stirring and heating at reflux for 8 h. The reaction mixture was cooled to room temperature, ethyl acetate was added (15 mL) and the mixture was washed with water (3 × 10 mL). After, the organic phase

was dried with anhydrous $MgSO_4$, the solution was filtered and the solvent was evaporated to dryness. The resulting crude product was purified by column chromatography (silica gel, DCM/MeOH (100:01)) and was obtained as yellow oil (11 mg, 10%).

^{1}H NMR (400 MHz, DMSO-d_6): δ = 3.04 (s, 6H, NMe_2), 6.84 (dd, J = 6.8 and 2.0 Hz, 2H, H2 and H6 aniline), 7.27–7.32 (m, 2H, 2 × H4 Ph), 7.34–7.39 (m, 4H, 2 × H2 and H6 Ph), 7.61 (d, J = 8.4 Hz, 4H, 2 × H3 and H5 Ph), 8.03 (dd, J = 6.8 and 2.0 Hz, 2H, H3 and H5 aniline) ppm.

^{13}C NMR (100.6 MHz, DMSO-d_6): δ = 40.36, 112.83, 119.39, 127.31, 127.70, 128.00, 128.20, 128.70, 129.10, 134.62, 147.71, 151.70 ppm.

IR (liquid film): ν = 3420, 2926, 2856, 1692, 1646, 1615, 1549, 1509, 1495, 1446, 1405, 1363, 1250, 1202, 1172, 1124, 1071, 1026, 1002, 966, 945, 822, 766, 696 cm^{-1}.

3.4 Results and disscusion

The synthesis of 4-(4,5-diphenyl-1*H*-imidazol-2-yl)-*N,N*-dimethylaniline (probe **1**) was published elsewhere (using different catalysts such as oxalic acid, $SnCl_4$ - SiO_2, H_3BO_3-ultrasounds).[26] In this study we used a one-step Radziszewski reaction between 4-dimethylamino benzaldehyde (**1a**) and 1,2-diphenylethane-1,2-dione (**1b**) in the presence of ammonium acetate in acidic media which directly yielded probe **1** in 10 % yield (or in 88 % yield in ethanol in presence of I_2) (see Scheme 1).

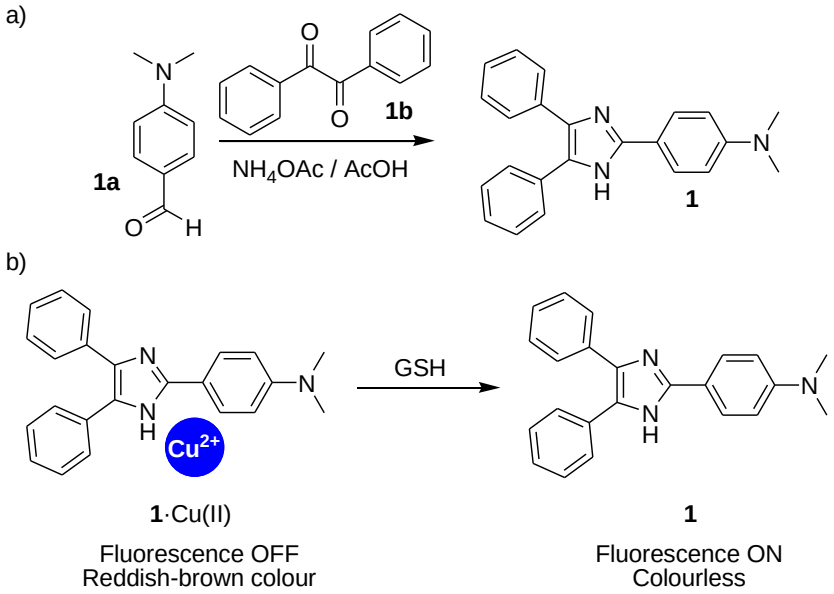

Scheme 1. (a) Synthesis of probe **1** and (b) GSH recognition mechanism using **1**·Cu(II) complex.

Probe **1** was not fully water soluble and, for this reason, we carried out the spectroscopic characterization in water-acetonitrile mixtures. In this respect, water (pH 7.4)-acetonitrile 1:1 (v/v) solutions of probe **1** (5.0×10^{-5} mol L^{-1}) presented an absorption band, of charge-transfer nature (due to the presence of a donor *N,N*-dimethylaniline moiety and an electron-deficient imidazole heterocycle as acceptor group), centred at ca. 320 nm. In a first step, UV–visible changes of probe **1** solutions were studied in the presence of 10 eq. of selected metal cations (i.e. Cu (II), Pb(II), Mg(II), Ge(II), Ca(II), Zn(II), Co(II), Ni(II), Ba(II), Cd(II), Hg (II), Fe(III), In(III), As(III), Al(III), Cr(III), Ga(III), K(I), Li(I) and Na(I)). The obtained results are shown in Fig. 1.

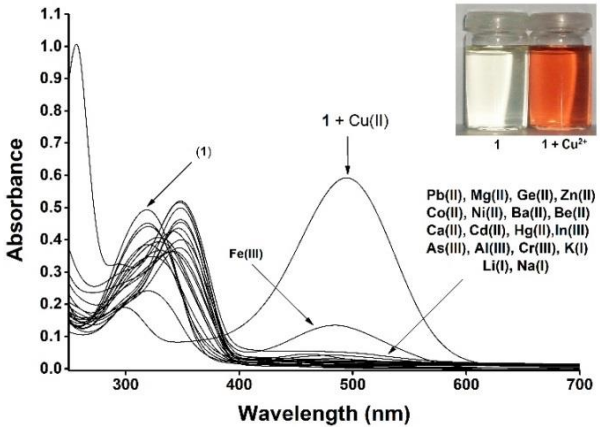

Figure 1. UV-visible spectra of **1** in water (pH 7.4)-acetonitrile 1:1 (v/v) (5.0×10^{-5} mol L^{-1}) alone and in the presence of 10 eq. of selected metal cations. The inset shows the change in colour of **1** in the presence of Cu(II).

As could be seen, among all cations tested, only Cu(II) was able to induce a remarkable appearance of a new red-shifted band centred at ca. 490 nm. These facts were reflected in a marked colour change from colourless to reddish-brown (Fig. 1). In more detail, addition of increasing quantities of Cu(II) induced a progressive decrease of the band centred at 320 nm with a growth in absorbance at 490 nm (see Supporting Information for the UV–visible titration profile of probe **1** with Cu(II)). The appearance of a red-shifted band upon addition of Cu(II) is tentatively attributed to an interaction of this cation with the acceptor part of the probe **1**, i.e the imidazole ring.

Changes in the UV–visible bands (reflected in marked colour changes) of probe **1** upon addition of Cu(II) were ascribed to the formation of a 1:1 stoichiometry complex as was assessed from the Job's plot shown in Fig. 2. From the UV–visible titration profile a logarithm of the stability constant for the formation of the 1·Cu(II) complex of 5.0 ± 0.1 was determined.

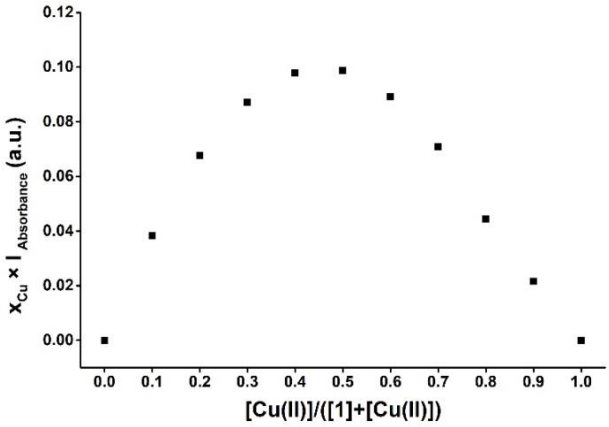

Figure 2. Job's plot of **1** and Cu(II) in water (pH 7.4)-acetonitrile 1:1 (v/v). Total concentration of **1** and Cu(II) of 2.0×10^{-5} mol L^{-1}.

Furthermore, probe **1** was also emissive and, upon excitation of water (pH 7.4)-acetonitrile 1:1 (v/v) solution of the probe at 320 nm, a marked fluorescence at 445 nm appeared (see Fig. 3). The emission behaviour of probe **1** in the presence of selected cations was also tested. As in the UV–visible studies, the unique cation able to induce changes in the emission band of probe **1** was Cu(II).

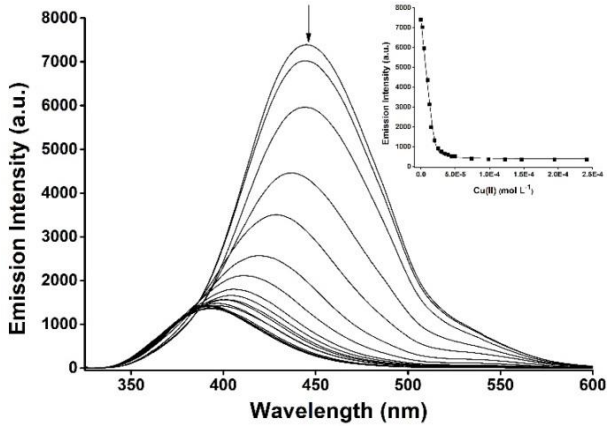

Figure 3. Fluorescence titration profile of **1** in water (pH 7.4)-acetonitrile 1:1 (V/V) (5.0×10^{-5} mol L^{-1}) upon addition of increasing amounts of Cu(II) (from 0 to 10 eq.). Inset: plot of the emission intensity at 445 nm vs Cu(II) concentration.

As could be seen in Fig. 3, addition of increasing amounts of Cu(II) to water (pH 7.4)-acetonitrile 1:1 (v/v) solution of probe **1** induced a progressive quenching of the 445 nm emission together with a moderate blue shift of the band. From the emission titration profile obtained, a limit of detection of 3.2 μM for Cu(II) was determined.

Taking into account the high affinity of Cu(II) toward thiol moieties[27] we envisioned that **1**·Cu(II) complex could be a promising ensemble for fluorescence "off-on" detection of certain biothiols via a Cu(II) displacement approach. For this purpose, water (pH 7.4)-acetonitrile 1:1 (v/v) solution of **1**·Cu(II) complex (6.2 × 10^{-6} mol L^{-1}) were prepared and the UV-absorption behaviour in the presence of GSH (2.0 eq.) and selected amino acids (2.0 eq. of Lys, Val, Gln, Leu, His, Thr, Trp, Gly, Phe, Arg, Ile, Met, Ser, Ala, Pro, Tyr, Gly, Asn, Asp, Glu, Cys and Hcy) was tested. The obtained results are shown in Fig. 4.

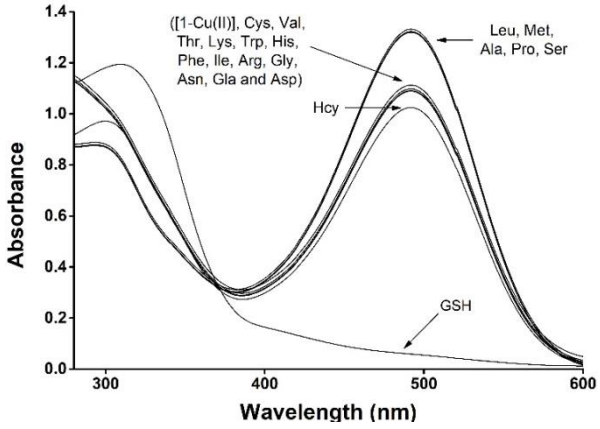

Figure 4. UV–visible changes of water (pH 7.4)-acetonitrile 1:1 (v/v) solution of **1**·Cu(II) complex (6.2 × 10^{-6} mol L^{-1}) in the presence of GSH (2.0 eq.) and selected amino acids (also 2.0 eq.).

As could be seen in Fig. 4, only GSH was able to induce a complete disappearance of the 490 nm band ascribed to the **1**·Cu(II) complex, which was reflected in a marked colour change from reddish-brown to colourless. In contrast, none of the amino acids tested induced remarkable changes in the

visible band. Addition of increasing quantities of GSH induced a progressive decrease of the absorbance at 490 nm (see Supporting Information). From the titration profile, a limit of detection for GSH of 3 μM was determined.

Additionally, the fluorescence response of water (pH 7.4)-acetonitrile 1:1 (v/v) solution of **1**·Cu(II) complex in the presence of GSH and selected amino acids was also tested. Upon excitation at 320 nm, water (pH 7.4) - acetonitrile 1:1 (v/v) solution of **1**·Cu(II) complex presented a weak emission band centred at 404 nm (see Fig. 5). Addition of amino acids induced negligible changes in the emission profile (data not shown) whereas in the presence of increasing quantities of GSH a marked emission enhancement together with a moderate red shift (to 411 nm) was observed (see Fig. 5).

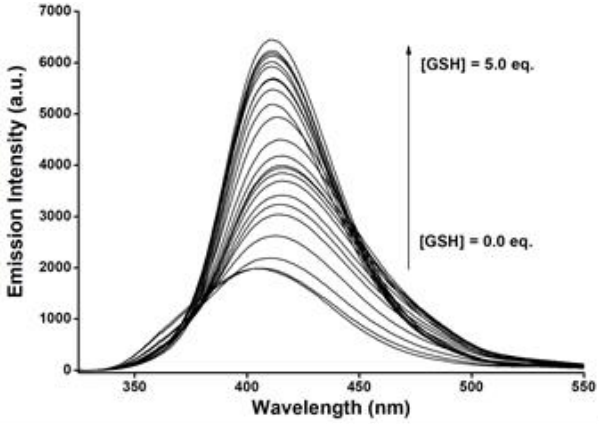

Figure 5. Fluorescence titration profile of **1**·Cu(II) complex in water (pH 7.4) acetonitrile 1:1 (V/V) (6.2×10^{-6} mol L^{-1}) upon addition of increasing amounts of GSH (excitation at 320 nm).

From the emission titration profile, obtained upon addition of increasing quantities of GSH, a limit of detection of 2 μM for GSH was calculated. The obtained limit of detection is similar to that found by Jiang *et al.* using a coumarin-Cu(II) complex (0.36 μM)[22] and by Kim and co-workers using and iminophenol-Cu(II) complex (5.86 μM).[24] However, Yan and co-workers measured a limit of detection of 0.02 μM for GSH using graphitic carbon nitride.[23]

The UV–visible and emission changes obtained when GSH was added to aqueous solutions of **1**·Cu(II) complex pointed to a demetallation process as mechanism of the optical response observed. GSH is able to displace Cu(II) from the **1**·Cu(II) complex restoring the UV–visible and emission spectra of probe **1**. The absence of optical response in the presence of thiol-containing amino acids Cys and Hcy and the remarkable selectivity of the **1**·Cu(II) complex toward GSH could be ascribed to a preferential coordination of the tripeptide with Cu(II). The structure of GSH presented several potential coordinating sites (amino, sulfhydryl and carboxylates) in a flexible backbone and could coordinate Cu(II) more effectively than Cys and Hcy which presented the same functional groups but in a more rigid skeleton.[28] This **1**·Cu(II) demetallation process regenerates the optical features of the free probe.

Besides, the selectivity of **1**·Cu(II) for GSH detection in the presence of other competitive biothiols (such as Cys and Hcy) was also tested (see Supporting Information). For this purpose, the emission intensity of **1**·Cu(II) (at 411 nm upon excitation at 320 nm) alone, in the presence of GSH (2.0 eq.) and with a mixture of GSH + Cys + Hcy (2.0 eq. of each biothiol) was measured. The emission intensity measured in the presence of GSH and with the three biothiols are nearly the same. This fact pointed to a selective response of **1**·Cu(II) toward GSH (this biothiol is the only able to demetallate **1**·Cu(II)) and opens the possible use of this complex for the detection of this tripeptide in real samples.

3.5 Conclusions

In summary, we described herein the use of probe **1** complexed with Cu(II) as selective and sensitive chromo-fluorogenic sensor for GSH. Probe **1** forms a coloured and weakly-emissive complex with Cu(II) in water (pH 7.4)-acetonitrile 1:1 (V/V) solution. Moreover, **1**·Cu(II) complex exhibits unique selectivity and sensitivity for GSH detection in aqueous environments. Addition of GSH to water

(pH 7.4)-acetonitrile 1:1 (V/V) solutions of **1**·Cu(II) complex induced a marked bleaching of the colour and the appearance of an intense emission band. The optical changes where ascribed to a GSH-induced demetallation of **1**·Cu(II) complex which regenerated the free probe. The response to GSH was quite selective because other biothiols tested (Cys and Hcy) were unable to induce any colour or emission changes. Besides, the system presented a competitive limit of detection for GSH (2 μM using emission measurements). Moreover, the **1**·Cu(II) complex is one of the few examples of chromo-fluorogenic probes which selectively detect GSH in the presence of Cys and Hcy in aqueous environments.

3.6 Acknowledgments

We thank the Spanish Government (MAT2015-64139-C4-1-R) and Generalitat Valenciana (PROMETEOII/2014/047). H. E. O. thanks Generalitat Valenciana for his Grisolia fellowship. Thanks are also due to Fundação para a Ciência e Tecnologia (Portugal) for financial support to the Portuguese NMR network (PTNMR, Bruker Avance III 400- Univ. Minho), FCT and FEDEReCOMPETEQREN-EU for financial support to the research centre CQUM (UID/QUI/0686/2016) and a doctoral grant to R.C.M. Ferreira (SFRH/BD/86408/2012). The NMR spectrometers are part of the National NMR Network (PTNMR) and are partially supported by Infrastructure Project No 022161 (co-financed by FEDER through COMPETE 2020, POCI and PORL and FCT through PIDDAC).

3.7 References and Notes

Keywords: Glutathione, Chromo-fluorogenic detection, Cu(II) complex, Displacement assay.

References

1. Z. A. Wood, E. Schroder, J. R. Harris, L. B. Poole, *Trends Biochem Sci*, **2003**, 28, 32–40.

2. S. K. Dey, S. Roy, *Bull Environ Contam Toxicol*, **2010**, 84, 385–9.

3. a) H. Sies, *Free Radic Biol Med*, **1999**, 27, 916–21; b) V. I. Lushchak, *J Amino Acids*, **2012**, 736837.

4. S. K. Biswas, I. Rahman, *Mol. Asp. Med*, **2009**, 30, 60–76.

5. F. H. Jay, Z. Hongqiao, A. Alessandra, *Mol. Asp. Med*, **2009**, 30, 1–12.

6. M. J. William, A. L. Wilson-Delfosse, J. J. Mieyal, *Nutrients*, **2012**, 4, 1399–440.

7. D. M. Townsend, K. D. Tew, H. Tapiero, *Biomed Pharmacother*, **2003**, 57, 145–55.

8. S. A. Hilderbrand, R. Weissleder, *Curr Opin Chem Biol*, **2010**, 14, 71–9.

9. M. L. James, S. S. Gambhir, *Physiol Rev*, **2012**, 92, 897–965.

10. Y. F. Huang, H. T. Chang, *Anal Chem*, **2007**, 79, 4852–9.

11. G. Chwatko, K. Elzbieta, P. Kubalczyk, K. Borowczyk, M. W. Rokiel, R. Glowacki, *Anal. Methods*, **2014**, 6, 8039–44.

12. T. Moore, L. Anthony, A. K. Niemi, T. Kwan, K. Cusmano-Ozog, M. E. Gregory, M. T. Cowan, *J Chromatogr B*, **2013**, 929, 51–5.

13. S. Timur, D. Odaci, A. Dincer, F. Zihnioglu, A. Telefoncu, *Talanta*, **2008**, 74, 1492–7.

14. S. Cavanillas, N. Serrano, J. M. Diaz-Cruz, C. Arino, M. Esteban, *Electroanalysis*, **2014**, 26, 581–7.

15. S. Arindam, J. R. Nikhil, *Anal Chem*, **2013**, 85, 9221–8.

16. M. Lv, H. Gu, X. Yuan, J. Gao, T. Cai, *J Mol Struct*, **2012**, 1029, 75–80.

17. L. Ouyang, L. Zhu, J. Jiang, H. Tang, *Anal Chim Acta*, **2014**, 816, 41–9.

18. A. Buryak, A. Severin, *J. Comb. Chem*, **2006**, 8, 540–3.

19. Y. H. Ahn, J. S. Lee, Y. T. Chang, *J Am Chem Soc*, **2007**, 129, 4510–1.

20. a) Y. Liu, Y. Hu, S. Lee, D. Lee, J. Yoon, *Bull Kor Chem Soc*, **2016**, 37, 1661–78; b) C. X. Yin, K. M. Xiong, F. J. Hu, J. C. Salamanca, R. M. Strongin, *Angew Chem Int Ed*, **2017**, 56, 13188–98; c) H. S. Jung, X. Chen, J. S. Kim, Y. Yoon, *Chem Soc Rev*, **2013**, 42, 6019–31.

21. a) Y. Hu, C. H. Heo, G. Kim, E. J. Jun, J. Yin, H. M. Kim, J. Yoon, *Anal Chem*, **2015**, 87, 3308–13; b) Y. G. Shi, J. H. Yao, Y. L. Duan, Q. L. Mi, J. H. Chen, Q. Q. Xu, G. Z. Gou, Y. Zhou, J. F. Zhang, *Bioorg Med Chem*, **2013**, 23, 2538–42; c) H. S. Jung, J. H. Han, Y. Habata, C. Kang, J. S. Kim, *Chem. Commun*, **2011**, 47, 5142–4; d) Q. H. You, A. W. M. Lee, W. H. Chan, X. M. Zhu, K. C. F. Leung, *Chem. Commun*, **2014**, 50, 6207–10; e) C. C. Zhao, Y. Chen, H. Y. Zhang, B. J. Zhou, X. J. Lv, W. F. Fu, *J. Photochem. Photobiol. A: Chem.*, **2014**, 282, 41–6; f) Z. H. Fu, L. B. Yan, X. Zhang, F. F. Zhu, X. L. Han, J. Fang, Y. W. Wang, Y. Peng, *Org Biomol Chem*, **2017**, 15, 4115–21; g) K. S. Lee, J. Park, H. J. Park, Y. K. Chung, S. B. Park, H. J. Kim, I. S. Shin, J. I. Hong, *Sens. Actuators B Chem.*, **2016**, 237, 256–61.

22. H. Z. Qiang, S. L. Li, G. Y. Ying, Y. Jiang, *Sens. Actuators B Chem.*, **2015**, 212, 220–4.

23. C. Yang, X. Wang, H. Liu, S. Ge, J. Yu, M. Yan, *New J. Chem*, **2017**, 41, 3374–9.

24. G. R. You, H. J. Jang, T. G. Jo, C. Kim, *RSC Adv*, **2016**, 6, 74400–8.

25. See for example: a) S. El Sayed, M. Licchelli, R. Martínez-Máñez, F. Sancenón, *Chem. As. J*, **2017**, 12, 2670–4; b) R. C. M. Ferreira, S. P. G. Costa, H. Gonçalves, M. M. M. Raposo, *New J Chem*,

2017, 41, 12866–78; c) C. Marín-Hernández, L. E. Santos-Figueroa, S. El Sayed, T. Pardo, M. M. M. Raposo, R. M. F. Batista, S. P. G. Costa, F. Sancenón, R. Martínez-Máñez, *Dyes Pigm*, **2015,** 122, 50–8; d) C. Marín-Hernández, L. E. Santos-Figueroa, M. E. Moragues, M. M. M. Raposo, R. M. F. Batista, S. P. G. Costa, T. Pardo, R. Martínez-Máñez, F. Sancenón, *J Org Chem,* **2014**, 79, 10752–61

26. See for example: a) A. Maleki, R. Paydar, *RSC Adv*, **2015**, 5, 33177–84; b) N. D. Kokare, J. N. Sangshetti, D. B. Shinde, *Synthesis*, **2007**, 2829–34; c) K. F. Shelke, S. B. Sapkal, S. S. Sonar, B. R. Madje, B. B. Shingate, M. S. Shingare, *Bull Kor Chem Soc*, **2009**, 30, 1057–60; d) S. Samai, G. C. Nandi, P. Singh, M. S. Singh, *Tetrahedron*, **2009**, 65, 10155–61

27. S. Mandal, G. Das, R. Singh, R. Shukla, P. K. Bharadwaj, *Coord Chem Rev*, **1997,** 160, 191–235.

28. Y. Shi, Y. Pan, H. Zhang, Z. Zhang, M. J. Li, C. Yi, M. Yang, *Biosensors Bioelectron*, **2014,** 56, 39–45.

3.8 Supporting Information

- ***Titration experiments:***

UV/vis and fluorescence titration experiments were carried out with a freshly prepared solution of probe **1** (5.0×10^{-5} mol L^{-1}) dissolved in water (pH 7.4)-acetonitrile 1:1 (v/v) and stored in a dry atmosphere. Moreover, a solution of copper(II) perchlorate hexahydrate salt (7.5×10^{-3} mol L^{-1}) in acetonitrile was also prepared. For the titrations we used a fluorimeter cuvette containing probe **1** (3 mL) and then we added, subsequently, 5-200 µL of the Cu(II) acetonitrile solution. After each addition, the UV-visible and the fluorescence were measured. The same procedure was used for the titration of **1**·Cu(II) with GSH but, in this case the complex (6.2×10^{-6} mol L^{-1}) was prepared in water (pH 7.4)-acetonitrile 1:1 (v/v) and the biothiol was dissolved in water (pH 7.4).

- ***Stability constant determination:***

The apparent binding constant for the formation of the respective complexes were evaluated using the Benesi−Hildebrand (B−H) plot (equation 1) [1-3]:

$$1/(A - A_0) = 1/\{K(A_{max} - A_0)C\} + 1/(A_{max} - A_0) \quad (1)$$

A_0 is the absorbance of **1**·Cu(II) complex at the absorbance maximum (λ = 490 nm), A is the observed absorbance at that particular wavelength in the presence of a certain concentration of Cu(II) (C), A_{max} is the maximum absorbance value that was obtained at λ = 490 nm during titration with varying Cu(II) concentrations, K is the apparent binding constant, which was determined from the slope of the linear plot, and C is the concentration of the Cu(II) added during titration studies.

- ***GSH limit of detection evaluation:***

The limit of detection of GSH using **1**·Cu(II) complex was calculated using the emission titration profiles obtained (see Figure S6) Detection limit was calculated with equation 2:

$$LOD = 3.3\ \sigma/k \quad (2)$$

Where σ is the standard deviation of the blank measurement, and k is the slope between the ratio of UV−vis absorbance versus GSH concentration.

- ***Selectivity assays of 1·Cu(II) complex for GSH in the presence of Cys and Hcy:***

In order to evaluate the selectivity of **1**·Cu(II) complex for GSH, competitive assays in the presence of other biothiols (such as Cys and Hcy) were carried out. For this purpose, the emission intensity at 404 nm (excitation at 320 nm) of a water (pH 7.4)-acetonitrile 1:1 (v/v) solution of **1**·Cu(II) complex was measured alone, in the presence of GSH (2.0 eq.) and in the presence of a mixture of GSH + Cys + Hcy (2.0 eq. of each biothiol). The obtained results are shown in Figure S7. As could be seen, nearly the same emission intensity was observed when **1**·Cu(II) complex was treated with GSH and with the mixture of the three biothiols. These results clearly demonstrated the selectivity of **1**·Cu(II) complex toward GSH because the presence of the other biothiols (Cys and Hcy) did not induce any emission enhancement.

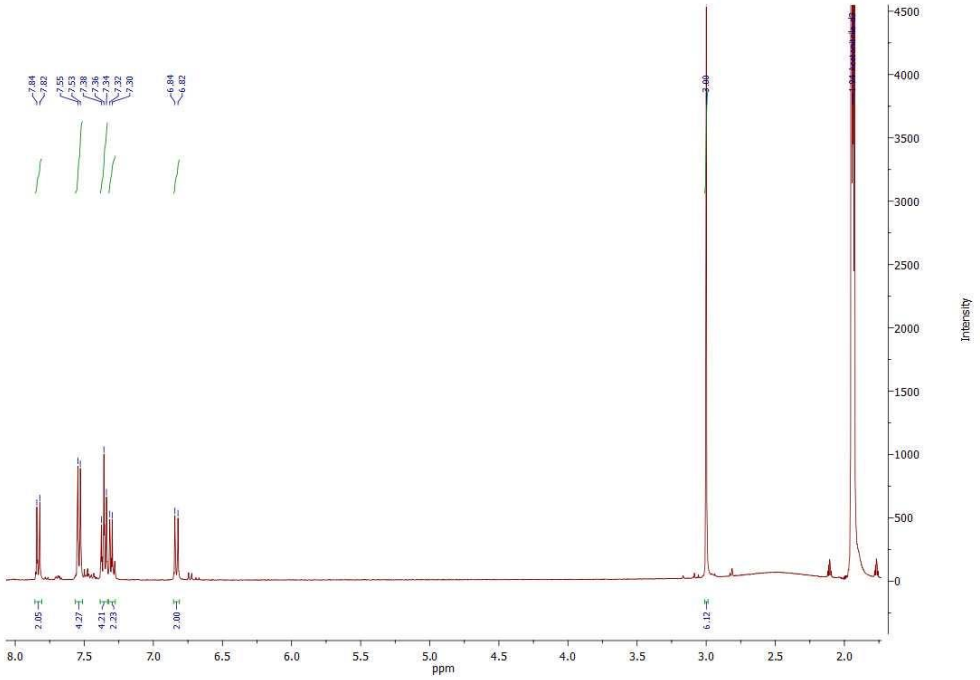

Figure S1. ^{1}H NMR spectra of probe **1** in DMSO-d_6.

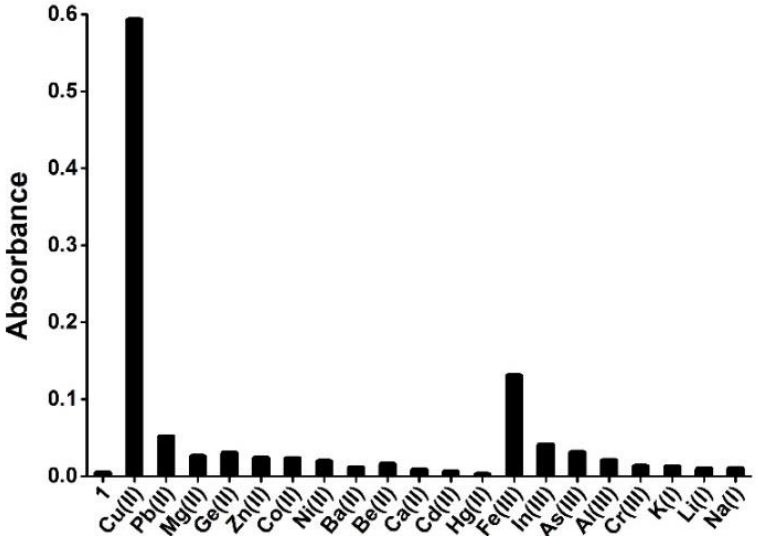

Figure S2. Absorbance at 489 nm of water (pH 7.4)-acetonitrile 1:1 (v/v) (5.0 x 10^{-5} mol L^{-1}) solutions of **1** alone and in the presence of selected metal cations (10 eq.).

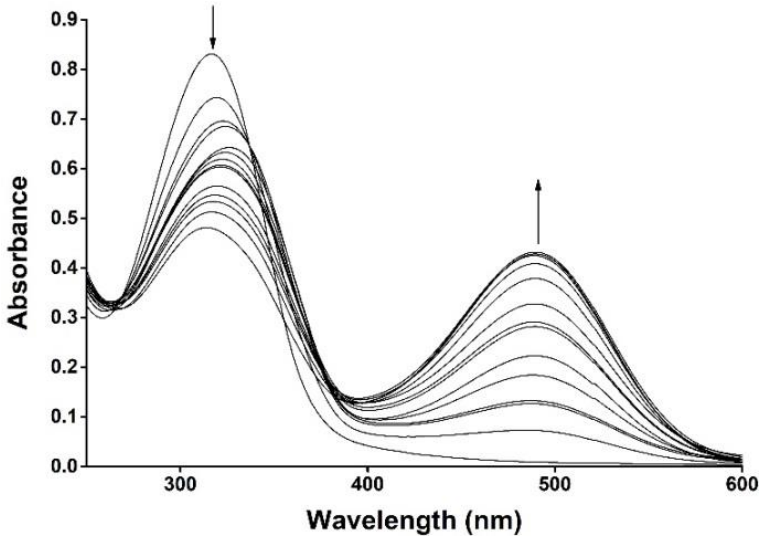

Figure S3. UV-visible titration profile of **1** in water (pH 7.4)-acetonitrile 1:1 (v/v) (5.0 x 10^{-5} mol L^{-1}) upon addition of increasing amounts of Cu(II) (from 0 to 10 eq.).

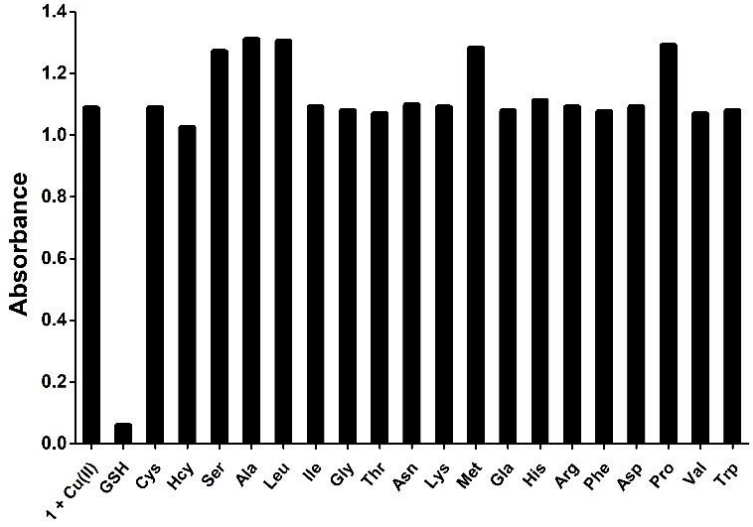

Figure S4. Absorbance at 489 nm of water (pH 7.4)-acetonitrile 1:1 (v/v) solutions of **1**·Cu(II) complex in the presence of GSH (2.0 eq.) and selected amino acids (2.0 eq.).

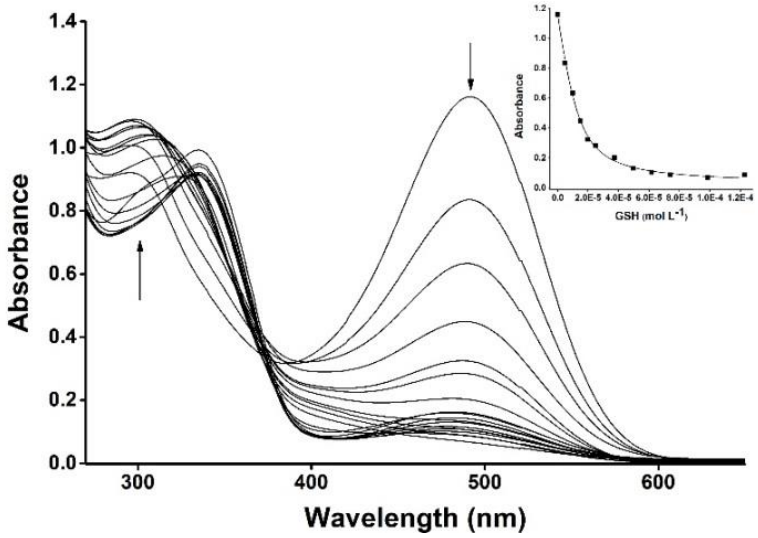

Figure S5. UV/Vis. titration profile of **1**·Cu(II) complex (6.2 x 10^{-6} mol L^{-1}) in water (pH 7.4)-acetonitrile 1:1 (v/v) upon addition of GSH (0-2.0 equivalents). Inset: plot of absorbance at 489 nm vs GSH concentration.

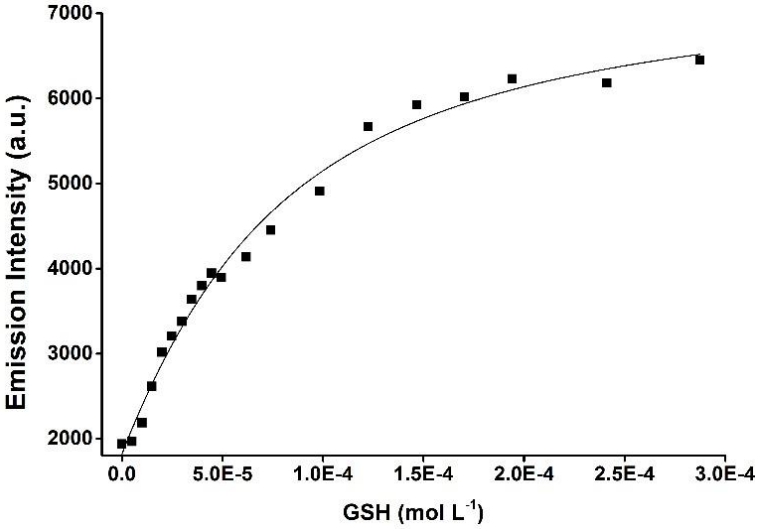

Figure S6. Emission intensity at 411 nm (excitation at 320 nm) of water (pH 7.4)-acetonitrile 1:1 v/v solutions of **1**·Cu(II) (5.0 x 10^{-5} mol L^{-1}) upon addition of increasing quantities GSH.

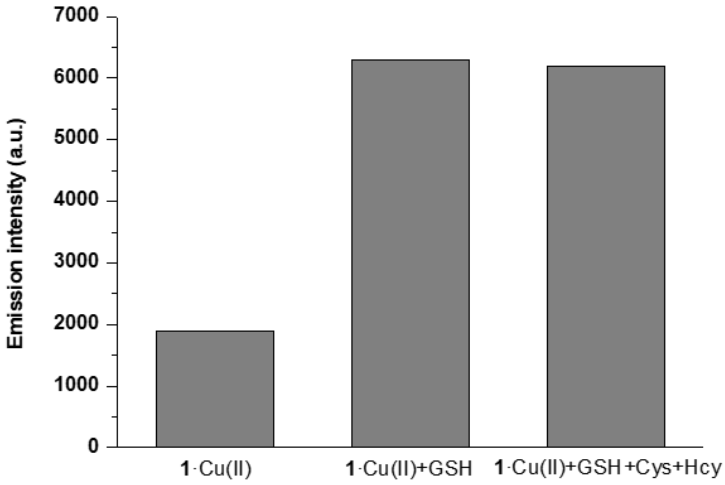

Figure S7. Emission intensity at 411 nm (excitation at 320 nm) of water (pH 7.4)-acetonitrile 1:1 v/v solutions of **1**·Cu(II) (5.0 x 10^{-5} mol L^{-1}) alone and in the presence of GSH (2.0 eq.) and a mixture of GSH+Cys+Hcy (2.0 eq. of each biothiol).

Table S1. Experimental features of the analytical methods used for GSH detection.

Method	Limit of detection (μM)	Interferences	Time (min)	Reference
Displacement assay of a Cu(II) complex	2	-	5	This paper
Gold nanoparticles assisted laser desorption/ionization mass spectrometry	Not reported	Not reported	Not reported	Anal. Chem. 2007; 79: 4852
HPLC with UV detection	5	-	10	Anal. Methods 2014; 6: 8039
HPLC-mass spectrometry	0.4	-	5	J. Chromatogr. B 2013; 929: 51
Chitosan membrane with glutathione reductase and	200	-	5	Talanta 2008; 74: 1492

sulfhydryl oxidase integrated onto the surface of graphite rods				
Voltammetric electronic tongue	3	Cys, Hcy	Not reported	Electroanalysis 2014; 26: 581
Surface enhanced Raman scattering	Not reported	-	60	Anal. Chem. 2013; 85: 9221
Surface enhanced Raman scattering	Not reported	Not reported	Not reported	J. Mol. Struct. 2012; 1029: 75
Surface enhanced Raman scattering	0.04	-	Not reported	Anal. Chim. Acta 2014; 816: 41
Dynamic combinatorial libraries of Cu(II) and Ni(II) complexes	Not reported	Not reported	Not reported	J. Comb. Chem. 2006; 8: 540
Dynamic combinatorial libraries of fluorophores	Not reported	-	30	J. Am. Chem. Soc. 2007; 129: 4510

Chapter 4.

A simple and easy-to-prepare imidazole-based probe for the selective chromo-fluorogenic recognition of biothiols and Cu(II) in aqueous environments

A simple and easy-to-prepare imidazole-based probe for the selective chromo-fluorogenic recognition of biothiols and Cu(II) in aqueous environments

Hazem Essam Okda,[abc] Sameh El Sayed,[abc] Ismael Otri,[abc] Rosa C.M. Ferreira,[d] Susana P.G. Costa,[d] M. Manuela M. Raposo,[d] Ramón Martínez-Máñez[abc]* and Félix Sancenón[abc]*

[a] *Instituto Interuniversitario de Investigación de Reconocimiento Molecular y Desarrollo Tecnológico (IDM), Universitat Politècnica de València, Universitat de València, Spain*

[b] *Departamento de Química, Universitat Politècnica de València, Camino de Vera s/n, 46022, València, Spain*

[c] *CIBER de Bioingeniería, Biomateriales y Nanomedicina (CIBER-BBN), Spain*

[d] *Centro de Química, Universidade do Minho, Campus de Gualtar, 4710-057, Braga,*

Received: May 22, 2018
Published online: October 12, 2018

Dyes and Pigments, **2019**, 162, 303–308

4.1 Abstract

A new simple and easy-to-prepare imidazole-based probe **1** was synthesized and used to detect Cu(II) and biothiols (Cys, Hcy and GSH) in aqueous environments. Addition of increasing amounts of Cu(II) to water (pH 7.4)-acetonitrile 90:10 v/v solutions of probe **1** induced the apperance of a red-shifted absorption together with a marked colour change from colorless to deep blue. In addition, probe **1** was fluorescent and a marked emission quenching in the presence of Cu(II) was observed. The optical response is selective and other cations tested do not induce significant chromo-fluorogenic modulations. Limits of detection for Cu(II) of 0.7 and 3.2 μM using UV–visible and fluorescence data were determined. On the other hand, addition of Cys, Hcy and GSH to the deep-blue water (pH 7.4)-acetonitrile 90:10 v/v solutions of the **1**-Cu(II) complex resulted in a marked bleaching together with the appearance of a highly emissive band centred at 475 nm. Other amino acids tested induced negligible response. The limits of detection for Cys, Hcy and GSH using **1**-Cu(II) and emission data are 6.5, 5.0 and 10.2 μM, respectively. These optical changes were ascribed to a biothiol-induced demetallation process of the **1**-Cu(II) complex that released the free probe. Besides, probe **1** is non-toxic and can be used for Cu(II) detection in HeLa cells.

4.2 Introduction

Transition metal cations are involved in several vital processes and are also used as diagnostic tools in medical, physiological and environmental fields.[1–3] In this scenario, the development of techniques for monitoring transition metal cations is an active area of research. Among transition metal cations, Cu(II) is the third most abundant essential element in the human body and plays vital roles in several physiological processes.[4–9] For instance, it has been reported that Cu(II) stimulates the proliferation of endothelial cells and is necessary for the secretion

of several angiogenic factors by tumour cells.[10,11] Aside from its biological and environmental importance, copper is widely used in metallurgical, pharmaceutical and agrochemical industries.[12] As a result of the extensive applications of Cu(II) in life science and industry, it has become one of the first hazard environmental pollutants.[13] Despite the important role played by Cu(II) in several biological processes, abnormal levels of this cation can cause serious health problems on humans due to its ability to displace other vital metal ions in some enzyme-catalysed reactions.[14] In addition, high concentrations of Cu(II) in cells was documented to cause toxicity and different neurodegenerative diseases such as Menkes, Wilson's and Alzheimer.[15] Therefore, simple and rapid sensing tools to monitor Cu(II) levels in biological and environmental media is of importance.

In the past years, electrochemical methods, spectrometry and chromatography have been employed to detect Cu(II). However, these methods are limited by their relatively high costs, are time consuming and are not usually suitable for in situ and on site analysis. As an alternative to these classical methods, the use of chemical optical probes has attracted great attention in the last years and several Cu(II) sensors have been reported.[16] Some of these probes are able to detect Cu(II) both in solution (by colour and/or emission changes) and in living cells (by using confocal microscopy).[17–21] In spite of these interesting features, some of these probes operate in organic solvents and often presented poor selectivity.[22,23] Thus, the preparation of selective probes that can detect Cu(II) in water or water/organic solvents mixtures is still a matter of interest.

On the other hand, biothiols (GSH, Cys and Hcy) are molecules that play fundamental roles in living systems because are involved in many important biological processes (such as tissue growth and defences).[24,25] Dysregulation of biothiol levels could induce the appearance of certain diseases such as Alzheimer and cardiovascular disorders.[26,27] For the above mentioned reasons, the sensitive and selective detection of biothiols has been a matter of concern. In this respect, in the last years, several probes for the chromo-fluorogenic detection of biothiols

have been published.[28–31] Most of the published examples are designed following the chemodosimeter paradigm, which makes use of the high nucleophilic reactivity of the thiol group. For example, biothiols reaction with fluorophores containing aldehyde,[32–34] and 4-methoxythiophenol moieties[35,36] have been recently reported. Besides, hydrolysis reactions induced by biothiols coupled with emission changes are also used.[37,38] However, among different approaches used for the design of biothiol chemosensors the use of Cu(II) complexes is perhaps one of the most promising. These probes worked using the well-known indicator displacement assay (IDA) paradigm.[39,40] These IDA assays are based on the use of fluorescent probes that coordinate selectively with Cu(II) (a highly effective quencher). As a consequence a non-emissive complex is formed. In the presence of biothiols, the non-emissive complex is demetallated (due to the preferential binding of Cu(II) with the thiol moieties in the biothiols) restoring the fluorescence of the free fluorophore. Using this IDA approach several systems for biothiols detection have been recently published.[41–46]

Bearing in mind our experience in the development of molecular probes for detection of anions, cations and neutral molecules of biological and environmental significance,[47–52] we report herein the synthesis and sensing behaviour of a new imidazole-based easy-to-prepare chromo-fluorogenic probe **1** able to detect Cu(II) in water (pH 7.4)-acetonitrile 90:10 v/v mixtures. Besides, the complex formed between probe **1** and Cu(II) was used for the selective chromo-fluorogenic detection of relevant biothiols (Cys, Hcy and GSH). Probe **1** was also successfully used for detection of Cu(II) in living cells.

4.3 Experimental section

- ***Chemicals:***

Commercially available reagents 4-(dimethylamino) benzaldehyde (**1a**), 1,2-di(thiophen-2-yl)ethane-1,2-dione (**1b**), ammonium acetate, $Na_2S_2O_3$, and I_2 were

purchased from Sigma-Aldrich and Acros and used as received. TLC analyses were carried out on 0.25 mm thick precoated silica plates (Merck Fertigplatten Kieselgel $60F_{254}$) and spots were visualized under UV light. Chromatography on silica gel was carried out on Merck Kieselgel (230–240 mesh). All the metal salts used for the UV–visible and fluorescence experiments are nitrates.

- ***Materials and methods:***

All melting points were measured on a Stuart SMP3 melting point apparatus. IR spectra were determined on a BOMEM MB 104 spectrophotometer using KBr discs. NMR spectra were obtained on a Bruker Avance III 400 at an operating frequency of 400 MHz for ^{1}H and 100.6 MHz for ^{13}C using the solvent peak as internal reference at 25 °C. All chemical shifts are given in ppm using δH Me_4Si=0 ppm as reference. Assignments were supported by spin decoupling-double resonance and bi-dimensional heteronuclear correlation techniques. High resolution mass spectrometry (HRMS) data were obtained with a TRIPLETOF T5600 (ABSciex, USA) spectrometer. UV/visible titration profiles were carried out with JASCO V-650 spectrophotometer (Easton, MD, USA). Fluorescence measurements were recorded with a JASCO FP-8500 spectrophotometer.

- ***Synthesis of probe 1 (method A):***

4-(Dimethylamino) benzaldehyde (**1a**, 0.15 g, 1 mmol), 1,2-di(thiophen-2-yl)ethane-1,2-dione (**1b**, 0.2 g, 1 mmol) and NH_4OAc (20 mmol) were dissolved in glacial acetic acid (5 mL), followed by stirring and heating at reflux for 8 h. Then, the reaction mixture was cooled to room temperature, ethyl acetate (15 mL) was added and the mixture was washed with water (3 × 10 mL). After, the organic phase was dried with anhydrous $MgSO_4$, filtered and the solvent was evaporated under reduced pressure. The resulting crude product was purified by column chromatography (silica gel, CH_2Cl_2/MeOH 100:1), given the pure product as a pink solid: yield (70 mg, 59%). ^{1}H NMR (400 MHz, DMSO-d_6): δ = 2.96 (s, 6H, NMe_2), 6.77 (dd, J=7.2 and 2.4 Hz, 2H, H3 and H5), 6.99 (dd, J=5.2 and 3.6 Hz, 1H), 7.13

(dd, J=3.6 and 1.2 Hz, 1H), 7.19 (dd, J=5.2 and 3.6 Hz, 1H), 7.36–7.39 (m, 2H), 7.65 (dd, J=5.2 and 1.2 Hz, 1H), 7.84 (dd, J=7.2 and 2.0 Hz, 2H, H2 and H6), 12.46 (s, 1H, NH) ppm. ^{13}C NMR (100.6 MHz, DMSO-d_6): δ = 40.12 (NMe_2), 111.86 (C3 and C5), 117.51 (C1), 119.51, 123.08, 124.52 (C2 and C6), 126.40, 126.98, 127.24, 127.51, 128.04, 131.27, 133.01, 137.87, 146.70 (C4), 150.45 ppm. IR (Nujol): ν =2855, 1615, 1510, 1201, 1167, 1116, 1078, 905, 841, 822, 687 cm^{-1}. HRMS-EI m/z: calcd for $C_{19}H_{17}N_3S_2 + H^+$: 352.0942; measured: 352.0936.

- ***Synthesis of probe 1 (method B):***

4-(Dimethylamino) benzaldehyde (**1a**, 0.15 g, 1 mmol), 1,2-di(thiophen-2-yl)ethane-1,2-dione (**1b**, 0.2 g, 1 mmol), NH_4OAc (20 mmol) and I_2 (5 mol %) were dissolved in ethanol (5 mL), followed by stirring and heating at reflux for 27 h. Then, the reaction mixture was diluted with water (15 mL) having a small amount of $Na_2S_2O_3$ and was cooled in an ice bath. The resulting crude product which precipitated was purified by recrystallization from ethanol given the pure compound **1** as a pink solid: yield (100 mg, 84%).

- ***Synthesis of complex 1-Cu(II):***

Probe **1** dissolved in acetonitrile (1.0 mmol) was mixed with $Cu(NO_3)_2$ (1.0 mmol) followed by stirring and heating at reflux for 4 h. Then $[NH_4][PF_6]$ was added and the solid product formed was collected, washed with cold acetonitrile and dried: yield (0.8 mmol, 80%). Elemental analysis, [**1**-Cu(II)]$[PF_6]_2$, Calculated: C, 54.98; H, 4.13; N, 10.12; Cu, 15.31; Found: C, 55.05; H, 4.06; N, 10.17; Cu, 15.25.

4.4 Results and discussion

Probe **1** is not completely water soluble and, for this reason, the spectroscopic behaviour was studied in water (pH 7.4)-acetonitrile 90:10 v/v mixture. In this

respect, water (pH 7.4)-acetonitrile 90:10 v/v solutions of probe **1** (1.0×10^{-5} mol L^{-1}) presented an absorption band centred at ca. 320 nm with a molar extinction coefficient of 28000M^{-1} cm^{-1} (see Fig. 1). Next, UV–visible changes in probe **1** upon addition of 10 eq. of Cu(II), Pb(II), Mg(II), Ge(II), Ca(II), Zn(II), Co(II), Ni(II), Ba(II), Cd(II), Hg(II), Fe(III), In(III), As(III), Al(III), Cr(III), Ga(III), K(I), Li(I) and Na(I) was studied. As could be seen in Fig. 1, among all cations tested, only Cu(II) was able to induce the appearance of a new absorption band centred at 555 nm (ε=32000M^{-1} cm^{-1}). The marked changes in the UV–visible spectrum of probe **1** upon addition of 10 eq. of Cu(II) is reflected in a clear colour modulation from colourless to deep blue (see also Fig. 1).

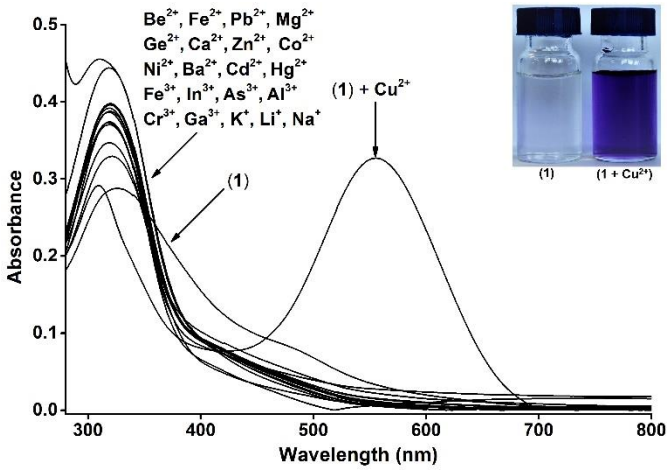

Figure 1. UV–visible spectra of probe **1** in water (pH 7.4)-acetonitrile 90:10 v/v (1.0×10^{-5} mol L^{-1}) alone and in the presence of 10 eq. of selected metal cations. The inset shows the change in colour of probe **1** in the presence of Cu (II).

Having assessed the highly selective response of probe **1** toward Cu(II) we studied, in the next step, the changes in the UV–visible spectra upon addition of increasing amounts of Cu(II). Addition of different amounts of Cu(II) to water (pH 7.4)-acetonitrile 90:10 v/v solutions of **1** (1.0×10^{-5} mol L^{-1}) induced the progressive decrease of the absorption centred at 320 nm together with the growth of the visible band at 555 nm. From the obtained titration profile a limit of

detection of 0.7 μM was determined (see Supporting Information) which is almost 100 times lower than the limit prescribed by the World Health Organization (WHO) guideline for drinking water (30 mM).[53,54]

In order to understand the mode of coordination between probe **1** and Cu(II) Job's plot were determined. As could be seen in Fig. 2, probe **1** clearly forms a 1:1 stoichiometry complex with Cu(II). From the UV–visible titration shown in Fig. 3 a logarithm of the stability constant for the formation of the **1**-Cu(II) complex of 3.50 ± 0.15 was determined.

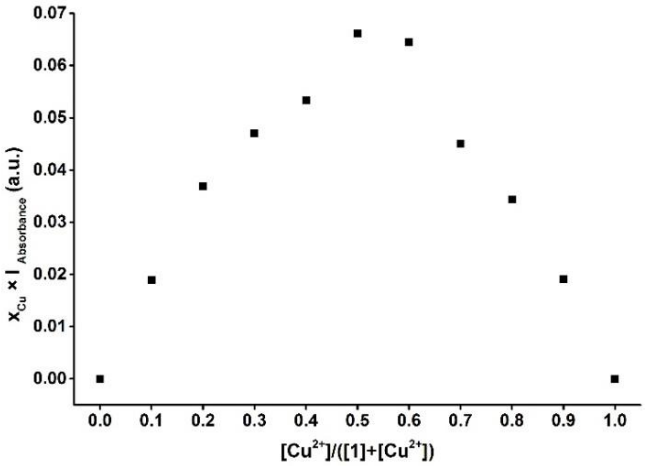

Figure 2. Job's plot of probe **1** and Cu(II) in water (pH 7.4)-acetonitrile 90:10 v/v. Total concentration of **1** and Cu(II) of 2.0×10^{-5} mol L^{-1}.

Probe **1** is also fluorescent. Excitation at 324 nm (one of the isosbestic points observed in the Cu(II) UV–visible titration profile) of water (pH 7.4)-acetonitrile 90:10 v/v solutions of probe **1** (1.0×10^{-5} mol L^{-1}) showed a marked emission band centred at 475 nm (quantum yield of 0.26). Among all cations tested, only Cu(II) induced emission quenching as could be seen in Fig. 3. From the emission titration profile (see Supporting Information) a linear ratio between the emission intensity and the amount of Cu(II) added was observed. Besides, a limit of detection of 3.7 μM of Cu(II) was determined.

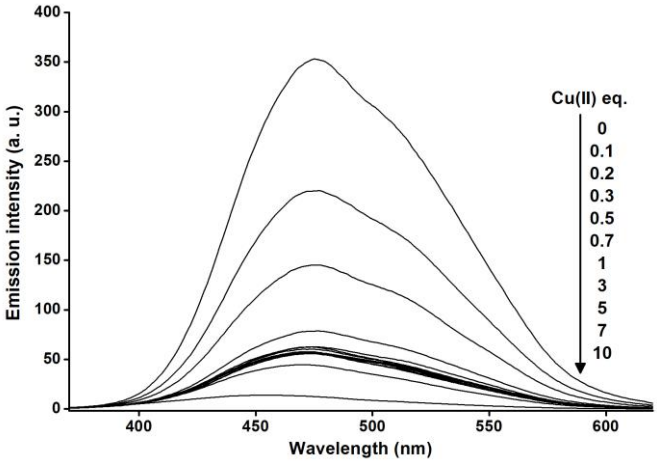

Figure 3. Fluorescence spectra of probe **1** in water (pH 7.4)-acetonitrile 90:10 v/v (1.0×10^{-5} mol L^{-1}) upon addition of increasing amounts of Cu(II) (from 0 to 10 eq.).

On the other hand, the emission of probe **1** in water-acetonitrile 90:10 v/v mixtures at acidic pH (5.0 and 6.0) remained nearly unchanged upon addition of Cu(II) cation (see Supporting Information). The observed emission quenching is remarkable, especially when compared with the results previously published obtained with a structurally related probe **2** (see Scheme 1).

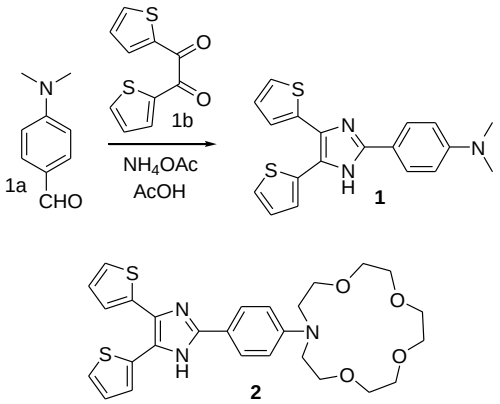

Scheme 1. Synthesis of probe **1** and structure of closely related macrocycle-containing imidazole-derivative **2**.

In this respect, ethanol solutions of macrocycle-containing probe **2** presented a weak emission band that was markedly increased upon addition of Cu(II).[55] The marked emission enhancement observed with **2** was ascribed to an increase in the rigidity of the probe upon formation of 2:1 metal-probe complexes in which one Cu(II) coordinated with the macrocycle and the other with the nitrogen atoms of the imidazole with a logarithm of the stability constant of 11.58 ± 0.01.

In our case, the fluorescence experiments were carried out in a more competitive media (water-acetonitrile 90:10 v/v) and probe **1** lacks the macrocycle binding domain presented in **2**. Taking into account the red shift observed in the UV–visible titration profile of probe **1** with Cu(II), and also the formation of 1:1 complexes, assessed from the Job's plot, we proposed that for **1**, the Cu(II) coordinates with one of the nitrogen atoms of the imidazole heterocycle. The observed quenching of the emission intensity of **1** upon Cu(II) binding is most likely due to an electron or energy transfer process between the probe and the cation.

Taking into account the non-emissive nature of **1**-Cu(II) complex (quantum yield of 0.07) and the high affinity of thiol moieties for Cu(II) we tested the possible use of this complex in an IDA assay for biothiols detection. As stated above, water (pH 7.4)-acetonitrile 90:10 v/v solutions of **1**-Cu(II) complex (6.2×10^{-6} mol L^{-1}) presented a marked deep blue colour due to a remarkable absorption band centred at 555 nm. In a first step, the chromogenic response of **1**-Cu(II) complex was tested in the presence of amino acids (Val, Leu, Thr, Lys, Trp, His, Phe, Ile, Arg, Met, Ala, Pro, Gly, Ser, Cys, Asn, Gln, Tyr, Asp, Glu and Hcy) and relevant biothiols (GSH).

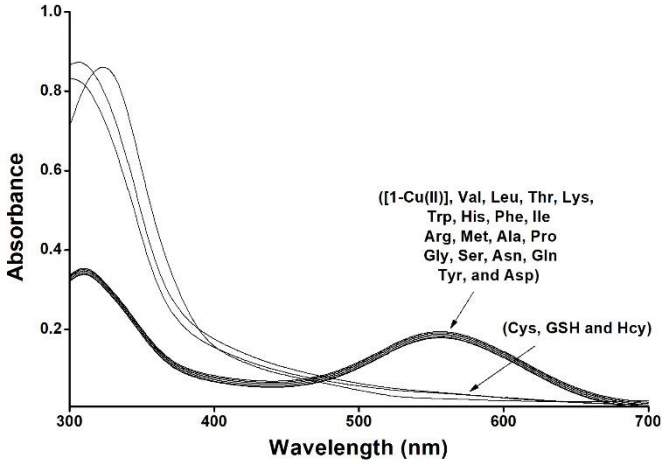

Figure 4. UV–visible changes of **1**-Cu(II) (6.2×10^{-6} mol L^{-1}) in water (pH 7.4) acetonitrile 90:10 v/v in the presence of selected amino acids (0.2 eq.) and biothiols (0.2 eq.).

As could be seen in Fig. 4 only Cys, Hcy and GSH were able to induce the bleaching of the solution of the **1**-Cu(II) complex reflected in the disappearance of the 555 nm band together with the appearance of an absorption centred at 320 nm. Besides, water (pH 7.4)-acetonitrile 90:10 v/v solutions of **1**-Cu(II) complex (6.2×10^{-6} mol L^{-1}) were weakly emissive and only addition of Cys, Hcy and GSH induced an emission enhancement (ca. 2.7-fold) at 475 nm (see Fig. 5).

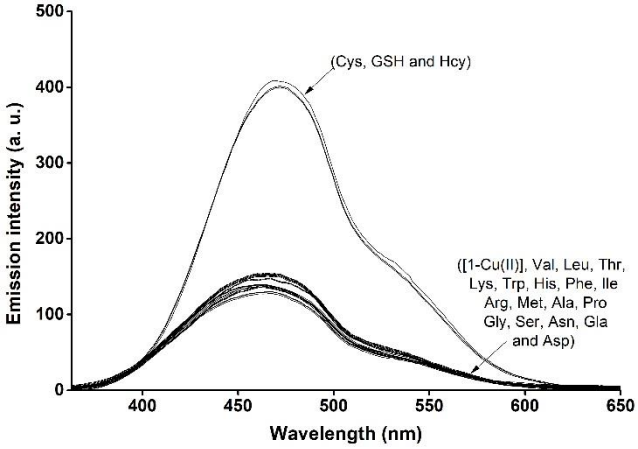

Figure 5. Changes in the emission band of **1**-Cu(II) complex (6.2×10^{-6} mol L^{-1}) in water (pH 7.4)-acetonitrile 90:10 v/v upon addition of biothiols (0.2 eq.) and selected amino acids (0.2 eq.).

From the emission titration profiles obtained upon addition of increasing quantities of biothiols (see Supporting Information) limits of detection of 6.5, 5.0 and 10.2 μM for Cys, Hcy and GSH were obtained. The chromo-fluorogenic changes observed upon addition of biothiols to the aqueous solutions of **1**-Cu(II) complex were ascribed to a demetallation of the complex, due to the high affinity of Cu(II) cation for thiol moieties, that released the free probe **1**.

On the other hand, we also tested the chromo-fluorogenic behavior of water (pH 7.4)-acetonitrile 90:10 v/v solutions of **1**-Cu(II) complex (3.2×10^{-6} mol L^{-1}) in the presence of selected anions (F^-, Cl^-, Br^-, I^-, AcO^-, BH_4^-, ClO_4^-, $H_2PO_4^-$, CN^-, HS^-, SCN^-, NO_3^-, HCO_3^- and $P_2O_7^{4-}$). Of all the anions tested only $P_2O_7^{4-}$ was able to induce the disappearance of the absorption band of the complex centred at 555 nm (with a marked bleaching of the solution) and an enhancement in the emission at 475 nm (see Supporting Information). These chromofluorogenic changes were also ascribed to a demetallation of **1**-Cu(II) complex, induced by $P_2O_7^{4-}$ anion, that produced the free probe.[56]

The selective emission quenching of **1** in the presence of Cu(II) and the recovery observed with GSH suggests that the probe can be used for the imaging of these species in living cells. Based on these observations, the cytotoxicity of **1** was first evaluated. HeLa cells were treated with **1** (5 μM) over half an hour period and cell viability was determined by a WST-1 assay. Moreover, the viability of probe **1** in the presence of Cu(II) (1 and 10 eq.) was also assessed. The obtained results are shown in Fig. 6. As could be seen, probe **1** was non-toxic to HeLa cells at the concentration tested. Besides, the concentrations of Cu(II) added (alone and in the presence of probe **1**) were also non-toxic to HeLa cells.

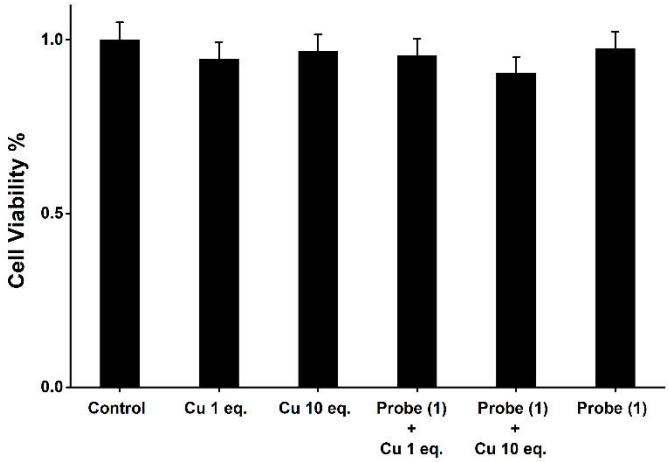

Figure 6. Cell viability assays. HeLa cells were treated with probe **1** (5 μM) for 30 min in the absence or in the presence of Cu(II) (1 and 10 eq.). Then, cell viability was quantified by means of WST-1 assay.

Then, in order to verify the feasibility of the developed probe to detect Cu(II) and GSH in highly competitive environments, we prospectively used probe **1** for the fluorescence imaging of both species in living cells. In a typical experiment, HeLa cells were incubated in DMEM supplemented with 10% fetal bovine serum. To conduct fluorescence microscopy studies, HeLa cells were seeded in 24mm glass coverslips in 6-well plates and were allowed to settle for 24 h. Cells were treated with probe **1** in DMSO (1%) at a final concentration of 5 μM. After 30 min, the medium was removed and solutions of different concentrations of $Cu(NO_3)_2$ in PBS were added (5 μM and 50 μM) and cells were incubated for another 10-min period. Finally, treated cells were incubated overnight in order to ascertain the intracellular GSH effect.

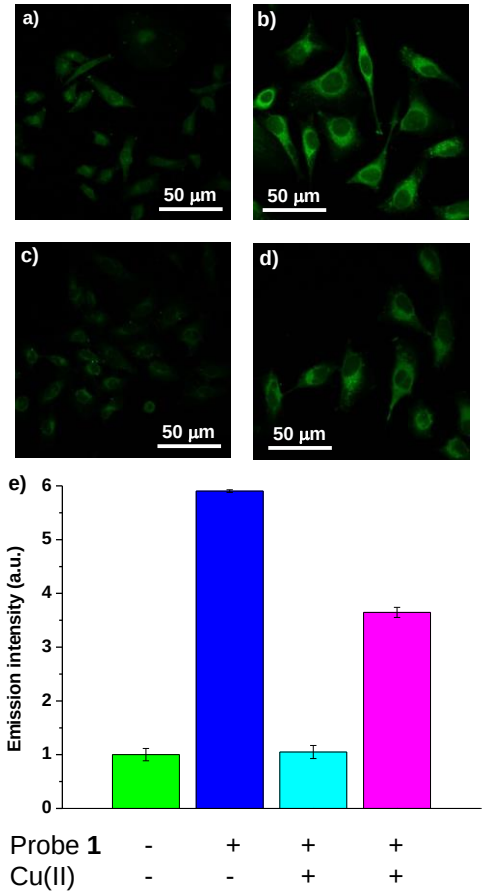

Figure 7. Confocal microscopy images of probe **1** in HeLa cells. HeLa cells were incubated with **1** (5 µM) for 30 min at 37 °C in DMEM. Cells images obtained using an excitation wavelength of 405 nm. (a) Fluorescence images of Hela cells, (b) Fluorescence images of Hela cells incubated with **1** (5 µM) for 30 min. (c) Fluorescence images of Hela cells incubated with probe **1** and pre-treated with Cu(II) 10 eq. (50 µM) for 10 min. (d) Fluorescence images of HeLa cells after the pre-treatment with probe **1** and Cu(II) and after incubation overnight. (e) Emission intensity quantification by the confocal images analysis.

As seen in the confocal fluorescence microscope images shown in Fig. 7a, the control experiment (HeLa cells without probe **1**) showed a weak fluorescence, and cells treated with **1** (5 µM) showed a marked intracellular emission (Fig. 7b). Moreover, a significant quenching in intracellular emission was observed in the

Cu(II)-treated cells (Fig. 7c), clearly indicating the possible use of **1** to detect this divalent metal cation in complex biological settings. Finally, after incubation overnight, a remarkable emission enhancement could be observed probably due to a intracellular GSH-induced demetallation of complex **1**-Cu(II) which generated the free probe (Fig. 7d). Besides, the emission intensity of the HeLa cells after each treatment was measured and the obtained results are presented in Fig. 7e.

4.5 Conclusions

In summary, we report herein an easy-to-prepare imidazole-based chromo-fluorogenic probe **1** for the selective and sensitive optical detection of Cu(II) and biothiols. Probe **1** was able to selectively detect Cu(II) in a highly competitive media (water-acetonitrile 90:10 v/v) by a marked colour change from colourless to deep blue. Besides, a significant quenching of the probe emission in the presence of Cu(II) was observed. Moreover, real-time fluorescence imaging measurements confirmed that probe **1** can be used to detect intracellular Cu(II) at micromolar concentrations. Moreover, **1**-Cu(II) complex was used for the development of an IDA assay for the selective chromo-fluorogenic sensing of biothiols (Cys, Hcy and GSH). Biothiols were able to demetallate **1**-Cu(II) complex with the subsequent release of free probe **1** assessed by a marked colour change from deep blue to colorless and by a significant emission enhancement. The sensing behaviour of probe **1** toward Cu(II) and of the **1**-Cu(II) complex toward biothiols are comparable to other sensing probes recently published (see Supporting Information for a comparative table). Besides, the results presented here showed the sequential detection of two analytes, which is an emerging area inside the design and synthesis of new molecular probes.[41–46, 57–59]

4.6 Acknowledgements

The authors thank the financial support from the Spanish Government (projects MAT2015-64139-C4-1-R and AGL2015-70235- C2-2-R) and the Generalitat Valenciana (project PROMETEOII/2014/ 047). Thanks are also due to Fundação para a Ciência e a Tecnologia for financial support to the Portuguese NMR network (PTNMR, Bruker Avance III 400-Univ. Minho), FCT and FEDER (European Fund for Regional Development)-COMPETEQREN-EU for financial support to the research centre CQ/UM (Ref. UID/QUI/00686/2013 and UID/QUI/0686/2016), and a PhD grant to R. C. M. Ferreira (SFRH/BD/86408/2012).

4.7 References and Notes

Keywords: Biothiols • Chromo-fluorogenic detection • Cu(II) complex • Displacement assay.

References

1. Maity D, Raj A, Karthigeyan D, Kundu TK, Govindaraju T., *Supramol Chem*, **2015**, 27, 589–94.

2. Ghosh S, Ganguly A, Bhattacharyya A, Alam MA, Guchhait N., *RSC Adv*, **2016**, 6, 67693–700.

3. Nandre J, Patil S, Patil V, Yu F, Chen L, Sahoo S, Prior T, Redshaw C, Mahulikar P, Patil U. *Biosens Bioelectron*, **2014**, 61, 612–7.

4. Xu H, Wang X, Zhang C, Wu Y, Liu Z., *Inorg Chem Commun*, **2013,** 34, 8–11.

5. Chereddy NR, Thennarasu S., *Dyes Pigments*, **2011**, 91, 378–82.

6. Lee HG, Kim KB, Park GJ, Na YJ, Jo HY, Lee SA, Kim C., *Inorg Chem Commun*, **2014**, 39, 61–5.

7. Dong M, Ma TH, Zhang AJ, Dong YM, Wang YW, Peng Y., *Dyes Pigments*, **2010**, 87, 164–72.

8. Chen X, Pradhan T, Wang F, Kim JS, Yoon J., *Chem Rev*, **2012**, 112, 1910–56.

9. Kim H, Na YJ, Song EJ, Kim KB, Bae JM, Kim C., *RSC Adv*, **2014**, 4, 22463–9.

10. Swaminathan S, Gangadaran P, Venkatesh T, Ghosh M*., J Pharmaceut Biomed Sci*, **2011**, 9, 1–15.

11. Kamble S, Utage B, Mogle P, Kamble R, Hese S, Dawane B, Gacche R., *AAPS Pharm Sci Tech*, **2016**, 17, 1030–41.

12. Jain AK, Singh RK, Jain S, Raisoni J., *Transition Met. Chem.*, **2008**, 33, 243–9.

13. Goswami S, Sen D, Das NK, Hazra G., *Tetrahedron Lett*, **2010**, 51, 5563–6.

14. Xie Q, Zhou T, Yen L, Shariff M, Nguyen T, Kami K, Gu P, Liang L, Rao J, Shi R., *Nutr Diet Suppl*, **2013**, 5, 1–6.

15. Choo XY, Alukaidey L, White AR, Grubman A., *Int J Alzheimer's Dis*, **2013**, 2013, 145345.

16. Udhayakumari D, Naha S, Velmathi S., *Anal. Methods*, **2017**, 9, 552–78.

17. Na YJ, Park GJ, Jo HY, Lee SA, Kim C., *New J Chem*, **2014**, 38, 5769–76.

18. Divya KP, Sreejith S, Balakrishna B, Jayamurthy P, Anees P, Ajayaghosh A. *Chem Commun (J Chem Soc Sect D)*, **2010**, 46, 6069–71.

19. Yu H, Fu M, Xiao Y., *Phys Chem Chem Phys*, **2010**, 12, 7386–91.

20. Kim H, Na YJ, Park GJ, Lee JJ, Kim YS, Lee SY, Kim C., *Inorg Chem Commun*, **2014**, 49, 68–71.

21. Noh JY, Park GJ, Na YJ, Jo HY, Lee SA, Kim C., *J Chem Soc, Dalton Trans*, **2014**, 43, 5652–6.

22. Trigo-López M, Muñoz A, Ibeas S, Serna F, García FC, García JM, *Sensor Actuator B Chem*, **2016**, 226, 118–26.

23. Kim KB, Park GJ, Kim H, Song EJ, Bae JM, Kim C., *Inorg Chem Commun*, **2014**, 46, 237–40.

24. Townsend DM, Tew KD, Tapiero H., *Biomed Pharmacother*, **2003**, 57, 145–55.

25. Miller JW, Beresford SA, Neuhouser ML, Cheng TY, Song X, Brown EC, Zheng Y, Rodriguez B, Green R, Ulrich CM., *Am J Clin Nutr*, **2013**, 97, 827–34.

26. Dorszewska J, Prendecki M, Oczkowska A, Dezor M, Kozubski W., *Curr Alzheimer Res*, **2016**, 13, 952–63.

27. Rozycka A, Jagodzinski PP, Kozubski W, Lianeri M, Dorszewska J, *Curr Genom*, **2013**, 14, 534–42.

28. Isik M, Ozdemir T, Turan IS, Kolemen S, Akkaya EU., *Org Lett*, **2013**, 15, 216–9.

29. Liao YC, Venkatesan P, Wei LF, Wu SP., *Sensor Actuator B Chem*, **2016**, 232, 732–7.

30. Liu T, Huo F, Yin C, Jianfang L, Jianbin C, Yongbin Z., *Dyes Pigments*, **2016**, 128, 209–14.

31. Lee KS, Park J, Park HJ, Chung YK, Park SB, Kim HJ, Shin IS, Hong JI., *Sensor Actuator B Chem*, **2016**, 237, 256–61.

32. Kong F, Liu R, Chu R, Wang X, Xu K, Tang B., *Chem Commun (J Chem Soc Sect D)*, **2013**, 49, 9176–8.

33. Zhang J, Jiang XD, Shao X, Zhao J, Su Y, Xi D, Yu H, Yue S, Xiao LJ, Zhao W., *RSC Adv*, **2014**, 4, 54080–3.

34. Wang YW, Liu SB, Ling WJ, Peng Y., *Chem Commun (J Chem Soc Sect D)*, **2016**, 52, 827–30.

35. Liu J, Sun YQ, Zhang H, Huo Y, Shi Y, Guo W., *Chem Sci*, **2014**, 5, 3183–8.

36. Guan YS, Niu LY, Chen YZ, Wu LZ, Tung CH, Yang QZ., *RSC Adv*, **2014**, 4, 8360–4.

37. Fu ZH, Han X, Shao Y, Fang J, Zhang ZH, Wang YW, Peng Y., *Anal Chem*, **2017**, 89, 1937–44.

38. Yang YL, Zhang FM, Wang YW, Zhang BX, Fang R, Fang JG, Peng Y., *Chem Aust J*, **2015**, 10, 422–6.

39. Zhao CC, Chen Y, Zhang HY, Zhou BJ, Lv XJ, Fu WF., *J Photochem Photobiol A*, **2014**, 282, 41–6.

40. Guangjie H, Meng Q, Zhao X, Cheng H, Zhoub P, Duan C., *Inorg Chem Commun*, **2016**, 65, 28–31.

41. Fu ZH, Yan LB, Zhang X, Zhu FF, Han XL, Fang J, Wang YW, Peng Y., *Org Biomol Chem*, **2017**, 15, 4115–21.

42. Singh Y, Arun S, Singh BK, Dutta PK, Ghosh T., *RSC Adv*, **2016**, 6, 80268–74.

43. Lee SH, Lee JJ, Shin JW, Min KS, Kim C., *Dyes Pigments*, **2015**, 116, 131–8.

44. Maheshwaran D, Nagendraraj T, Manimaran P, Ashokkumar B, Kumar M, Mayilmurugan R., *Eur J Inorg Chem*, **2017**, 1007–16.

45. Kim YS, Park GJ, Lee SA, Kim C., *RSC Adv*, **2015**, 5, 31179–88.

46. You GR, Lee JJ, Choi YW, Lee SY, Kim C., *Tetrahedron*, **2016**, 72, 875–81.

47. Santos-Figueroa LE, Llopis-Lorente A, Royo S, Sancenón F, Martínez-Máñez R, Costero AM, Gil S, Parra M, *ChemPlusChem*, **2015**, 80, 800–4.

48. Marín-Hernández C, Santos-Figueroa LE, El Sayed S, Pardo T, Raposo MMM, Batista RMF, Costa SPG, Sancenón F, Martínez-Máñez R., *Dyes Pigments*, **2015**, 122, 50–8.

49. Lo Presti M, El Sayed S, Martínez-Máñez R, Costero AM, Gil S, Parra M, Sancenón F., *New J Chem*, **2016**, 40, 9042–5.

50. El Sayed S, de la Torre C, Santos-Figueroa LE, Pérez-Paya E, Martínez-Máñez R, Sancenón F, Costero AM, Parra M, Gil S., *RSC Adv*, **2013**, 3, 25690–3.

51. El Sayed S, de la Torre C, Santos-Figueroa LE, Martínez-Máñez R, Sancenón F., *Supramol Chem*, **2015**, 4, 244–54.

52. Marín-Hernández C, Santos-Figueroa LE, Moragues ME, Raposo MMM, Batista RMF, Costa SPG, Pardo T, Martínez-Máñez R, Sancenón F., *J Org Chem*, **2014**, 79, 10752–61.

53. Sarkar B., *Chem Rev*, **1999**, 99, 2535–44.

54. Barnham KJ, Masters CL, Bush AI., *Nat Rev Drug Discov*, **2004**, 3, 205–14.

55. Oliveira E, Baptista RMF, Costa SPG, Raposo MMM, Lodeiro C., *Inorg Chem*, **2010**, 49, 10847–57.

56. Huang X, Guo Z, Zhu W, Xie Y, Tian H., *Chem Commun (J Chem Soc Sect D)*, **2008**, 5143–5.

57. Dong YM, Peng Y, Dong M, Wang YW., *J Org Chem*, **2011**, 76, 6962–6.

58. Peng Y, Dong YM, Dong M, Wang YW., *J Org Chem* **2012**, 77, 9072–80.

59. Dong M, Peng Y, Dong YM, Tang N, Wang YW., *Org. Letture*, **2012**, 14, 130–3.

4.8 Supporting Information

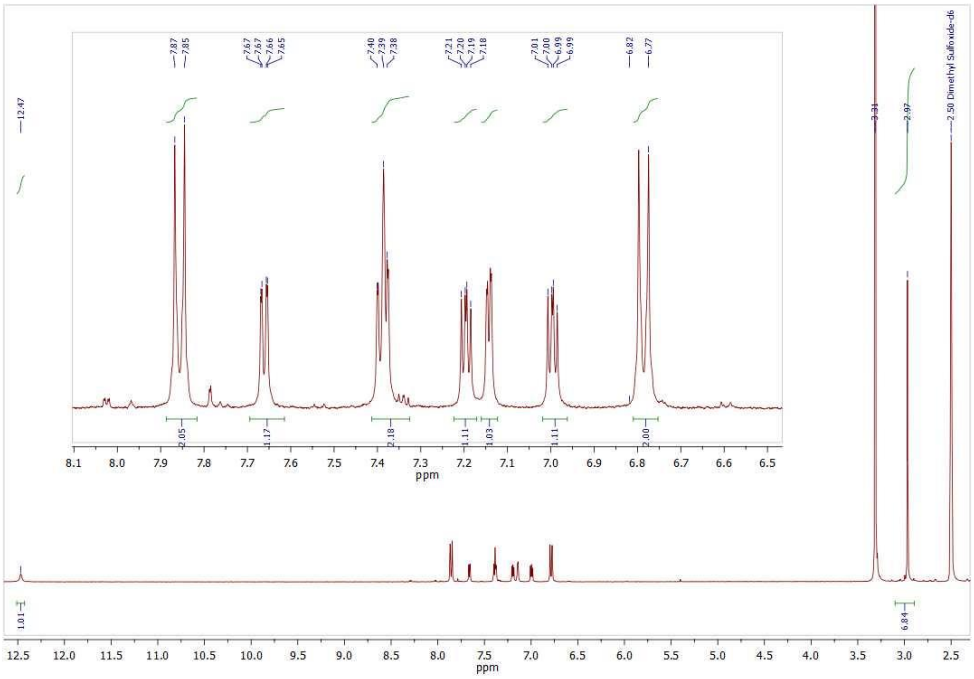

Figure S1. ^{1}H NMR spectra of probe **1** in DMSO-d_6.

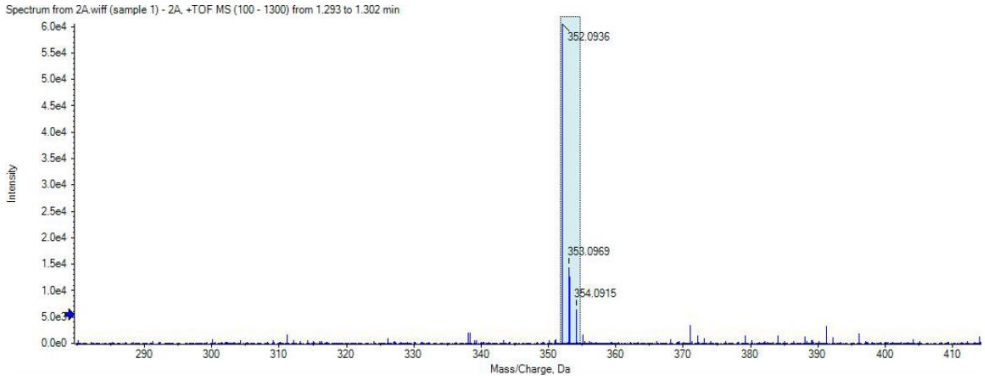

Figure S2. ESI-MS spectra of probe **1**.

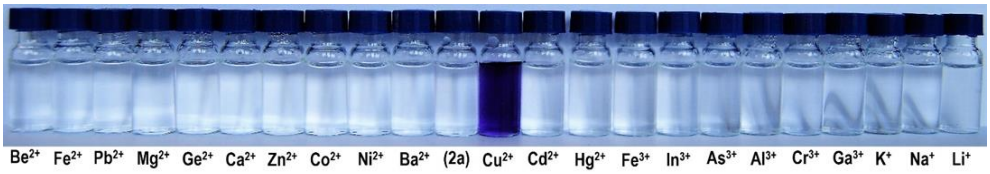

Figure S3. Colour changes observed in acetonitrile solutions of probe **1** (1.0 x 10^{-5} mol L^{-1}) upon addition of 10 equiv. of selected metal cations.

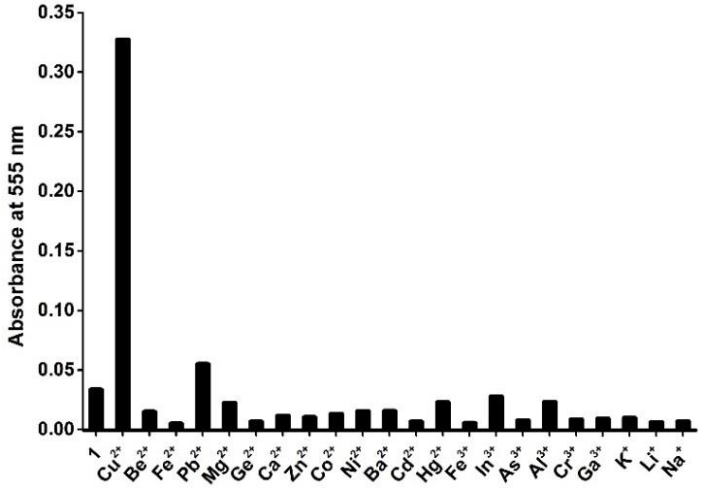

Figure S4. Absorbance at 555 nm of water (pH 7.4)-acetonitrile 90:10 v/v (1.0 x 10^{-5} mol L^{-1}) solutions of probe **1** alone and in the presence of selected metal cations (10 eq.).

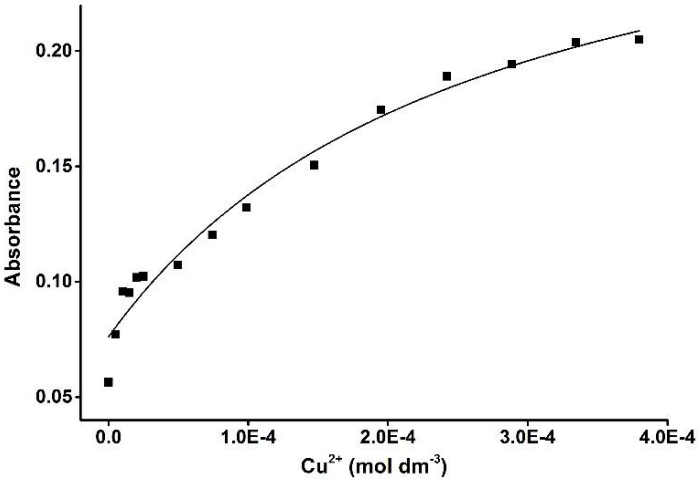

Figure S5. Absorbance at 555 nm of water (pH 7.4)-acetonitrile 90:10 v/v (1.0 x 10^{-5} mol L^{-1}) solutions of probe **1** upon addition of increasing quantities of Cu(II).

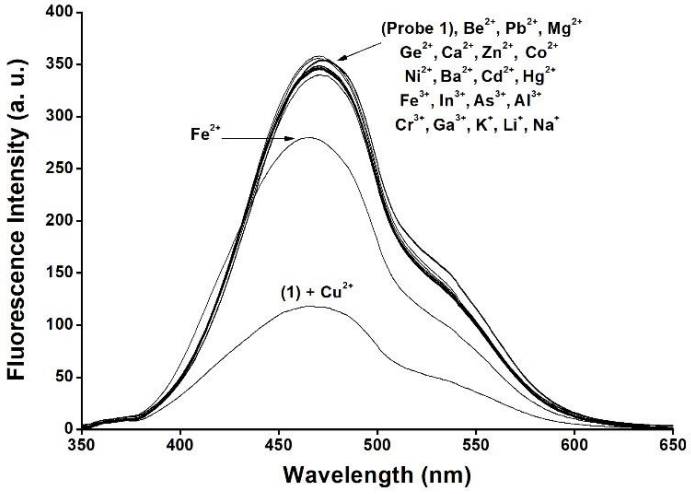

Figure S6. Fluorescence spectra (excitation at 320 nm) of probe **1** in water (pH 7.4)-acetonitrile 90:10 v/v (1.0 x 10^{-5} mol L^{-1}) upon addition of selected metal cations (10 eq.).

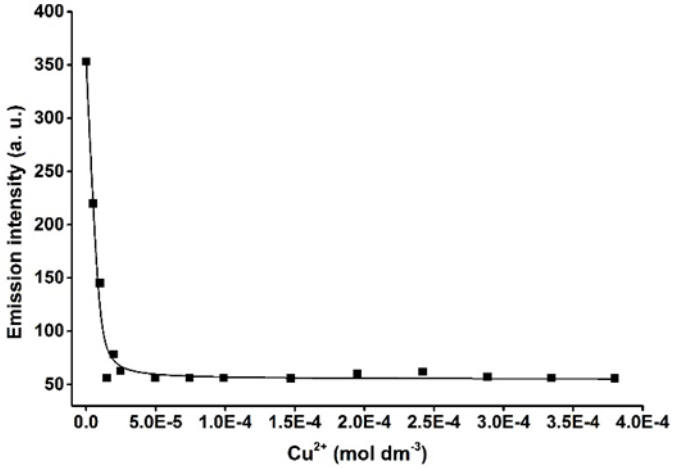

Figure S7. Fluorescence at 475 nm (excitation at 320 nm) of water (pH 7.4)-acetonitrile 90:10 v/v (1.0×10^{-5} mol L^{-1}) solutions of probe **1** upon addition of increasing quantities of Cu(II).

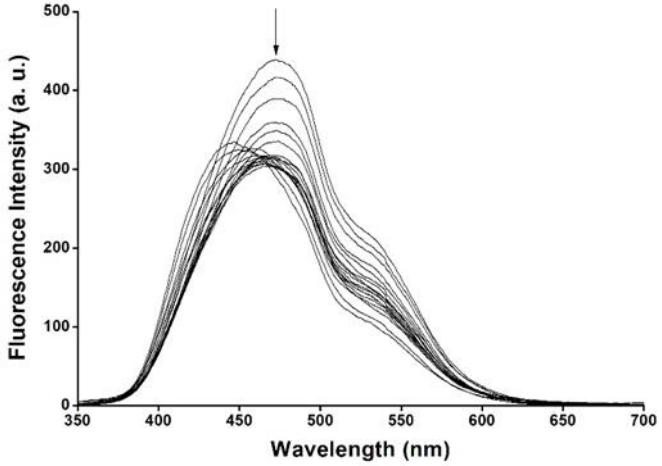

Figure S8. Emission spectra of probe **1** in water (pH 5.0)-acetonitrile 90:10 v/v (1.0×10^{-5} mol L^{-1}) solutions of probe **1** upon addition of increasing quantities of Cu(II).

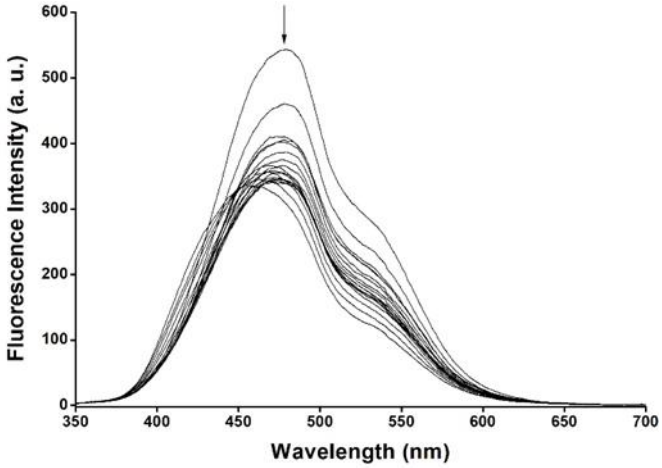

Figure S9. Emission spectra of probe **1** in water (pH 6.0)-acetonitrile 90:10 v/v (1.0 x 10^{-5} mol L^{-1}) solutions of probe **1** upon addition of increasing quantities of Cu(II).

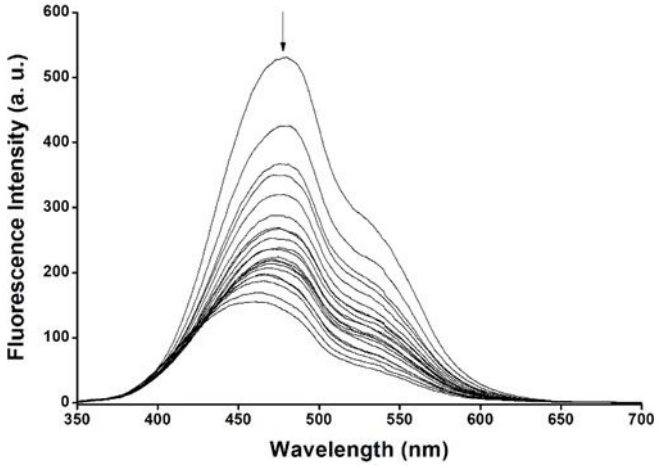

Figure S10. Emission spectra of probe **1** in water (pH 8.0)-acetonitrile 90:10 v/v (1.0 x 10^{-5} mol L^{-1}) solutions of probe **1** upon addition of increasing quantities of Cu(II).

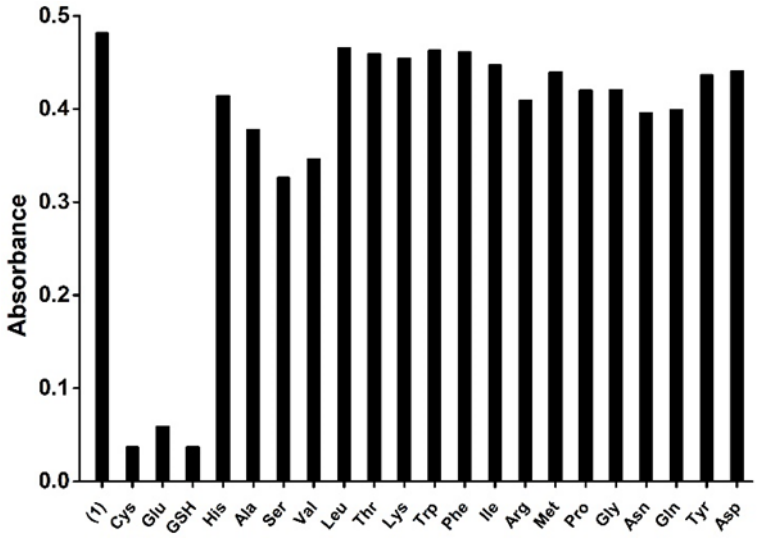

Figure S11. Absorbance at 555 nm of water (pH 7.4)-acetonitrile 90:10 v/v solutions of **1**·Cu(II) complex (6.2 x 10-6 mol L-1) in the presence of Cys, Hcy and GSH (0.3 eq.) and selected amino acids (0.3 eq.).

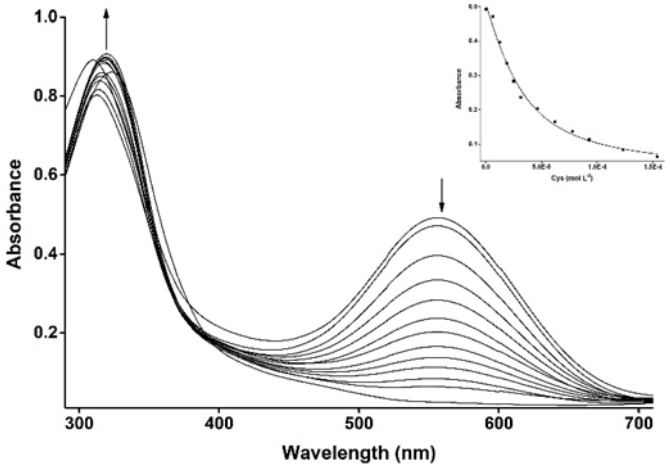

Figure S12. UV/Vis. titration profile of **1**·Cu(II) complex (6.2 x 10^{-6} mol L^{-1}) in water (pH 7.4)-acetonitrile 90:10 v/v upon addition of Cys (0 - 1.0 equivalents). Inset: Absorbance at 555 nm vs Cys concentration.

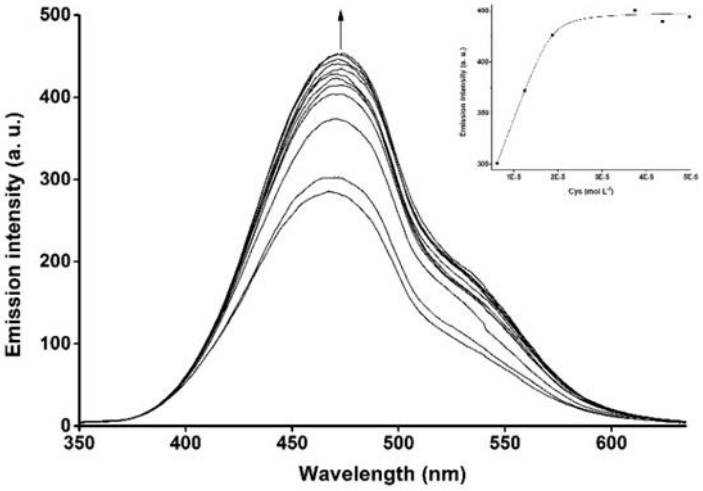

Figure S13. Fluorescence spectral changes of water (pH 7.4)-acetonitrile 90:10 v/v solutions of **1**·Cu(II) complex (6.2 x 10^{-6} mol L^{-1}) upon addition of increasing quantities of Cys (excitation at 324 nm). Inset emission at 475 nm vs. Cys concentration.

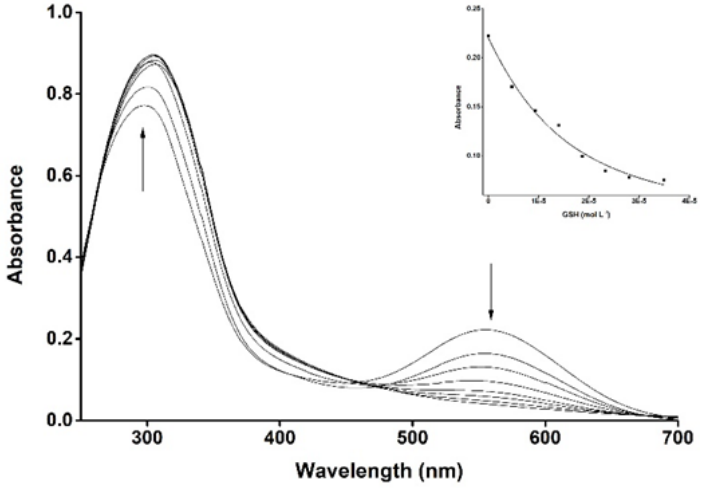

Figure S14. UV/Vis. titration profile of **1**·Cu(II) complex (6.2 x 10^{-6} mol L^{-1}) in water (pH 7.4)-acetonitrile 90:10 v/v upon addition of GSH (0 – 0.8 equivalents). Inset: Absorbance at 555 nm vs GSH concentration.

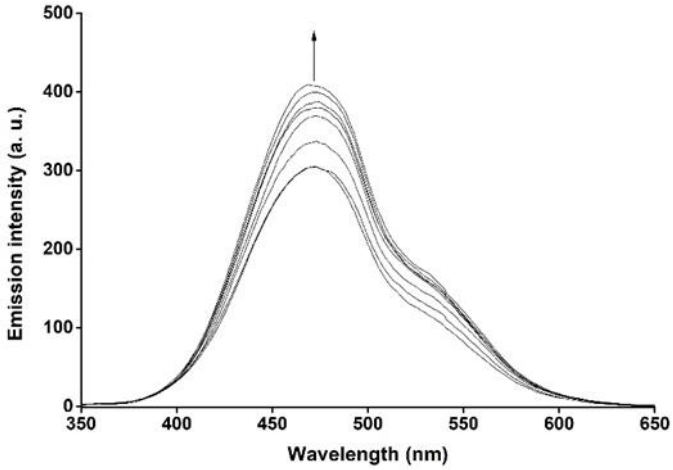

Figure S15. Fluorescence spectral changes of water (pH 7.4)-acetonitrile 90:10 v/v solutions of **1**·Cu(II) complex (6.2 x 10^{-6} mol L^{-1}) upon addition of increasing quantities of GSH (excitation at 324 nm).

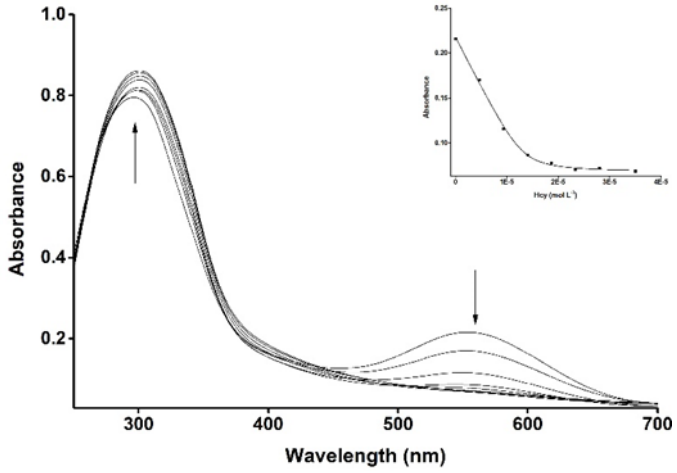

Figure S16. UV/Vis. titration profile of **1**·Cu(II) complex (6.2 x 10^{-6} mol L^{-1}) in water (pH 7.4)-acetonitrile 90:10 v/v upon addition of Hcy (0 – 0.8 equivalents). Inset: Absorbance at 555 nm vs Hcy concentration.

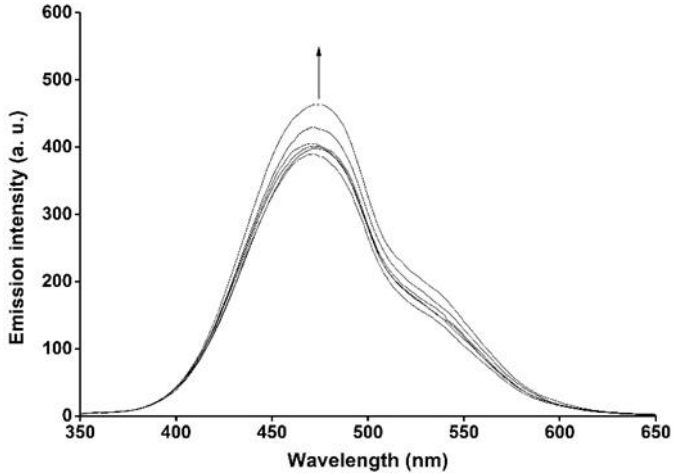

Figure S17. Fluorescence spectral changes of water (pH 7.4)-acetonitrile 90:10 v/v solutions of **1**·Cu(II) complex (6.2 x 10^{-6} mol L^{-1}) upon addition of increasing quantities of Hcy (excitation at 324 nm).

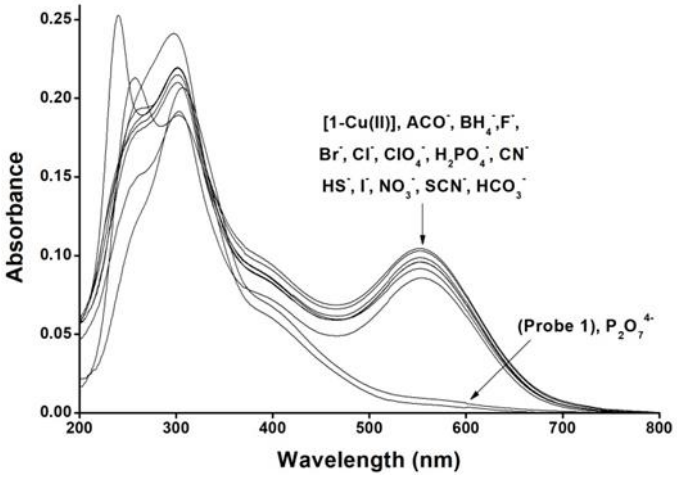

Figure S18. UV-visible changes of **1**-Cu(II) (3.2 x 10^{-6} mol L^{-1}) in water (pH 7.4)-acetonitrile 90:10 v/v in the presence of selected anions (0.2 eq.).

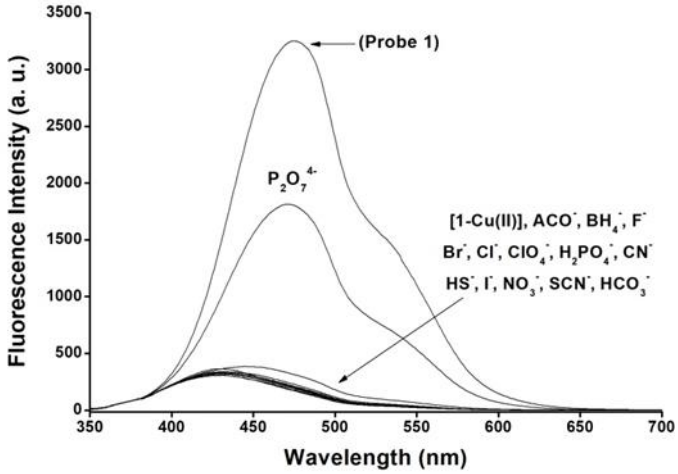

Figure S19. Changes in the emission band of **1**-Cu(II) complex (3.2 x 10^{-6} mol L^{-1}) in water (pH 7.4)-acetonitrile 90:10 v/v upon addition of selected anions (0.2 eq.).

Table S1. Analytical features of recently chromo-fluorogenic probes for biothiols detection recently published.

Probe	**Mechanism**	**Media**	**Response**	**Limit of detection (μM)**	**Reference**
Imidazole derivative-Cu(II) complex	Demetallation	Water-ACN 9:1	Cys, Hcy, GSH	6.5 (Cys); 5.0 (Hcy); 10.2 (GSH)	This paper
Fluorescein derivative-Cu(II) complex	Demetallation	Hepes	Cys, Hcy, GSH	0.12 (Cys); 0.036 (Hcy); 0.024 (GSH)	41
Naphthol derivative-Cu(II) complex	Demetallation	Water-DMSO 7:3	Cys (Hcy and GSH not tested)	2.9	42
Hydroxynaphthalene derivative-Cu(II) complex	Demetallation	Tris-DMSO 1:1	Cys	10.77	43

Anthracenyl derivative-Cu(II) complex	Demetallation	Hepes-ACN 3:7	Cys	0.019	44
Hydorxyjulolidine derivative-Cu(II) complex	Demetallation	Tris-DMF 5:1	Cys	3.6	45
Hydorxyjulolidine derivative-Cu(II) complex	Demetallation	Tris-DMSO 2:8	Cys	7.82	46
BODIPY derivative	Michael addition	Hepes-ACN 8:2	Cys	Not reported	28
Coumarin derivative	Michael addition	Water-MeOH 1:1	Cys, Hcy, GSH	0.192 (Cys); 0.158 (Hcy); 0.155 (GSH)	29
Triphenylamine derivative	Michael addition	Hepes-MeOH 1:1	Cys, Hcy, GSH	0.13 (Cys); 0.12 (Hcy); 0.085 (GSH)	30
Coumarin derivative-Cu(II) complex	Cu(II)/Cu(I) conversion	Hepes	Cys, Hcy, GSH	Not reported (Cys); not reported (Hcy); 15 (GSH)	31
Cyanine derivative	Aldehyde-thiazoline conversion	PBS	Cys, Hcy	0.008 (Cys); 0.008 (Hcy)	32
BODIPY derivative	Aldehyde-thiazoline conversion	Water-ACN 2:8	Cys, Hcy	Not reported (Cys); 2 (Hcy)	33

Binaphthyl derivative	Aldehyde-thiazoline conversion	Hepes-EtOH 2:98	Hcy	54	34
Pyronin derivative containing 4-methoxythiophenol	Nucleophilic aromatic substitution	PBS	Cys, Hcy, GSH	Not reported (Cys); not reported (Hcy); not reported (GSH)	35
Cyanine derivative containing 4-methoxythiophenol	Nucleophilic aromatic substitution	Hepes-DMSO 4:1	Cys	1.26	36
Fluorescein derivative	Hydrolysis of an acrylate ester	PBS-DMSO 7:3	Cys	0.084	37
Iminocoumarin derivative	Hydrolysis of a 2,4-dinitrobenzenesulfonyl moiety	PBS	Cys, Hcy, GSH	5.0 (Cys); 10.0 (Hcy); 5.0 (GSH)	38

- ***Fluorescence quantum yield measurements***

The fluorescence quantum yield of pyrene in cyclohexane (φ_f = 0.32) was used as a reference to measure the fluorescence quantum yields of probe **1** and complex [**1**·Cu(II)]. The following equation was used to calculate the fluorescence quantum yield:

$$\varphi_s = \varphi_f \frac{I_s A_f \eta_s^2}{I_f A_s \eta_r^2}$$

Here φ_f is the fluorescence quantum yield of reference. I stand for the integrated area under the emission curves. The subscripts s and r stand for sample and reference, respectively. A is the absorbance at a particular excitation wavelength. η is the refractive index of the medium. The absorbance of the dye at

the excitation wavelength was always kept ~0.1. The steady state absorption and emission spectra were fitted by the log normal line shape function. Consequently the fluorescence quantum yield for probe **1** is φ = 0.26 and for [**1**·Cu(II)] complex is φ = 0.07.

Chapter 5.
N,N-diphenylanilino-heterocyclic aldehydes based chemosensors for UV-vis/NIR and fluorescence Cu(II) detection

N,N-diphenylanilino-heterocyclic aldehydes based chemosensors for UV-vis/NIR and fluorescence Cu(II) detection

Hazem Essam Okda,[abc] Sameh El Sayed,[abc] Rosa C. M. Ferreira,[d] Raquel C. R. Gonçalves, [d] Susana P. G. Costa,[d] M. Manuela M. Raposo,[d] Ramón Martínez-Máñez,[abc]* and Félix Sancenón[abc]*

[a] *Instituto Interuniversitario de Investigación de Reconocimiento Molecular y Desarrollo Tecnológico (IDM), Universitat Politècnica de València, Universitat de València, Spain*

[b] *Departamento de Química, Universitat Politècnica de València, Camino de Vera s/n, 46022, València, Spain*

[c] *CIBER de Bioingeniería, Biomateriales y Nanomedicina (CIBER-BBN), Spain*

[d] *Centro de Química, Universidade do Minho, Campus de Gualtar, 4710-057, Braga,*

New Journal of Chemistry, **2019**, 43, 7393-7402

(Reproduced with permission of The Royal Society of Chemistry)

5.1 Abstract

Herein, three *N*,*N*-diphenylanilino-heterocyclic aldehyde probes (**5**, **6** and **7**) are synthesized, characterized and their sensing behaviour against metal cations tested. Acetonitrile solutions of the three probes show an intramolecular charge-transfer band in the 360-420 nm range due to the presence of an electron donor *N*,*N*-diphenylanilino group and an electron acceptor aldehyde moiety. Besides, all three probes are moderately emissive with bands in the 540-580 nm range in acetronitrile. The chromo-fluorogeic behaviour of the three probes in acetonitrile in the presence of selected metal cations is assessed. Of all the metal cations tested only Cu(II) induces marked colour and emission changes. In this respect, addition of Cu(II) cation to solutions of probes induces the appearance of NIR absorptions at 756 nm for **5**, at 852 nm for **6** and at 527, 625 and 1072 nm for **7**. Besides, Cu(II) induces a marqued quenching of the emission of the three probes. The observed spectral changes are ascribed to the formation of 1:1 probe-Cu(II) complexes in which the metal cation interacts with the acceptor part of the chemosensors. In addition, the limits of detection determined using UV-visible and fluorescence titrations are in the 0.21-5.12 μM range, which are values lower than the minimum concentration prescribed by the World Health Organization (WHO) guideline for drinking water for copper (30 mM). Besides, probe **7** is used for the detection of Cu(II) in aqueous environments using SDS anionic surfactant.

5.2 Introduction

In recent years, the development of new chromo-fluorogenic molecular chemosensors for biologically active metal ions has been extensively investigated because of their potential applications in life sciences, medicine, chemistry, and biotechnology.[1] These chromo-fluorogenic probes are generally formed by two components covalently linked, namely the binding site and the reporter unit. Interaction of transition metal cations with the binding site can induce a

rearrangement of the π-conjugated system of the reporter unit, which may be reflected in colour and/or emission changes. However, the covalent linking of highly selective binding sites with reporter units require, in most cases, great synthetic efforts in order to achieve certain selectivity to the guest and to impart the desired functionality in terms of color and/or emission changes upon coordination. In order to minimize synthetic requirements, recently, the preparation of simple chemical species that integrated binding sites into the structure of certain dyes or fluorophores has deserved great attention.[2]

On the other hand, copper is the third cation in abundance in human bodies besides zinc and iron. Cu(II) plays an important role in biological and environmental areas as an essential trace element for both plants and animals, including humans.[3] In addition, copper plays a key role in copper-containing enzymes in different catalytic and physiological processes.[4,5] Based on research findings, it has been suggested that copper deficiency can increase the risk of developing coronary heart disease,[6] while the excessive concentrations of this cation leads to variation in brain function.[7] It has been also reported that the disturbance in Cu(II) levels results in human genetic disorders like, Wilson's diseases[8] and Menke's syndrome.[9] Moreover, Cu(II) could lead to detrimental effects by causing oxidative stress and disorders associated with neurodegenerative diseases[10] such as Parkinson's,[11] Alzheimer's,[12] prion,[13] Huntington's diseases[14] and metabolic disorders such as obesity and diabetes.[15] Taking into account the above mentioned facts, several analytical methods for Cu(II) detection such as photometric measurements,[16] inductively coupled plasma emission or mass spectroscopy (ICP-ES, ICP-MS),[17] atomic absorption spectroscopy (AAS),[18] anodic stripping voltammetry (ASV),[19] and total reflection X-ray fluorimetry (TXRF)[20] have been used. However, these techniques involve complicated procedures, required high cost instrumentation, and trained personnel.

Owing to the significant physiological relevance and associated biomedical implications, there is a considerable interest in developing highly selective chemosensors for real time detection of Cu(II) in environmental and biological samples.[21] Moreover, very recently, the development of Cu(II) chromo-fluorogenic chemosensors with a marked optical response (changes in colour or in fluorescence) in the NIR zone (700-1100 nm) has deserved great attention.[22] Compared with UV-visible light, the NIR region has many advantages such as the possibility of reduced interferences of background absorption, fluorescence and light scattering. However, despite these interesting features, NIR probes for the sensing of cations are still scarce.[23]

From another point of view, heterocyclic aldehydes are versatile building blocks that can further react to yield a diversity of more complex molecules.[24] Heterocyclic aldehydes can be synthesized following different methods such as Vilsmeier formylation, metalation followed by addition of DMF, Vilsmeier-Haack-Arnold reaction, Stille, Suzuki and Sonogashira cross couplings and Clauson-Kaas reactions.[25] Heterocyclic aldehydes prepared by these procedures can subsequently be used for the synthesis of more complex push-pull π-conjugated heterocyclic systems intended for several applications such as nonlinear optics (SHG, TPA), optical chemosensors, fluorescent probes, heterogeneous catalysts, OLEDs, DSSCs, and synthesis of functionalized heterocyclic based unnatural amino acids.[26]

Motivated by previous studies by us,[27] we decided to further explore the potential use of *N*,*N*-diphenylanilino-heterocyclic aldehydes, bearing aryl and thienyl spacers as optical probes, for the detection of cations. In particular, we report herein the synthesis, characterization and sensing studies toward metal cations of three chromo-fluorogenic probes (**5**, **6** and **7**) based on the *N*,*N*-diphenylanilino-heterocyclic aldehydes skeleton. Interaction of the three probes with Cu(II) induced the appearance of absorption bands in the NIR zone and a remarkable quenching of the fluorescence.

5.3 Results and discussion

- ***Synthesis and characterization of the probes.***

Aldehydes **5**, **6** and **7**, functionalized with *N*,*N*-diphenylanilino as a donor group and different π-spacers (benzene and thiophene) were designed in order to study the effect of the heterocyclic π-bridges (i.e. length and electronic nature) on the optical properties and selectivity and sensitivity of the prepared probes. Thiophene spacers were selected due to their excellent charge-transfer properties and high thermal and photophysical stability.[24-26] In fact, compared with benzene derivatives, thiophenes offer a more effective conjugation and a lower energy for charge transfer transitions[28] due to their smaller resonance energy (thiophene, 29 kcal/mol; benzene, 36 kcal/mol).[29] On the other hand, *N*,*N*-diphenylanilino was chosen as donor group due to its well-known photophysical properties and its significantly higher thermo and photophysical stability compared to their *N*,*N*-dialkylaniline analogues.[30,31]

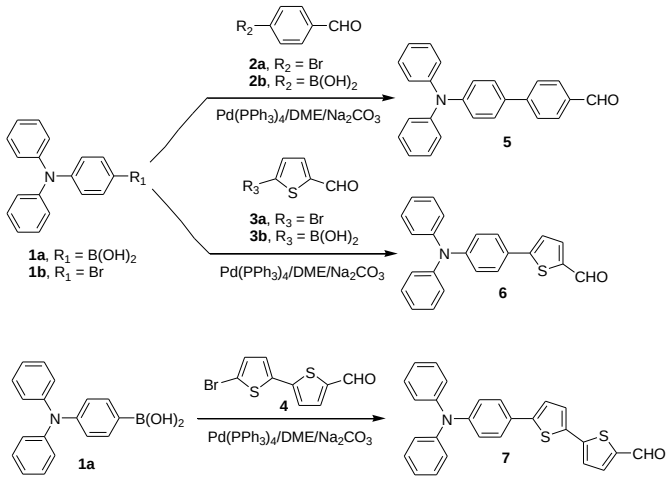

Scheme 1. Synthesis of probes **5**, **6** and **7**.

The synthetic protocols used to obtain probes **5**, **6** and **7** is shown in Scheme 1, following well-known procedures reported elsewhere.[25b,25c,26a,26c,26d,32] Suzuki coupling was selected as the method of synthesis due to well-known advantages of this coupling procedure (i.e. availability of the reagents, mild reaction conditions unaffected by the presence of water, tolerability of a broad range of functional groups and formation of non-toxic and easily removable inorganic by-product from the reaction mixture) compared to other coupling methods.[33]

Two different pairs of coupling components were used in order to determine the influence of the structure of the boronic acids as well as the brominated compounds on the yield of the Suzuki-Miyaura coupling reaction. Thus, probes **5**, **6** and **7** were prepared by Suzuki coupling with 4-(diphenylamino)phenylboronic acid **1a** and (hetero)aromatic brominated aldehydes **2a**, **3a** and **4** (*via* a) or using 4-bromo-*N,N*-diphenylaniline **1b** and heterocyclic boronic acids **2b** and **3b** as coupling components (*via* b).

According to table 1, aldehydes **5**, **6** synthesised using *via a* were obtained in higher yields (95-96 %), compared to those observed for *via b* (42-84 %). These results are not unexpected having in mind that in the Suzuki-Miyaura coupling the boronic acid is the nucleophilic coupling component and the aryl halide is the electrophilic coupling part. Therefore, boronic acids functionalized with electron donor groups are activated for the coupling reaction, as well as electron acceptor groups would activate the (hetero) aryl halides (*via* a).

The synthesis of aldehyde **6** using a Suzuki coupling reaction with 4-(diphenylamino)phenylboronic acid as one of the coupling components in a 75% yield was previously described.[34] Using another approach, when 4-iodophenyldiphenylamine was used as coupling reagent for the preparation of aldehyde **6**, a 92% yield was obtained.[35] However, in this last paper 4-iodophenyldiphenylamine was prepared with an overall yield for the two steps of 53%. The synthetic procedure (though Suzuki coupling) described in this paper is a

clear alternative to the published methods because uses commercially available coupling components and allows the preparation of **6** in a one-step process with a 96% yield (by means of *via* a).

Table 1. Yields, UV-visible and fluorescence data for *N,N*-diphenylanilino aldehydes **5**, **6** and **7** in acetonitrile solutions.

	Yield (%)		UV/Vis		Fluorescence		
	Via a	*Via* b	λ_{max} (nm)	Log ε	λ_{em} (nm)	ϕ_f	Stokes' shift (nm)
5	95	84	367	4.53	554	0.01	187
6	96	42	398	4.43	559	0.02	161
7	88	-	419	4.32	577	0.22	158

On the other hand, compound **7** was previously synthesized using Stille or Suzuki coupling reactions. The synthesis that used Stille couplings presented fair yields (68% and 74%)[36,37] and used, in both cases, toxic stannates as precursors. **7** was also prepared following Suzuki coupling with 4-(diphenylamino)phenylboronic and 5-iodo-2,2´-bithiophenyl-5-carboxaldehyde in a 91% yield.[36b] In this case, the iodine precursor was also prepared from 2,2´-bithiophenyl-5-carboxaldehyde with an overall yield of 81 % for aldehyde **7**. Besides, more recently, probe **7** was prepared using a Suzuki coupling reaction between 4-iodophenyldiphenylamine and 5´-(4,4,5,5-tetramethyl-[1,3,2] dioxaborolan-2-yl)-[2,2´]-bithiophenyl-5-carboxaldehyde. In this case, 4-iodophenyldiphenylamine was prepared by a Ullmann coupling reaction involving copper catalyzed iodoarylation of diphenylamine with 1,4-diiodobenzene (overall yield of 34% for **7**).[38] Using our synthetic methodology, we were able to obtain probe **7** in a higher yield compared to the methods described above. Compound **7** was synthesized with an 88 % yield in a one-step synthetic process through Suzuki coupling, using as precursors commercially available 4-(diphenylamino)phenylboronic and 5-bromo-2,2´-bithiophenyl-5-carboxaldehyde (via *a*).

Compounds **5**, **6** and **7** were characterized by spectroscopic techniques (see Table 1 for UV-visible and fluorescence data). The most distinctive signals in the ^{1}H NMR spectra for probes **5**, **6** and **7** were those corresponding to the aldehyde protons at ca. 9.86-10.05 ppm. FT-IR spectroscopy was also used in order to identify the typical band of the carbonyl group in aldehydes **5**, **6** and **7** that appeared in the 1656-1698 cm^{-1} range.

- ***Photophysical studies in acetonitrile solutions.***

The photophysical properties (absorption and emission) of the three *N*,*N*-diphenylanilino-heterocyclic aldehyde derivatives were studied in acetonitrile (Table 1). Electronic absorption spectra of heterocyclic aldehydes **5**, **6** and **7** in acetonitrile solutions showed an intense absorption band in the UV-visible region, in the 360-420 nm range, which can be attributed to an intramolecular charge-transfer (ICT) transition as consequence of the presence of *N*,*N*-diphenylanilino electron donor moiety directly linked to (hetero)aromatic bridges functionalized with the aldehyde electron acceptor group (see Figure 1). The wavelengths of the ICT absorption bands of the three probes were directly related with the π-spacer (length, and electronic nature of the aromatic or heteroaromatic rings). In this respect, a less effective conjugation and a higher energy for charge transfer transitions due to the higher resonance energy of the phenyl ring in probe **5** accounted for the lower wavelength of the ICT band (367 nm). On the other hand, the presence of one (probe **6**) or two (probe **7**) thiophene heterocycles induced an increase in the ICT character, which was reflected in redshifted wavelengths of the absorption bands (398 and 419 nm for **6** and **7** respectively). These facts are clearly related with the more effective conjugation, lower energy for the ICT transition and smaller resonance energy of thiophenes when compared to benzene derivatives.[25,29]

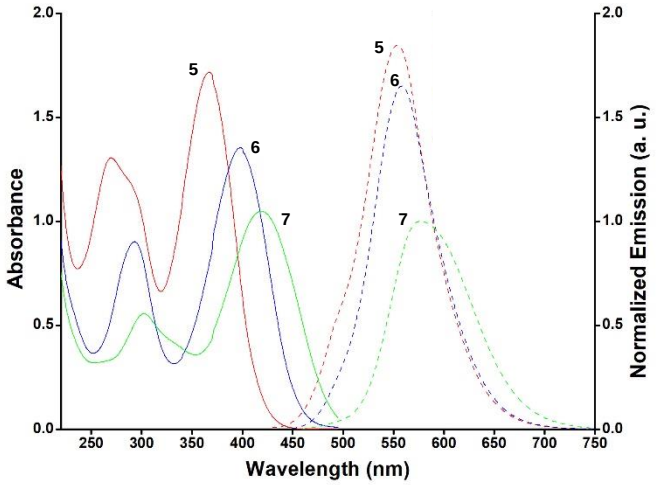

Figure 1. UV/Vis (solid lines) and fluoresence (dashed lines) spectra of the three probes in acetonitrile. Red lines: **5** (λ_{ex} = 367 nm); blue lines: **6** (λ_{ex} = 398 nm); green lines: **7** (λ_{ex} = 419 nm).

The three probes are weakly to moderate emissive upon excitation in the maximum of the corresponding absorption bands (see also Table 1). Upon excitation, the three probes showed broad unstructured emission bands in the 550-580 nm range (Figure 1). The relative fluorescence quantum yields were determined by using 10^{-6} M solutions of 9,10-diphenylanthracene (DPA) in ethanol as standard (Φ_F = 0.95).[39] Probes **5**, **6** and **7** exhibited low to moderate fluorescence quantum yields in acetonitrile? (Φ_F = 0.01-0.22, Table 1). Besides, all probes showed large Stokes' shifts from 158 to 187 nm (Table 1 and Figure 1). The large Stokes' shifts presented by **5-7** are a desired feature for fluorescent probes because allowed an improved separation of the light inherent to the matrix and the light dispersed by the sample.[40]

To further characterize the ICT nature of the absorption and emission bands and to understand the solvent relaxation mechanism of probes **5**, **6** and **7**, fluorescence solvatochromism measurements were performed.[41] As it has been reported, upon excitation of fluorophores with D-π-A (donor-π-acceptor) structures an intramolecular charge transfer (ICT) occurs and this process is expected to be sensitive to solvent changes. In fact, the emission spectra of the

ICT fluorophores have been reported to shift in response to the changes of the solvent polarity.[42] Taking into account the above mentioned facts, we measured the emission of probe **5** in different dioxane-acetonitrile mixtures ranging from pure dioxane to pure acetonitrile. The obtained results are depicted in Figure 2. As could be seen, upon increasing the relative solvent polarity (water as standard for the polarity of 1.000) from 0.164 (pure dioxane) to 0.460 (pure acetonitrile),[43] the emission maximum shifted from 463 to 552 nm. Besides, a progressive increase of acetonitrile content in the mixture induced moderate shifts of the emission of probe **5**. The obtained shifts could be ascribed to a solvent relaxation process. At this respect, the strong dipole-dipole interaction between the probe in its excited state and the surrounding solvent molecules induced a decrease in the emission energy that was reflected in the observed redshifted bands. The photophysical features of the three probes were also investigated in ethanol (see Table S1 in Supporting Information).

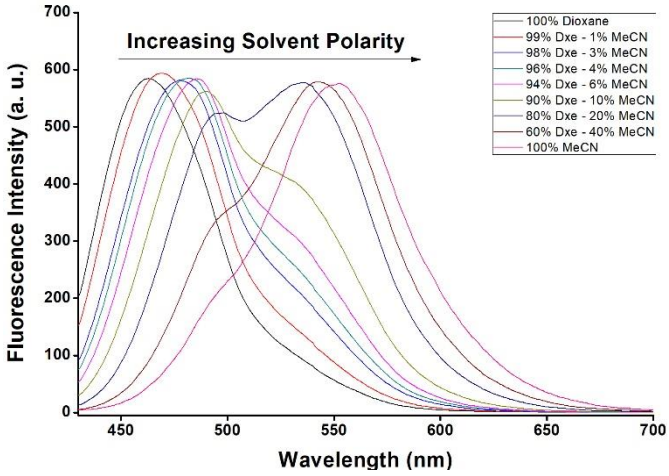

Figure 2. Emission band shifts of probe **5** in different dioxane-acetonitrile mixtures.

- ***UV-visible studies in the presence of cations.***

After the photophysical characterization of aldehyde-functionalyzed probes **5-7** their sensing behaviour in acetonitrile in the presence of selected metal cations was evaluated. Figure 3 shows the UV-visible spectra of probe **5** in acetonitrile (1.0×10^{-5} mol L^{-1}) alone and in the presence of 10 eq. of selected metal cations. As could be seen, probe **5** presents an absorption band centred at 367 nm that remained unchanged in the presence of Pb(II), Mg(II), Ge (II), Ca(II), Zn(II), Co(II), Ni(II), Ba(II), Cd(II), Hg(II), Fe(III), In(III), As(III), Al(III), Cr(III), Ga(III), K(I), Li(I) and Na(I). However, a remarkable response was obtained upon Cu(II) addition, which induced the appearance of a marked red-shifted absorption centred at 756 nm together with a marked colour change from colourless to green (see Figure 3).

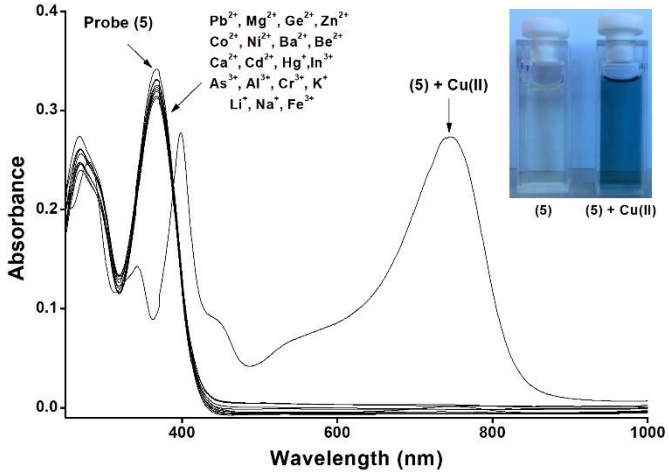

Figure 3. UV-visible spectra of probe **5** in acetonitrile (1.0×10^{-5} mol L^{-1}) alone and in the presence of 10 eq. of selected metal cations. The inset shows the change in colour of acetonitrile solutions of probe **5** alone and in the presence of Cu(II) cation.

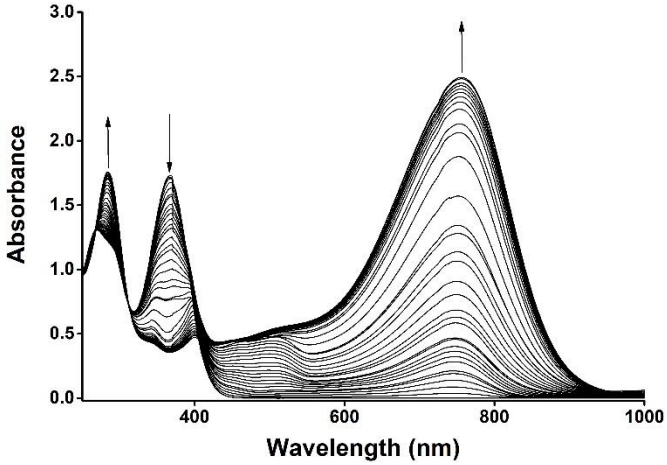

Figure 4. UV-visible titration profile of probe **5** in acetonitrile (5.0×10^{-5} mol L^{-1}) upon addition of increasing amounts of Cu(II) cation (from 0 to 10 eq.).

Then, UV-visible changes of acetonitrile solutions of probe **5** (5.0×10^{-5} mol L^{-1}) in the presence of increasing amounts of Cu(II) cation was studied. The obtained set of UV-visible spectra is shown in Figure 4. As could be seen, addition of progressive amounts of Cu(II) induced a gradual decrease of the absorption at 367 nm and the appearance of a new sharp band at 756 nm (see Figure 4). It is also remarkable the appearance of two isosbestic points at 315 and 420 nm that indicated the formation of only one species between probe **5** and Cu(II) cation. Moreover, from the titration profile a limit of detection for Cu(II) of 1.60 μM was determined (see Supporting Information, Figure S3).

Nearly the same response was obtained for probes **6** and **7**. Again, of all the cations tested, only Cu(II) induced remarkable changes in the UV-visible spectra which consisted in the appearance of red-shifted absorptions in the NIR zone at 852 and 1072 nm for probes **6** and **7** respectively (see Supporting Information, Figures S1-S2). UV-visible titration profiles of probes **6** and **7** upon addition of increasing amounts of Cu(II) cation were also obtained. As could be seen in Figure 5, addition of increasing quantities of Cu(II) cation to acetonitrile solutions of probe **6** induced a progressive decrease of the absorption centred at 398 nm

together with the growth of a band at 852 nm. This is reflected in a colour change from faint yellow to brownish-red. Besides, during the course of the titration, isosbestic points appeared at 305, 360 and 440 nm. From the titration profile (see Supporting Information, Figure S4) a limit of detection for Cu(II) of 5.12 µM was determined using probe **6**.

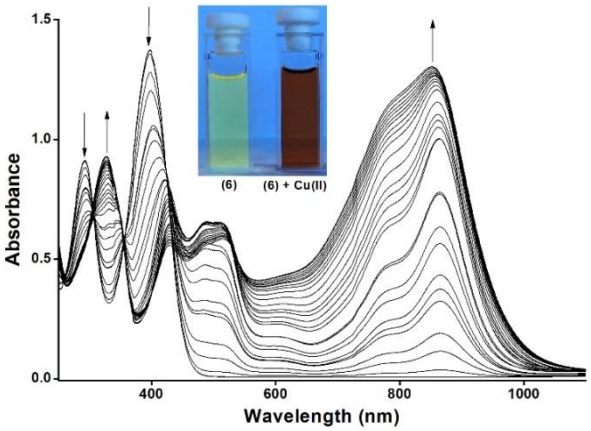

Figure 5. UV-visible titration profile of probe **6** in acetonitrile (5.0 x 10^{-5} mol L^{-1}) upon addition of increasing amounts of Cu(II) cation (from 0 to 10 eq.). The inset shows the change in colour of acetonitrile solutions of probe **6** alone and in the presence of Cu(II) cation.

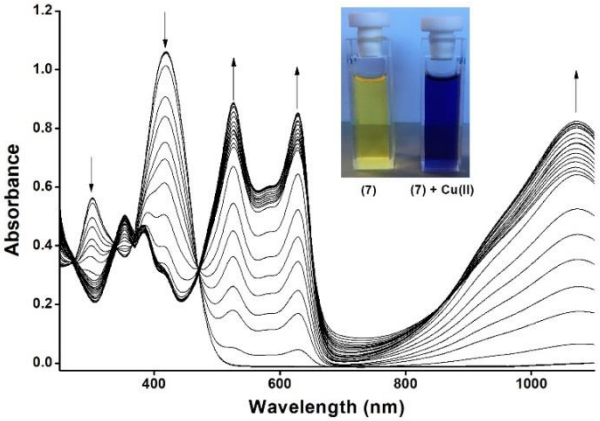

Figure 6. UV-visible titration profile of probe **7** in acetonitrile (5.0 x 10^{-5} mol L^{-1}) upon addition of increasing amounts of Cu(II) cation (from 0 to 10 eq.). The inset shows the change in colour of acetonitrile solutions of probe **7** alone and in the presence of Cu(II) cation.

Dealing with probe **7**, addition of increasing amounts of Cu(II) cation induced the progressive appearance of a main absorption band in the NIR zone at 1072 nm together with the gradual decrease of the band at 419 nm (see Figure 6). In addition, the colour changed from faint yellow to deep violet. Again, the appearance of isosbestic points at 275, 340, 370 and 450 nm indicated the presence of only one equilibrium in the interaction of probe **7** with Cu(II) cation. Finally, from the titration profile shown in Figure 6, a limit of detection for Cu(II) of 2.14 μM was found (see Supporting Information, Figure S5). The obtained limits of detection of Cu(II) for probes **5**, **6** and **7** are lower than the minimum concentration prescribed by the World Health Organization (WHO) guideline for drinking water (30 mM).[44]

In order to assess the mode of coordination between probes **5**-**7** and Cu(II) cation, Job's plot were measured. Moreover, the strength of coordination was studied *via* the evaluation of the corresponding stability constants, which were determined by UV-visible spectroscopic titrations between probes **5**, **6** and **7** and Cu(II) using Benesi−Hildebrand equation (Table 2).[45] The Job's plot obtained for probe **5** and Cu(II) cation (see Figure 7) clearly indicated the formation of 1:1 stoichiometry complexes. The same results, namely formation of 1:1 complexes, were obtained for the interaction of probes **6** and **7** with Cu(II) cation (see Supporting Information, Figures S6-S7). In order to assess if Cu(II) coordination with probes **5**-**7** was the responsible of the NIR generated bands, titrations of the complexes with EDTA were carried out. At this respect, addition of increasing amounts of EDTA to acetonitrile solutions of Cu(II)-**5**, Cu(II)-**6** and Cu(II)-**7** complexes induced the progressive disappearance of the NIR bands and the UV-visible spectra of the free probes were obtained (see Supporting Information, Figures S8 and S9). These facts clearly pointed out that observed chromogenic changes (generation of NIR bands) were due to Cu(II) coordination with probes **5**-**7**.

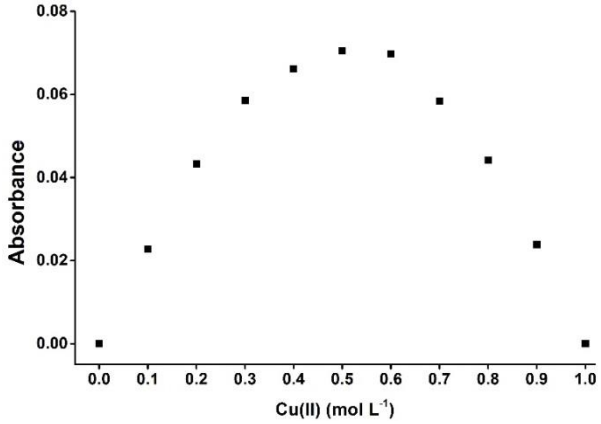

Figure 7. Job's plot for probe **5** and Cu(II) in acetonitrile. Total concentration of **5** and Cu(II) of 2.0 x 10^{-5} mol L^{-1}.

Table 2. Logarithms of the stability constants measured for the interaction of probes **5**, **6** and **7** with Cu(II) cation.

	5	**6**	**7**
Log K_a	5.39 ± 0.09	5.40 ± 0.12	6.50 ± 0.24

Moreover, the appearance of red-shifted UV-visible bands upon coordination of **5**-**7** with Cu(II) cation suggested the participation of the acceptor part of the probes in the interaction with copper. Taking into account this fact, i.e. interaction of Cu(II) cation with the electron acceptor aldehyde group in **5**-**7**, one should expect very similar stability constants for all three probes. However, although stability constants for probes **5** and **6** are quite similar (see Table 2), that found for **7** is significantly larger. This indicates that the presence of phenyl or thienyl rings, in probes **5** and **6**, as linkers of the *N*,*N*-diphenylaniline donor group with the electron acceptor aldehyde moiety seems to have negligible effect in the strength of the coordination with Cu(II) cation. On the other hand, the presence of two

electronically connected thienyl heterocycles in probe **7** increased one order of magnitude the strength of the interaction with Cu(II) cation when compared to that obtained for **5** and **6**. This fact could tentatively be indicative of the involvement of the second thienyl heterocycle in biding Cu(II) or to a more extended conjugation in probe **7** when compared with **6** (with only one thienyl linker).

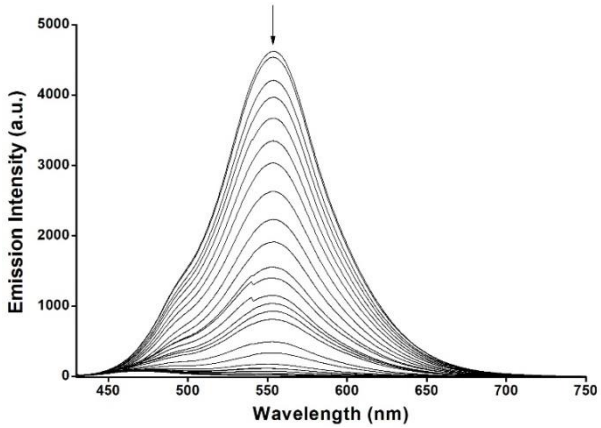

Figure 8. Fluorescence titration profile of **5** in acetonitrile (5.0 x 10^{-5} mol L^{-1}) upon addition of increasing amounts of Cu(II) cation (from 0 to 10 eq.) (λ_{ex} = 420 nm).

- ***Fluorescence studies in the presence of cations.***

Having assessed the chromogenic behaviour of the three probes in the presence of selected metal cations, in this section we carried out studies of the fluorescence response toward the same targets. At this respect, excitation at 420 nm (i.e. an isosbestic point in the Cu(II)-**5** titration profile) of acetonitrile solution of **5** (5.0 x 10^{-5} mol L^{-1}) induced the appearance of a broad emission band centred at 554 nm (see Figure 8). The response observed toward selected metal cations showed that only Cu(II) induced a progressive emission quenching (see also Figure

8). From the emission titration profile obtained, a limit of detection of 1.98 μM for Cu(II) was determined (see Supporting Information, Figure S10).

Nearly the same results were obtained for acetonitrile solutions (5.0×10^{-5} mol L^{-1}) of probes **6** and **7**, namely a marked quenching of the broad emission bands (at 559 nm after excitation at 440 nm for **6** and at 577 nm after excitation at 450 nm for **7**) after addition of increasing amounts of Cu(II) cation (see Figures in Supporting Information). Again, from the titration profiles (see Supporting Information, Figures S9-S10), limits of detection of 0.21 and 2.50 μM were measured for probes **6** and **7** respectively (see Supporting Information, Figures S11-S12).

- ***Chromo-fluorogenic studies in the presence of cations in aqueous environments.***

Finally, we tested the possible use of probes **5**-**7** in aqueous environments because this is an essential issue for monitoring environmental, biological, and industrial samples. Unfortunately, the selective chromogenic response toward Cu(II) cation in acetonitrile was not observed in the presence of small amounts of water. At this respect, water content as low as 4% prevents the formation of the corresponding complexes between probes **5** and **6** and Cu(II) cation (see Supporting Information, Figures S13-S14). On the other hand, the chromogenic response of probe **7** in the presence of Cu(II) was observed even with a ca. 7% of water (see Supporting Information, Figure S17). The absence of response of probes **5**-**7** when water was used is ascribed to the high solvation energy of Cu(II) which is not energetically compensated by the moderate interaction of Cu(II) cation with the probes.

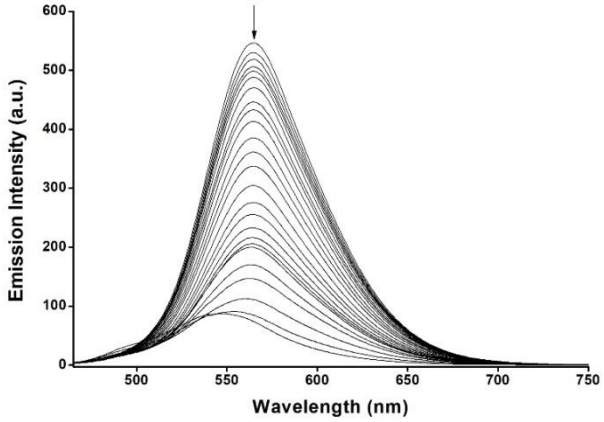

Figure 9. Fluorescence titration profile of SDS (20 mM, pH 7.5)-acetonitrile 90:10 v/v solution of probe **7** (1.0 x 10^{-5} mol L^{-1}) upon addition of increasing amounts of Cu(II) cation (from 0 to 15 eq.) (λ_{ex} = 450 nm).

One common alternative used to overcome the strong solvation effects of metal cations, that impose a highly effective energetic barrier that inhibits sensing processes in aqueous solution, is the use of surfactants. The use of chemical probes embedded in micelles for the chromo-fluorogenic detection of analytes in water is a well stablished field. Several authors showed that selected binding sites and fluorophores can be arranged in micelles of surfactants allowing detection of metal cations in water by changes in fluorescence.[46]

Taking into account these facts, and considering that chromogenic response of **7** toward Cu(II) cation was observed even with a ca. 7% of water, we studied the fluorogenic response of this probe to metal cations in sodium dodecyl sulfate (SDS) (20 mM, pH 7.5)-acetonitrile 90:10 v/v solution. Probe **7** is weakly soluble in pure water but is completely solubilized in SDS (20 mM, pH 7.5)-acetonitrile 90:10 v/v mixture. This solubilisation could be ascribed to the inclusion of probe **7** into the inner hydrophobic core of the SDS micelles. SDS aqueous solution of probe **7** presented a marked emission band centred at 565 nm upon excitation at 450 nm. Addition of 10 eq. of Ba(II), Pb(II), Mg(II), Co(II), Ni(II), Be(II), Ca(II), Cd(II), In(III),

As(III), Al(III), Cr(III), K(I), Li(I), Na(I) induced negligible changes in the emission of probe **7**. As clear contrast, in the presence of Zn(II) a moderate emission quenching (ca. 30% of the initial probe fluorescence) the was observed. However, addition of Cu(II) induced a marked ca. 80% reduction in the emission intensity of the probe (see Supporting Information, Figure S18). This emission quenching was ascribed to a proper SDS-assisted internalization of Cu(II) cation into the inner micellar core with subsequent interaction with probe **7**.

Once assessed the selective response of probe **7** in SDS (20 mM, pH 7.5)-acetonitrile 90:10 v/v solution, the emission behaviour upon addition of increasing amounts of Cu(II) cation was tested. The obtained results are shown in Figure 9. As could be seen, addition of increasing amounts of Cu(II) cation induced a progressive quenching of the emission band centred at 565 nm. From the titration profile (shown in the Supporting Information, Figure S19) a limit of detection of 3.8 μM for Cu(II) was determined. This limit of detection is very similar to that obtained with **7** in acetonitrile (2.50 μM) which indicated a small reduction in probe sensitivity toward Cu(II) cation. These results clearly indicated that probe **7** could be used to detect Cu(II) in real aqueous samples, with remarkable selectivity and sensitivity, using an anionic surfactant such as SDS.

5.4 Conclusions

In summary, we described herein the synthesis (using Suzuki coupling reactions), photophysical characterization and chromo-fluorogenic studies toward metal cations in acetonitrile of three heterocyclic aldehydes (**5**, **6** and **7**). The three probes presented intramolecular charge-transfer broad absorption bands in the 360-420 nm range due to the presence of *N*,*N*-diphenylanilino donor moieties electronically conjugated with aldehyde acceptor group through aryl or thienyl spacers. Besides, the probes are weakly to moderate emissive with fluorescence bands in the 540-580 nm range. Of all the cations tested, only Cu(II) induced the

appearance of strong absorption bands in the NIR zone together with remarkable colour changes for the three probes. Besides, Cu(II) cation induced marked emission quenching for the three probes. The observed colour/emission modulations were ascribed to the formation of 1:1 probe-Cu(II) complexes in which the metal cation interacts with the acceptor part of the probes. In addition, the limits of detection determined using UV-visible and fluorescence titrations are in the 0.21-5.12 μM range. This is below the minimum concentration prescribed by the World Health Organization (WHO) guideline for drinking water is set at 30 mM. Inclusion of probe **7** inside SDS micelles allowed Cu(II) detection in aqueous environments.

5.5 Experimental

- ***Synthesis and characterization of the probes.***

Reaction progress was monitored by thin layer chromatography (0.25 mm thick pre-coated silica plates: Merck Fertigplatten Kieselgel 60 F_{254}), while purification was carried out by silica gel column chromatography (Merck Kieselgel 60; 230-400 mesh). NMR spectra were obtained on a Bruker Avance III 400 at an operating frequency of 400 MHz for ^{1}H and 100.6 MHz for ^{13}C using the solvent peak as internal reference. The solvents are indicated in parenthesis before the chemical shift values (δ relative to TMS and given in ppm). Melting points were determined on a Gallenkamp apparatus. Infrared spectra were recorded on a BOMEM MB 104 spectrophotometer. Mass spectrometry analyses were performed at the "C.A.C.T.I.-Unidad de Espectrometria de Masas" at the University of Vigo, Spain. All commercially available reagents were used as received. Boronic acids **1a**, **2b** and **3b** and brominated derivatives **2a** and **3a** were commercially available. We have previously reported the synthesis of the precursor aldehyde **4**.[47]

- ***General procedure for the synthesis of heterocyclic aldehydes 5, 6 and 7 (via a).***

4-(Diphenylamino)phenylboronic acid **1a** (2.5 mmol) and aromatic or heterocyclic bromides **2a**, **3a** and **4** (1.9 mmol) were coupled in a mixture of DME (30 mL), ethanol (2 mL), aqueous Na_2CO_3 (2 mL, 2 M) and $Pd(PPh_3)_4$ (3 mol %) at 80 °C, by stirring under nitrogen. The reaction was monitored by TLC, which determined the reaction time (12 h). After cooling, the mixture was extracted with ethyl acetate (30 mL), a saturated solution of NaCl was added (15 mL) and the phases were separated. The organic phase was washed with water (3 × 20 mL) and with a 10% solution of NaOH (30 mL). The organic phase obtained was dried with anhydrous $MgSO_4$, filtered, and the solvent removed to give a crude mixture. The crude product was purified using column chromatography (silica gel, and chloroform as eluent) to afford the pure coupled products **5** (95%), **6** (96%) and **7** (88%).

4-(4'-(Diphenylamino)phenyl)phenyl-carbaldehyde (5).

Yellow solid (168 mg, 95%). Mp: 113.6-114.1 °C. FTIR (CH_2Cl_2): *v* = 3420, 3036, 2828, 2734, 1698, 1592, 1491, 1329, 1282, 1170, 816, 696 cm^{-1}. ^1H NMR (DMSO-d_6): δ = 7.12 (dt, J = 7.2 and 1.2 Hz, 2H, 2×H-4''), 7.18 – 7.21 (m, 6H, H-3', H-5', 2× H-2'' and 2×H-6''), 7.32 (dt, J = 7.2 and 1.2 Hz, 4H, 2×H-3'' and 2×H-5''), 7.55 (dd, J = 6.8 and 2.0 Hz, 2H, H-2' and H-6'), 7.75 (dd, J = 6.8 and 2.0 Hz, 2H, H-3 and H-5), 7.95 (dd, J = 6.8 and 2.0 Hz, 2H, H-2 and H-6), 10.05 (s, 1H, CHO) ppm. ^{13}C NMR (DMSO-d_6): δ = 122.92 (C-3' and C-5'), 123.33 (C-4''), 124.69 (C-2'' and C-6''), 126.66 (C-3 and C-5), 127.85 (C-2' and C-6'), 129.26 (C-3'' and C-5''), 130.14 (C-2 and C-6), 132.53 (C-1'), 134.50 (C-1), 146.29 (C-4), 147.12 (C-1''), 148.21 (C-4'), 191.52 (CHO) ppm. Anal. Calcd for $C_{25}H_{19}NO$: C, 85.90; H, 5.50; N, 4.00. Found: C, 85.79; H, 5.50; N, 3.80.

5-(4'-(Diphenylamino)phenyl)thiophene-2-carbaldehyde (6).[34]

Green solid (83 mg, 96%). Mp: 120.2-121.0 °C. FTIR (CH_2Cl_2): *v* = 3423, 1660, 1591, 1530, 1490, 1444, 1329, 1283, 1228, 1193, 1179, 804, 755, 696 cm^{-1}. ^1H NMR (DMSO-d_6): δ = 7.07 – 7.17 (m, 8H, H-3', H-5', 2× H-2'', 2× H-4'' and 2×H-6''), 7.29 – 7.33 (m, 5H, H-4 and 2× H-3'' and 2×H-5''), 7.52 (dd, J = 6.8 and 2.0 Hz, 2H, H-2' and H-6'), 7.71 (d, J = 4.0 Hz, 1H, H-3), 9.86 (s, 1H, CHO) ppm. ^{13}C NMR (DMSO-d_6): δ = 122.24 (C-4''), 122.78 (C-4), 123.78 (C-3' and C-5'), 125.06 (C-2'' and C-6''), 126.00 (C-1'), 127.13 (C-2' and C-6'), 129.39 (C-3'' and C-5''), 137.66 (C-3), 141.19 (C-5), 146.84 (C-1''), 149.01 (C-4'), 154.40 (C-2), 182.45 (CHO) ppm.

5-(4'-(Diphenylamino)phenyl)-2,2''-bithiophene-5''-carbaldehyde (7).[36]

Orange solid (176 mg, 88%). Mp: 152.6-153.0 °C. FTIR (CH_2Cl_2): *v* = 3424, 2362, 2094, 1656, 1490, 1453, 1382, 1329, 1276, 1225, 1050, 870, 797, 753, 695, 664 cm^{-1}. ^1H NMR (DMSO-d_6): δ = 7.05 – 7.15 (m, 8H, H-3', H-5', 2× H-2'', 2× H-4'' and 2×H-6''), 7.18 (d, J = 3.6 Hz, 1H, H-4'''), 7.25 (d, J = 4.0 Hz, 1H, H-3'''), 7.27 – 7.31 (m, 4H, 2× H-3'' and 2×H-5''), 7.33 (d, J = 4.0 Hz, 1H, H-4), 7.47 (dd, J = 8.8 and 2.4 Hz, 2H, H-2' and H-6'), 7.68 (d, J = 3.6 Hz, 1H, H-3), 9.86 (s, 1H, CHO) ppm. ^{13}C NMR (DMSO-d_6): δ = 123.12 (C-4'''), 123.17 (C-3'''), 123.46 (C-3' and C-5'), 123.73 (C-4), 124.80 (C-3), 126.61 (C-2'' and C-6''), 127.08 (C-2' and C-6'), 127.23 (C-5), 129.39 (C-3'' and C-5''), 134.05 (C-5'''), 137.43 (C-4'''), 141.26 (C-2'''), 146.27 (C-1'), 147.24 (C-1''), 147.44 (C-2), 148.04 (C-4'), 182.40 (CHO) ppm.

- ***General procedure for the synthesis of heterocyclic aldehydes 5 and 6 (via b).***

4-Bromo-*N,N*-diphenylaniline **1b** (1.9 mmol) and boronic acids **2b** and **3b** (2.5 mmol), were coupled in a mixture of DME (30 mL), ethanol (2 mL), aqueous Na_2CO_3 (2 mL, 2 M) and $Pd(PPh_3)_4$ (3 mol %) at 80 ^oC, by stirring under nitrogen. The reaction was monitored by TLC, which determined the reaction time (12 h). After cooling, the mixture was extracted with ethyl acetate (30 mL), a saturated solution of NaCl was added (15 mL) and the phases were separated. The organic phase was washed with water (3 × 20 mL) and with a 10% solution of NaOH (30 mL). The organic phase obtained was dried with anhydrous $MgSO_4$, filtered, and the solvent removed to give a crude mixture. The crude product was purified using column chromatography (silica gel, and chloroform as eluent) to afford the pure coupled products **5**, and **6**, in 84 and 42 % yield, respectively.

- ***General methods.***

All cations, in the form of perchlorate salts, were purchased from Sigma–Aldrich Chemical Co., stored in a desiccator under vacuum containing self-indicating silica, and used without any further purification. Solvents were dried according to standard procedures. Unless stated otherwise, commercial grade chemicals were used without further purification. All the photophysical experiments were performed with freshly prepared, air-equilibrated solutions at room temperature (293 K). UV-visible absorption spectra (200–1100 nm) were recorded using a JASCO V-650 spectrophotometer (Easton, MD, USA). Fluorescence spectra were collected using a FluoroMax-4 spectrofluorometer and fluorescence quantum yields were determined according to literature procedures using dilute solutions (1.0×10^{-5} M) of the compounds and 9,10-diphenylanthracene (DPA) in ethanol as fluorescence standard ($\Phi_F = 0.95$).[39]

- ***Sensing measurements.***

Acetonitrile solutions of the three probes (1.0×10^{-5} mol L^{-1} for UV-visible measurements and 5.0×10^{-5} mol L^{-1} for emission studies) were prepared and stored in the dry atmosphere. Solutions of perchlorate salts of the respective cations (1.5×10^{-3} mol L^{-1}) were prepared in distilled acetonitrile and were stored under a dry atmosphere.

5.6 Acknowledgements

We thank the Spanish Government (MAT2015-64139-C4-1-R) and Generalitat Valenciana (PROMETEO2018/024). H. E. O. thanks Generalitat Valenciana for his Grisolia fellowship. Thanks are due to *Fundação para a Ciência e Tecnologia (FCT)* for a PhD grant to R. C. M. Ferreira (SFRH/BD/86408/2012), and FEDER (European Fund for Regional Development)-COMPETE-QREN-EU for financial support through the Chemistry Research Centre of the University of Minho (Ref. UID/QUI/00686/2016 and UID/QUI/0686/2019). The NMR spectrometer Bruker Avance III 400 is part of the National NMR Network and was purchased within the framework of the National Program for Scientific Re-equipment, contract REDE/1517/RMN/2005 with funds from POCI 2010 (FEDER) and FCT.

5.7 References and Notes

1. (a) P. R. Sahoo, K. Prakash, S. Kumar, *Coord. Chem. Rev.*, 2018, **357**, 18-49; (b) K. Baljeet, K. Navneet, S. Kumar, *Coord. Chem. Rev.*, 2018, **358**, 13-69; (c) S. Gandhi, M. Iniya, T. Anand, N. G. Kotla, O. Sunnapu, S. Singaravadivel, A. Gulyani, D. Chellappa, *Coord. Chem. Rev.*, 2018, **357**, 50-104; (d) Y. Zhang, S. Yuan, G. Day, X. Wang, X. Yang, H. C. Zhou, *Coord. Chem. Rev.*, 2018, **354**, 28-45.

2. (a) N. Kwon, H. Ying, Y. Juyoung, *ACS Omega*, 2018, **3**, 13731−13751; (b) T. Rasheed, M. Bilal, F. Nabeel, H. M. N. Iqbal, L. Chuanlong, Y. Zhou, *Sci Total Environ*, 2018, **615**, 476–485.

3. (a) D.G.J. Barceloux, *Clin. Toxicol.*, 1999, **37**, 217-230; (b) M. C. Linder, M. H. Azam, *Am. J. Clin. Nutr.*, 1996, **63**, 797S − 811S.

4. (a) R. Uauy, M. Olivares, M. Gonzalez, *Am. J. Clin. Nutr.*, 1998, **67**, 952S – 959S; (b) G. E. Cartwright, M. M. Wintrobe, *Am. J. Clin. Nutr.*, 1964, **14**, 224 – 232; (c) D. Strausak, J. F. Mrcer, H. H. Dieter, W. Stremmel, G. Multhaup, *Brain Res. Bull.*, 2001, **55**, 175 – 185.

5. (a) E. Gaggelli, H. Kozlowski, D. Valensin, G. Valensin, *Chem. Rev.*, 2006, **106**, 1995−2044; (b) T. V. O. Halloran, V. C. Culotta, *J. Biol. Chem.*, 2000, **275**, 25057−25060; (c) A. C. Rosenzweig, T. V. O. Halloran, *Curr. Opin. Chem. Biol.* 2000, **4**, 140−147; (d) A. Singh, Q. Yao, L. Tong, W. C. Still, D. Sames, *Tetrahedron Lett.*, 2000, **41**, 9601−9605.

6. (a) B. Atreyee, *Sci. Revs. Chem. Commun.*, 2015, **5**, 77-87; (b) D. M. Medeiros, *Biol. Trace Elem. Res.*, 2017, **176**, 10-19; (c) X. Jingshu, P. Begley, S. J. Church, S. Patassini, S. McHarg, N. Kureishy, K. A. Hollywood, H. J. Waldvogel, H. Liu, S. Zhang, *Sci. Rep.*, 2016, **6**, 27524; (d) P. M. Shetty, P. J. Hauptman, L. K. Landfried, K. Patel, E. P. Weiss, *J. Card. Fail.*, 2015, **21**, 968-972.

7. I. F. Scheiber, J. F. B. Mercer, R. Dringen, *Prog. Neurobiol.*, 2014, **116**, 33-57.

8. S. Lutsenko, *Biochem. Soc. Trans.*, 2008, **36**, 1233.

9. S. G. Kaler, *Nat. Rev. Neurol.*, 2011, **7**, 15-29.

10. E. L. Que, D. W. Domaille, C. J. Chang, *Chem. Rev.*, 2008, **108**, 1517-1549.

11. P. Davies, P. C. McHugh, V. J. Hammond, F. Marken, D. R. Brown, *Biochemistry,* 2011, **50**, 10781-10791.

12. M. G. Savelieff, S. Lee, Y. Liu, M. H. Lim, *ACS Chem. Biol.*, 2013, **8**, 856–865.

13. G. Xiao, Q. Fan, X. Wang, B. Zhou, *Proc. Natl. Acad. Sci. U.S.A.*, 2013, **110**, 14995-15000.

14. L. J. Hayward, J. A. Rodriguez, J. W. Kim, A. Tiwari, J. J. Goto, D. E. Cabelli, J. S. Valentine, R. H. J. Brown, *J. Biol Chem.*, 2002, **277**, 15923–15931.

15. D. Huster, S. Lutsenko, *Mol. BioSyst.*, 2007, **3**, 816-824.

16. J. S. Zavahir, Y. Nolvachai, P. J. Marriott, *Trends Anal. Chem.*, 2018, **99**, 47-65

17. L. Zhao, S. Zhong, K. Fang, Z. Qian, J. Chen, *J. Hazard. Mater.*, 2012, **239–240**, 206–212.

18. M. Porento, V. Sutinen, T. Julku, R. Oikari, *Appl. Spectrosc.*, 2011, **65**, 678–683.

19. C. M. Q. Montalvána, L. E. G. Pineda, L. Á. Contreras, R. Valdez, N. Arjona, M. T. O. Guzmán, *J. Electrochem. Soc.*, 2017, **164**, B304-B313.

20. K. Kukuś, D. Banaś, J. Braziewicz, U. Majewska, M. Pajek, J. W. Mościko, G. Antczak, B. Borkowska, S. Góźdź, J. S. Kalwat. *Biol. Trace Elem. Res.*, 2014, **158**, 22–28.

21. G. G. V. Kumar, M. P. Kesavan, G. Sivaraman, J. Annaraj, K. Anitha, A. Tamilselvi, S. Athimoolam, B. Sridhar, J. Rajesh, *Sens. Actuators B Chem.*, 2018, **255**, 3235-3247.

22. Q. Wang, K. Huang, S. Cai, C. Liu, X. Jiao, S. He, L. Zhao, X. Zeng, *Org. Biomol. Chem.*, 2018, **16**, 7163-7169.

23. P. Li, X. Duan, Z. Chen, Y. Liu, T. Xie, L. Fang, X. Li, M. Yin, B. Tang, *Chem. Commun.*, 2011, **47**, 7755-7757.

24. (a) J. Roncali, Macromol. *Rapid Commun.*, 2007, **28**, 1761-1775; (b) A. Mishra, C.-Q. Ma, P. Bäuerle, *Chem. Rev.*, 2009, **109**, 1141-1276; (c) L. R. Dalton, P. A. Sullivan, D. H. Bale, *Chem. Rev.*, 2010, **110**, 25-55; (d) Y. Wu, W. Zhu, *Chem. Soc. Rev.*, 2013, **42**, 2039-2058; (e) F. Bures, *RSC Adv.*, 2014, **4**, 58826-58851.

25. See for example: (a) M. M. M. Raposo, G. Kirsch, *Tetrahedron*, 2003, **59**, 4891-4899; (b) E. Genin, V. Hugues, G. Clermont, C. Herbivo, A. Comel, M. C. R. Castro, M. M. M. Raposo, M. Blanchard-Desce, *Photochem. Photobiol. Sci.*, 2012, **11**, 1756-1766; (c) M. M. M. Raposo, C. Herbivo, V. Hugues, G. Clermont, M. C. R. Castro, A. Comel, M. B. Desce, *Eur. J. Org. Chem.*, 2016, **31**, 5263-5273.

26. See for example: (a) C. Marín-Hernández, L. E. Santos-Figueroa, M. E. Moragues, M. M. M. Raposo, R. M. F. Batista, S. P. G. Costa, T. Pardo, R. Martínez-Máñez, F. Sancenón, *J. Org. Chem.*, 2014, **79**, 10752-10761; (b) J. Pina, J. S. Seixas de Melo, R. M. F. Batista, S. P. G. Costa, M. M. M. Raposo, *J. Org. Chem.*, 2013, **78**, 11389-11395; (c) S. S. M. Fernandes, M. C. R. Castro, I. Mesquita, L. Andrade, A. Mendes, M. M. M. Raposo, *Dyes Pigm.,* 2017, **136**, 46-53; (d) R. C. M. Ferreira, S. P. G. Costa, M. M. M. Raposo, *New J. Chem.* 2018, **42**, 3483-3492.

27. (a) M. M. M. Raposo, B. García-Acosta, T. Ábalos, P. Calero, R. Martínez-Máñez, J. V. Ros-Lis, J. Soto, *J. Org. Chem.*, 2010, **75**, 2922-2933; (b) L. E. Santos-Figueiroa, M. Moragues, M. M. M. Raposo, R. M. F. Batista, S. P. G. Costa, R. C. M. Ferreira, F. Sancénon, R. Martínez-Máñez, J. V. Ros-Lis, J. Soto, *Org. Biomol. Chem.*, 2012, **10**, 7418-7428; (c) T. Ábalos, D. Jiménez, R. Martínez-Máñez, J. V. Ros-Lis, S. Royo, F. Sancenón, J. Soto, A. M. Costero, S. Gil, M. Parra, *Tetrahedron Lett.*, 2009, **50**, 3885-3888; (d) T. Ábalos, D. Jiménez, M. Moragues, S. Royo, R. Martínez-Máñez, F. Sancenón, J. Soto, A. M. Costero, M. Parra, S. Gil, *Dalton Trans.*, 2010, **39**, 3449-3459; (e) A. Barba-Bon, A. M. Costero, S. Gil, M. Parra, J. Soto, R. Martínez-Máñez, F. Sancenón, *Chem. Commun.*, 2012, **48**, 3000-3002; (f) T. Ábalos, M. Moragues, S. Royo, D. Jiménez, R. Martínez-Máñez, J. Soto, F. Sancenón, S. Gil, J. Cano, *Eur. J. Inorg. Chem.*, 2012, 76-84; (g) M. Lo Presti, S. El Sayed, R. Martínez-Máñez, A. M. Costero, S. Gil, M. Parra, F. Sancenón, *New. J. Chem.*, 2016, **40**, 9042-9045; (h) B. Lozano-Torres, S. El Sayed, A. M. Costero, S. Gil, M. Parra, R. Martínez-Máñez, F. Sancenón, *Bull. Chem. Soc. Japan*, 2016, **89**, 498-500.

28. J. O. Morley, D. Push, *J. Chem. Soc. Faraday Trans.*, 1991, **87**, 3021-3025.

29. J. March, "Advanced Organic Chemistry: reactions, mechanisms, and structure", *4th ed. Wiley: New York*, 1992, **45**.

30. a) V. Hrobároková, P. Hrobárik, P. Gajdos, I. Fitilis, M. Fakis, P. Persephonis, P. Zahradník, *J. Org. Chem.*, 2010, **75**, 3053-3068; (b) V. Parthasarathy, S. Fery-Forgues, E. Campioli, G. Recher, F. Terenziani, M. Blanchard-Desce, *Small.*, 2011, **7**, 3219-3229; (c) P. Hrobárik, V. Hrobáriková, V. Semak, P. Kasák, E. Rakovský, I. Polyzos, M. Fakis, P. Persephonis, *Org. Lett.*, 2014, **16**, 6358-6361; (d) D. Cvejn, E. Michail, K. Seintis, M. Klikar, O. Pytela, T. Mikysek, N. Almonasy, M. Ludwig, V. Giannetas, M. Fakis, F. Bures, *RSC Adv.*, 2016, **6**, 12819-12828.

31. (a) J. Wang, K. Liu, L. Ma, *Chem. Rev.*, 2016, **116**, 14675-14725; (b) A. Mahmood, *Sol. Energy*, 2016, **123**, 127-144; (c) F. Liu, H. Xiao, Y. Yang, H. Wang, H. Zhang, J. Liu, S. Bo, Z. Zhen, X. Liu, L. Qiu, *Dyes Pigm.*, 2016, **130**, 138-147; (d) J. Wu, B. A. Wilson, D. W. J. Smith, S. O. Nielsen, *J. Mater. Chem. C*, 2014, **2**, 2591-2599; (e) Y.-J. Cheng, J. Luo, S. Hau, D. H. Bale, T.-D. Kim, Z. Shi, D. B. Lao, N. M. Tucker, Y. Tian, L. R. Dalton, P. J. Reid, A. K.-Y. Jen, *Chem. Mater.*, 2007, **19**, 1154-1163; (f) S. Suresh, H. Zengin, B. K. Spraul, T. Sassa, T. Wada, D. W. Smith, *Tetrahedron Lett.*, 2005, **46**, 3913-3916; (g) C. Cai, I. Liakatas, M.-S. Wong, M. Bosch, C. Bosshard, P. Günter, S. Concilio, N. Tirelli, U. W. Suter, *Org. Lett.*, 1999, **1**, 1847-1849.

32. (a) N. Robertson, *Angew. Chem. Int. Ed.,* 2006, **45**, 2338–2345; (b) S. Zhu, Z. An, X. Sun, Z. Wu, X. Chen, P. Chen, *Dyes Pigm.*, 2015, **120**, 85–92; (c) M. Liang, J. Chen, *Chem. Soc. Rev.*, 2013, **42,** 3453–3488. (d) M. Velusamy, K. R. J. Thomas, J. T. Lin, Y. C. Hsu, K. C. Ho, *Org. Lett.*, 2005, **7,** 1899–1902; (e) W. Zhu, Y. Wu, S. Wang, W. Li, X. Li, J. Chen, *Adv. Funct. Mater.*, 2011, **21**, 756–763; (f) H. H. Chou, Y. Chen, H. J. Huang, T. H. Lee, J. T. Lin, C. Tsai, *J. Mater. Chem.*, 2012, **22**, 10929–10938; (g) D. H. Roh, K. M. Kim, J. S. Nam, U. Y. Kim, B. M. Kim, J. S. Kim, *J. Phys. Chem. C*, 2016, **120,** 24655–24666.

33. (a) A. Suzuki, *J. Organomet. Chem.*, 1999, **576**, 147-168; (b) F. Bellina, A. Carpita, R. Rossi, *Synthesis*, 2004, **15**, 2419-2440.

34. D. P. Hagberg, T. Marinado, K. M. Karlsson, K. Nonomura, P. Qin, G. Boschloo, T. Brinck, A. Hagfeldt, L. Sun, *J. Org. Chem.*, 2007, **72**, 9550-9556.

35. C. Sissa, V. Parthasarathy, D. Drouin-Kucma, M. H. V. Werts, M. Blanchard-Desce, F. Terenziani, *Phys. Chem. Chem. Phys.*, 2010, **12**, 11715-11727.

36. (a) Y. J. Chang, T. J. Chow, *Tetrahedron*, 2009, **65**, 4726-4734; (b) A. Gupta, A. Ali, A. Bilic, M. Gao, K. Hegedus, B. Singh, S. E. Watkins, G. J. Wilson, U. Bach, R. A. Evans, *Chem. Commun.*, 2012, **48**, 1889-1891.

37. K. R. J. Thomas, Y. C. Hsu, J. T. Lin, K. M. Lee, K. C. Ho, C. H. Lai, Y. M. Cheng, P.-T. Chou, *Chem. Mater.*, 2008, **20**, 1830-1840.

38. K. Amro, J. Daniel, G. Clermont, T. Bsaibess, M. Pucheault, E. Genin, M. Vaultier, M. D. Blanchard, *Tetrahedron*, 2014, **70**, 1903-1909.

39. J. V. Morris, M. A. Mahaney, R. Huberr, *J. Phys. Chem.*, 1976, **80**, 969-974.

40. M. G. Holler, L. F. Campo, A. Brandelli, V. Stefani, J. *Photochem. Photobiol. A Chem.*, 2002, **149**, 217-225.

41. B. Pullman, J. Jortner, Intramolecular dynamics, in: Proceedings of the 15th Jerusalem Symposium, Israel, 1982, vol. 15, D. Reidel Publishing Company, Dordrecht, Holland, 1982.

42. (a) K. C. Moss, K. N. Bourdakos, V. Bhalla, K. T. Kamtekar, M. R. Bryce, M. A. Fox, H. L. Vaughan, F. B. Dias, A. P. Monkman, *J. Org. Chem.*, 2010, **75**, 6771– 6781; (b) G. L. Fu, H. Y. Zhang, Y.Q. Yan, C.H. Zhao, *J. Org. Chem.,* 2012, **77**, 1983–1990.

43. C. Reichardt, Solvents and solvents effects in organic chemistry, Wiley-VCH Publishers, 3rd Ed., 2003.

44. Environmental Protection Agency, National Primary Drinking Water Regulations for Lead and Copper, 2007, **195**.

45. (a) H. Benesi, J. Hildebrand, *J. Am. Chem. Soc.*, 1949, **71**, 2703–2707; (b) B. Arnold, A. Euler, K. Fields, R. Zaini, *J. Phys. Org. Chem.*, 2000, **13**, 729–34.

46. See for example: (a) P. Grandini, F. Mancin, P. Scrimin, U. Tonellato, *Angew. Chem. Int. Ed.*, 1999, **38**, 3061-3064; (b) M. Arduini, E. Rampazzo, F. Mancin, P. Tecilla, U. Tonellato, *Inorg.*

Chim. Acta, 2007, **360**, 721-727; (c) P. Pallavicini, L. Pasotti, S. Patroni, *Dalton Trans.*, 2007, 5670-5677.

47. S. P. G. Costa, R. M. F. Batista, M. M. M. Raposo, *Tetrahedron*, 2008, **64**, 9733-9737.

5.8 Supporting information

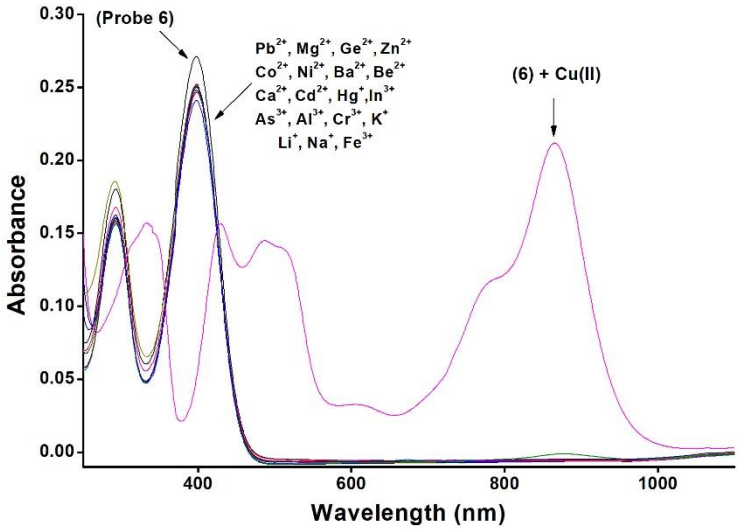

Figure S1. UV/visible spectra of probe **6** (1.0 x 10^{-5} mol L^{-1}) in acetonitrile alone and in the presence of 10 eq. of selected metal cations.

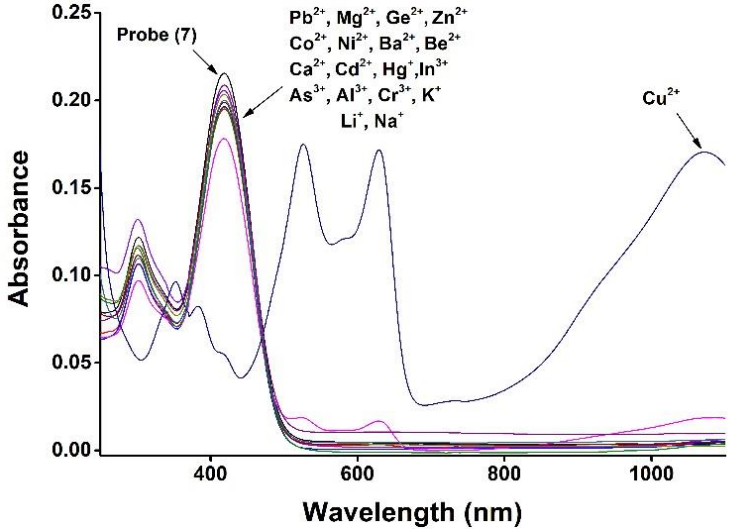

Figure S2. UV/visible spectra of probe **7** (1.0 x 10^{-5} mol L^{-1}) in acetonitrile alone and in the presence of 10 eq. of selected metal cations.

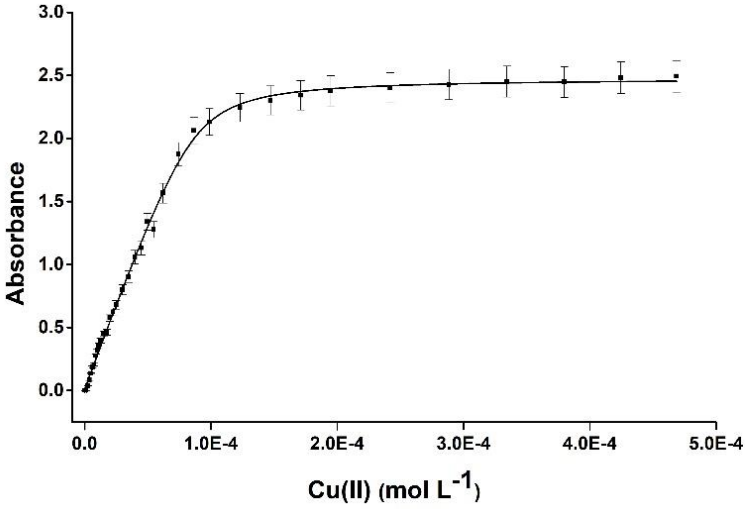

Figure S3. Absorbance of probe **5** (1.0 x 10^{-5} mol L^{-1} in acetonitrile) at 756 nm vs Cu(II) concentration.

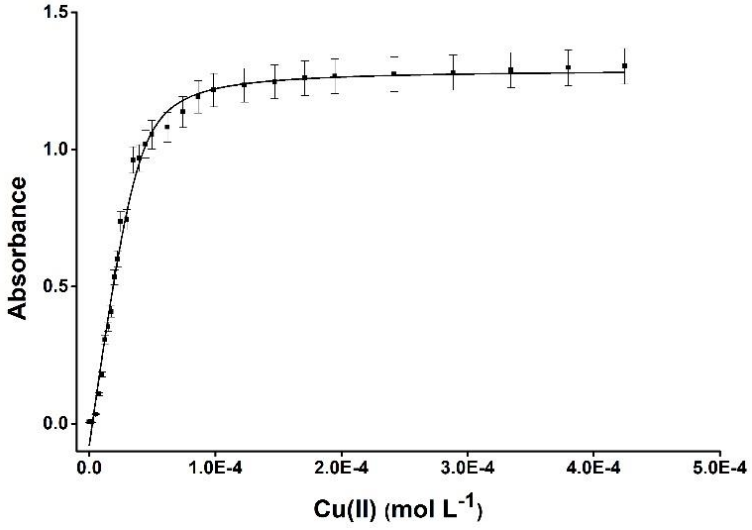

Figure S4. Absorbance of probe **6** (1.0 x 10^{-5} mol L^{-1} in acetonitrile) at 852 nm vs Cu(II) concentration.

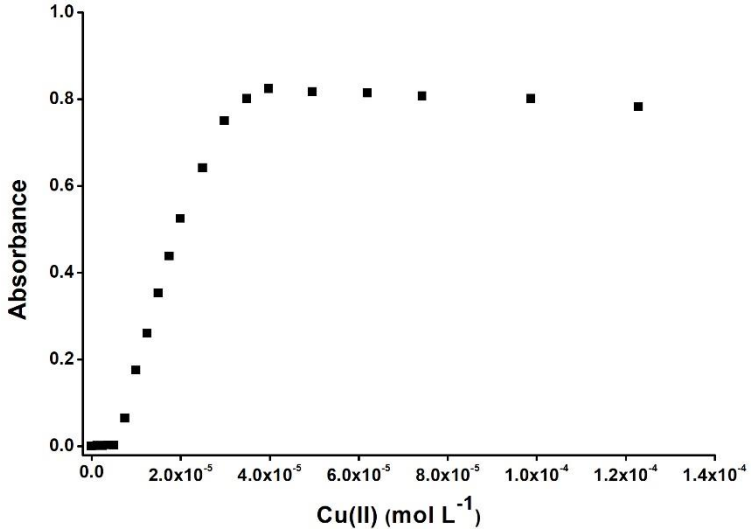

Figure S5. Absorbance of probe **7** (1.0 x 10^{-5} mol L^{-1} in acetonitrile) at 852 nm vs Cu(II) concentration.

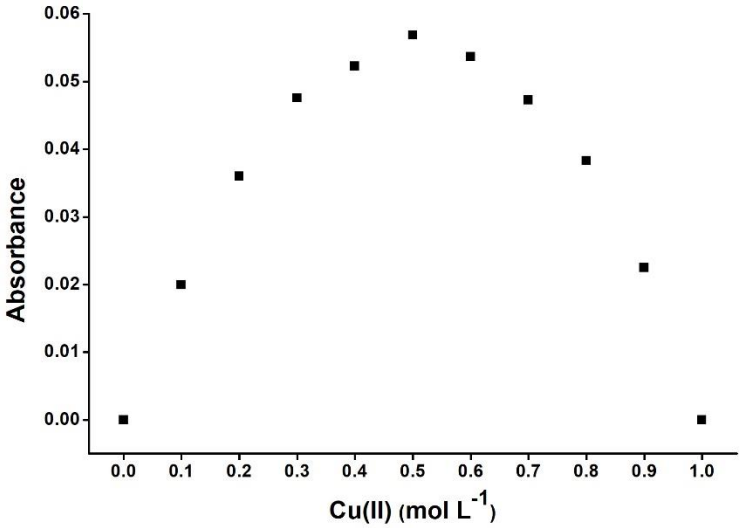

Figure S6. Job's plot for probe **6** and Cu(II) in acetonitrile. Total concentration of **6** and Cu(II) of 2.0 x 10^{-5} mol L^{-1}.

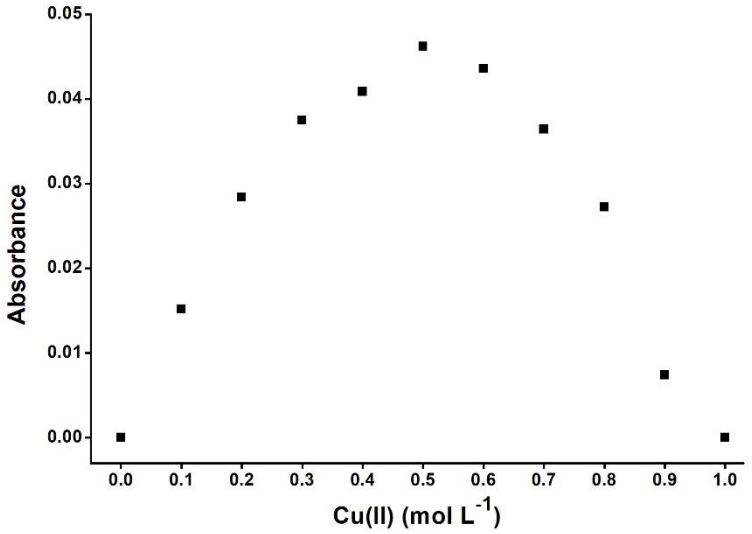

Figure S7. Job's plot for probe **7** and Cu(II) in acetonitrile. Total concentration of **7** and Cu(II) of 2.0 x 10^{-5} mol L^{-1}.

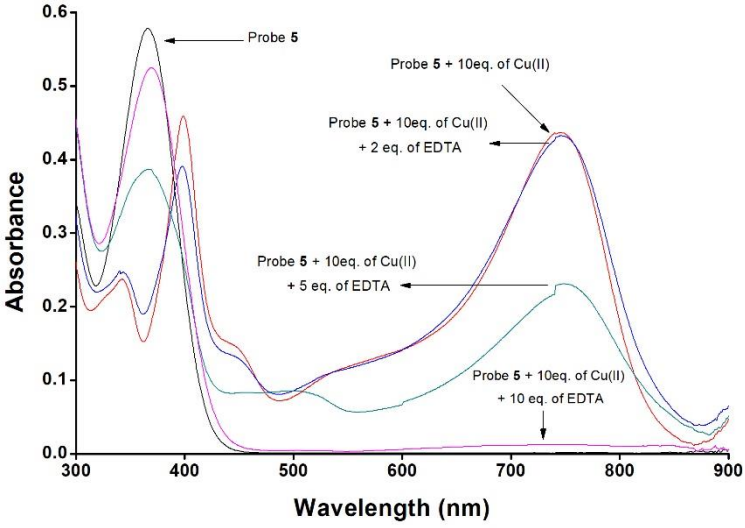

Figure S8. UV-visible profile of probe **5** in acetonitrile (1.0 x 10^{-5} mol L^{-1}) and of Cu(II)-**5** complex alone and upon addition of EDTA (2, 5 and 10 eq.).

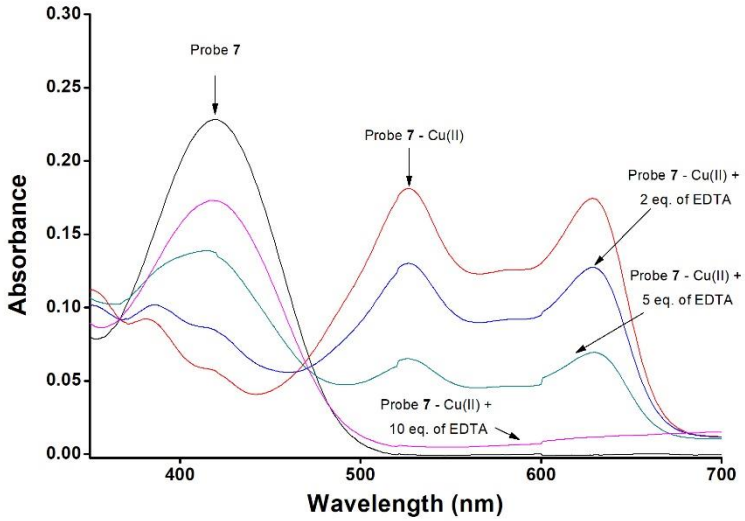

Figure S9. UV-visible profile of probe **7** in acetonitrile (1.0 x 10^{-5} mol L^{-1}) and of Cu(II)-**7** complex alone and upon addition of EDTA (2, 5 and 10 eq.).

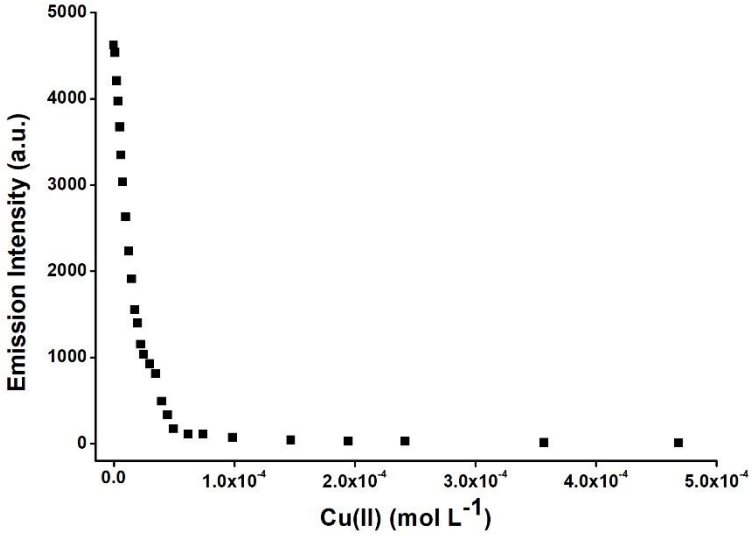

Figure S10. Emission intensity of probe **5** (5.0 x 10^{-5} mol L^{-1} in acetonitrile) at 554 nm vs Cu(II) concentration.

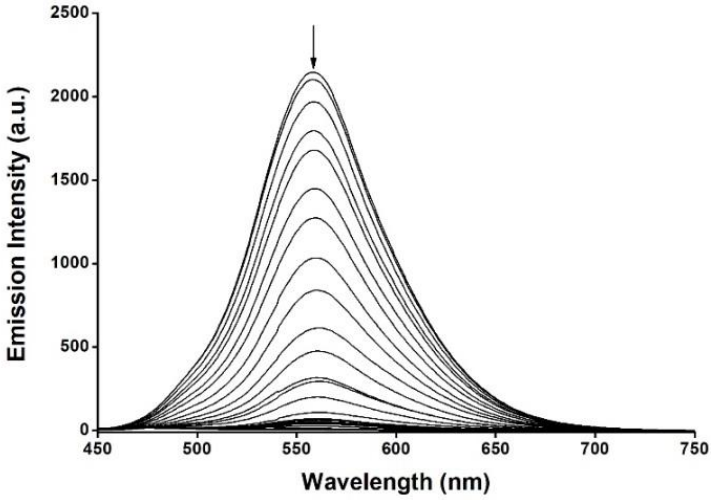

Figure S11. Fluorescence titration profile of **6** in acetonitrile (5.0 x 10^{-5} mol L^{-1}) upon addition of increasing amounts of Cu(II) cation (from 0 to 10 eq.) (λ_{ex} = 440 nm).

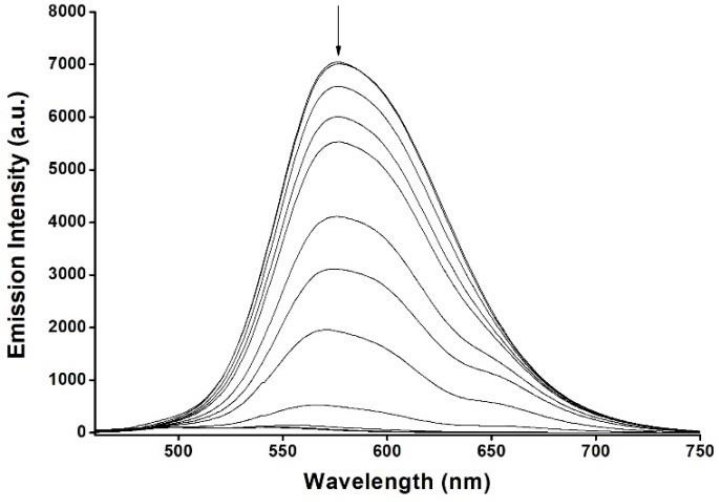

Figure S12. Fluorescence titration profile of **7** in acetonitrile (5.0 x 10^{-5} mol L^{-1}) upon addition of increasing amounts of Cu(II) cation (from 0 to 10 eq.) (λ_{ex} = 450 nm).

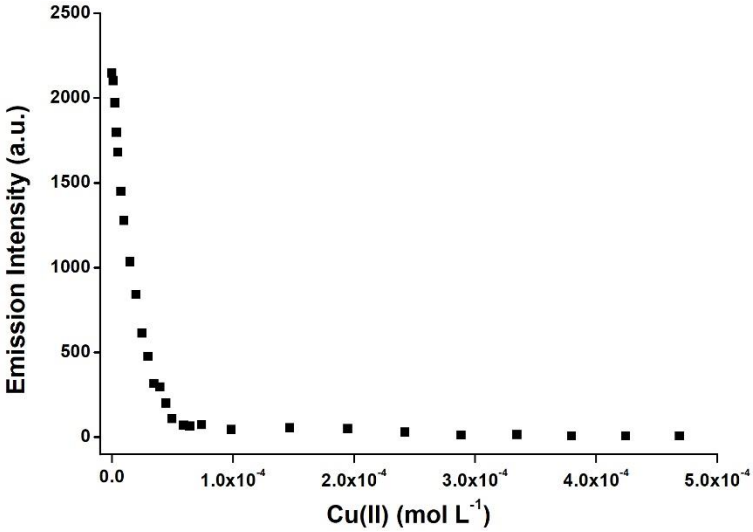

Figure S13. Emission intensity of probe **6** (5.0 x 10^{-5} mol L^{-1} in acetonitrile) at 559 nm vs Cu(II) concentration.

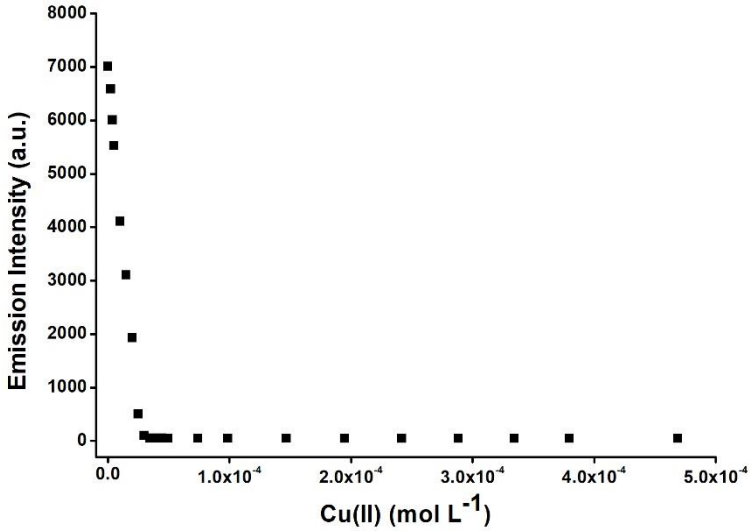

Figure S14. Emission intensity of probe **7** (5.0 x 10^{-5} mol L^{-1} in acetonitrile) at 577 nm vs Cu(II) concentration.

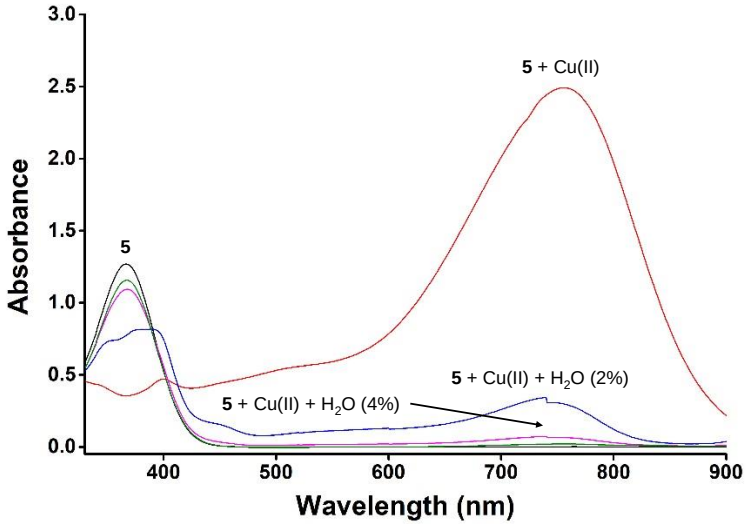

Figure S15. UV-visible profile of probe **5** in acetonitrile (5.0 x 10^{-5} mol L^{-1}) alone and containing water (2 and 4 %) upon addition of 10 eq. of Cu(II) cation.

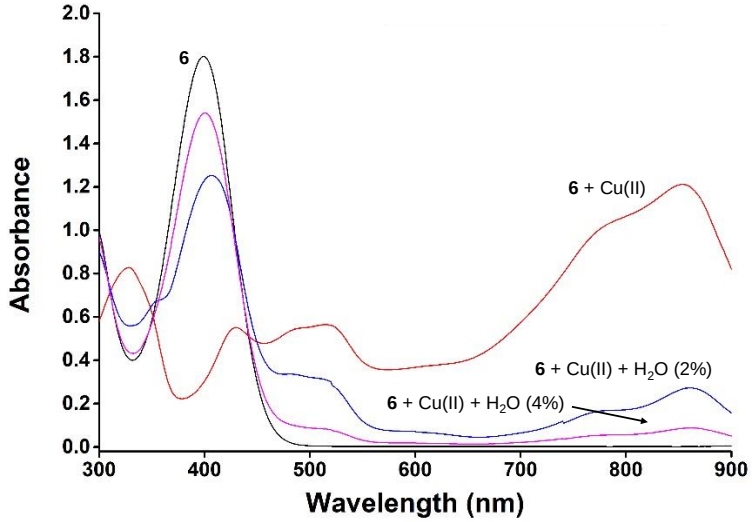

Figure S16. UV-visible profile of probe **6** in acetonitrile (5.0 x 10^{-5} mol L^{-1}) alone and containing water (2 and 4 %) upon addition of 10 eq. of Cu(II) cation.

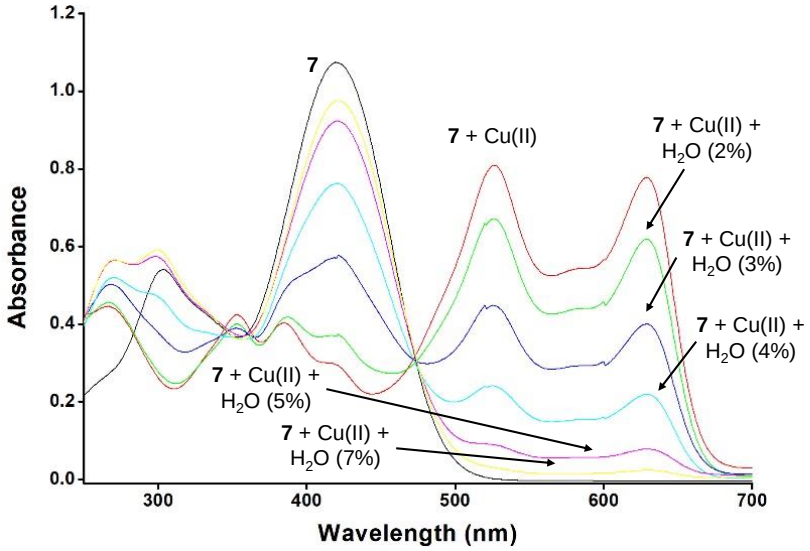

Figure S17. UV-visible profile of probe **7** in acetonitrile (5.0 x 10^{-5} mol L^{-1}) alone and containing water (2, 3, 4, 5 and 7 %) upon addition of 10 eq. of Cu(II) cation.

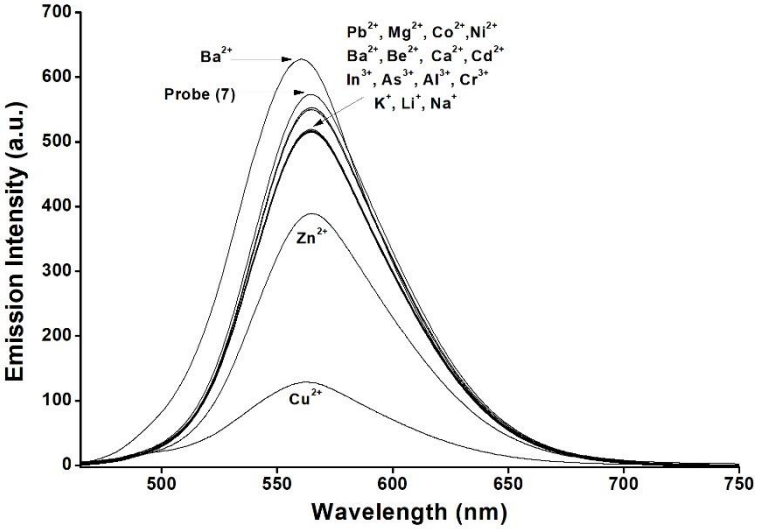

Figure S18. Emission spectra (excitation at 450 nm) of SDS (20 mM, pH 7.5)-acetonitrile 90:10 v/v solutions of probe **7** (1.0 x 10^{-5} mol L^{-1}) in the presence of 10 eq. of selected cations.

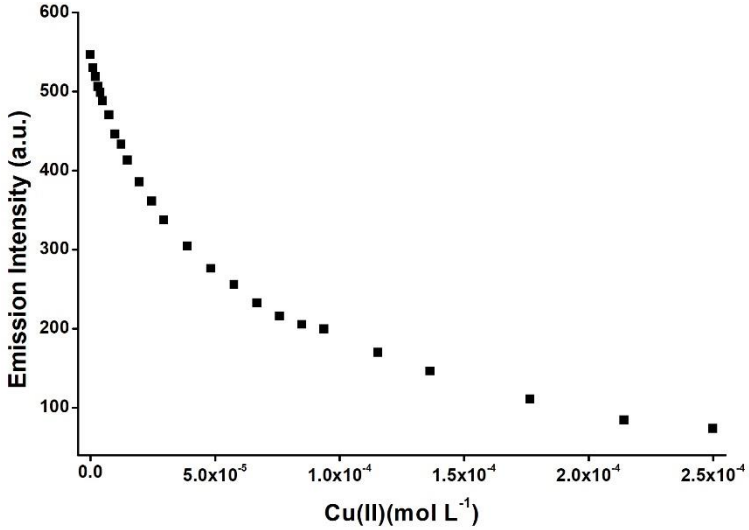

Figure S19. Plot of the emission intensity of **7** in SDS (20 mM, pH 7.5)-acetonitrile 90:10 v/v at 565 nm vs Cu(II) concentration.

Table S1. UV-visible and fluorescence data for *N,N*-diphenylanilino aldehydes **5**, **6** and **7** in ethanol.

	UV/Vis		Fluorescence		
	log ε	λ_{max} (nm)	λ_{em} (nm)	Φ_F	Stokes' shift (nm)
5	4.00	368	498	0.01	130
6	4.08	402	566	0.02	164
7	3.85	423	600	0.22	177

Chapter 6.
2,4,5-triaryl imidazole probes for the selective chromo-fluorogenic detection of Cu(II). Prospective use of the Cu(II) complexes for the optical recognition of biothiols

2,4,5-triaryl imidazole probes for the selective chromo-fluorogenic detection of Cu(II). Prospective use of the Cu(II) complexes for the optical recognition of biothiols

Hazem Essam Okda, [a,b,c] Sameh El Sayed, [a,b,c] Ismael Otri, [a,b,c] R. Cristina M. Ferreira, [d] Susana P. G. Costa, [d] M. Manuela M. Raposo,[d] Ramón Martínez-Máñez, [a,b,c]* and Félix Sancenón [a,b,c]*

[a] *Instituto Interuniversitario de Investigación de Reconocimiento Molecular y Desarrollo Tecnológico (IDM), Universitat Politècnica de València, Universitat de València, Spain. rmaez@qim.upv.es*

[b] *Departamento de Química, Universitat Politècnica de València, Camino de Vera s/n, 46022, València, Spain.*

[c] *CIBER de Bioingeniería, Biomateriales y Nanomedicina (CIBER-BBN).*

[d] *Centro de Química, Universidade do Minho, Campus de Gualtar, 4710-057, Braga, Portugal. E-mail: mfox@quimica.uminho.pt*

Polyhedron, **2019**, 170, 388-394

(Reproduced with permission of Elsevier Ltd.)

6.1 Abstract

The sensing behaviour toward metal cations and biothiols of two 2,4,5-triarylimidazole probes (**3a** and **3b**) is tested in acetonitrile and in acetonitrile-water. In acetonitrile the two probes present charge-transfer absorption bands in the 320-350 nm interval. Among all cations tested only Cu(II) is able to induce bathochromic shifts of the absorption band in the two probes, which is reflected in marked colour changes. Colour modulations are ascribed to the formation of 1:1 Cu(II)-probe complexes in which the cation interacts with the imidazole acceptor heterocycle. Besides, the two probes present intense emission bands (at 404 and 437 nm for **3a** and **3b** respectively) in acetonitrile that are quenched selectively by Cu(II). Probe **3a** is soluble in acetonitrile-water 1:1 (v/v) and Cu(II) also induces bathochromic shifts of the absorption bands. Moreover, the emission bands of probe **3a** in this mixed aqueous solutions is quenched in the presence of Cu(II). The potential use of the 1:1 complex formed between **3a** and Cu(II) for the chromo-fluorogenic detection of biothiols (GSH, Cys and Hcy) in aqueous environments is also tested. At this respect, addition of GSH, Cys and Hcy to acetonitrile-water 1:1 v/v solutions of **3a**-Cu(II) complex induces a hypsochromic shift of the visible band (reflected in a bleaching of the solutions) with a marked emission increase at 470 nm.

Keywords: Imidazole-based probes • Cu(II) detection • biothiols recognition • Cu(II) imaging • GSH imaging

6.2 Introduction

In the last years, the development of chromo-fluorogenic chemosensors for transition metal cations has attracted the attention of researchers around the world.[1] These chromo-fluorogenic chemosensors are generally formed by two subunits, namely the binding site and the signalling group, that can be covalently linked or forming a supramolecular assembly.[2] In the first case, interaction of

transition metal cations with the binding sites induce rearrangements in the π-conjugated system of the signalling unit which are reflected in colour and/or emission changes.[3] In the second approach, interaction of the transition metal cation with the binding site induced the displacement of the signalling unit from the initial complex to the solution.[4]

Among transition metal cations, Cu(II) is one of the most abundant essential element in the human body and plays vital roles in several physiological processes. For instance, it has been reported that Cu(II) stimulates the proliferation of endothelial cells and is necessary for the secretion of several angiogenic factors by tumour cells.[5,6] Aside from its biological and environmental importance, copper is widely used in metallurgical, pharmaceutical and agrochemical industries.[7] As a result of the extensive applications of Cu(II) in life science and industry, it has become one of the first hazard environmental pollutants.[8] Despite the important role played by Cu(II) in several biological processes, abnormal levels of this cation can cause serious health problems on humans due to its ability to displace other vital metal ions in some enzyme-catalysed reactions.[9] In addition, high concentrations of Cu(II) in cells was documented to cause toxicity and different neurodegenerative diseases such as Menkes, Wilson's and Alzheimer.[10] Therefore, simple and rapid sensing tools to monitor Cu(II) levels in biological and environmental media are of importance. Besides, the World Health Organization (WHO) has recommended the maximum allowable level of Cu(II) in drinking water at 2.0 ppm (~30 μM).[11,12]

Currently, several complex analytical techniques are used to detect metal ions such as electrochemical measurements, atomic absorption spectrometry and inductively coupled plasma mass spectroscopy.[13,14] However, these techniques are time-consuming, needs sample pre-treatment, used expensive equipment's, required trained personnel and cannot be used *in situ*.

On the other hand, biothiols (such as the amino acids cysteine (Cys) and homocysteine (Hcy) and the tripeptide glutathione (GSH)) play vital roles in cellular processes related with the damage of cellular components by reactive oxygen species (ROS).[15,16] Levels of biothiols in cells are controlled by the equilibrium between thiols and disulfides. Besides, the relative levels of biothiols can be used as biomarkers for aging, neurodegenerative pathologies and many other diseases such as cancer, AIDS and cystic fibrosis among others.[17,18] Thus, taking into account the above mentioned facts, determination of biothiols especially in biological samples is an important issue. Actually, different analytical methods are available to determination of biothiol levels including HPLC, capillary electrophoresis, and mass spectrometry.[19-21]

As an alternative to these classical techniques, in the past two decades, a number of chromo-fluorogenic probes for biothiol detection have been reported.[22-24] Most of the described examples are based on the chemodosimeter approach and are synthesized taking into account the nucleophilic character of thiol moieties in these biomolecules.[25-31] Also, the displacement approach has been extensively used to design biothiol selective chromo-fluorogenic probes. For this purpose, the emission quenching features of transition metal ions such as Cu(II) has been widely used. The basis of these probes is the generation of non-emissive Cu(II) complexes with fluorophores equipped with coordinating subunits. In the presence of biothiols, there is a demetallation process, restoring the full emission of the fluorophore.[32-37] However, many of the described biothiols chemosensors did not work in pure water or in mixed aqueous environments. Besides, the selectivity achieved in most cases is low because probes are unable to distinguish between Cys, Hcy and GSH. In fact, the synthesis and characterization of probes for the selective recognition of individual biothiol in aqueous environments is of interest.

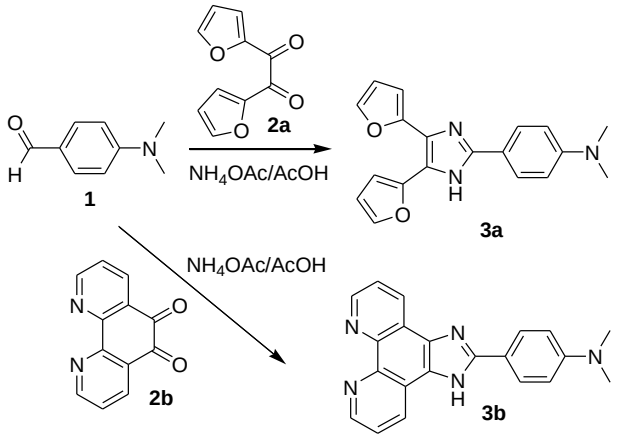

Scheme 1. One pot synthesis of imidazole probes **3a** and **3b**.

Taking into account our interest in the development of chromo-fluorogenic probes for biomolecules [38-45] we report herein the synthesis, characterization and binding studies toward Cu(II) and biothiols (GSH, Hcy and Cys), of two probes containing 2,4,5-trisubstitued imidazole moieties (**3a** and **3b** in Scheme 1). The prepared probes contain electron donor (furan) and electron acceptor (phenanthroline) rings of different strength covalently linked with an imidazole heterocycle. 2,4,5-triaryl(heteroaryl)-imidazole based chromophores have received increasing attention due to their distinctive optical properties, applications in medicinal chemistry and materials sciences, and as nonlinear optical materials (SHG chromophores, two-photon absorbing molecules) and thermally stable luminescent materials for several applications (such as OLEDs and fluorescent probes).

6.3 Experimental section

Materials and methods. All melting points were measured on a Stuart SMP3 melting point apparatus. TLC analyses were carried out on 0.25 mm thick pre-coated silica plates (Merck Fertigplatten Kieselgel $60F_{254}$) and spots were visualised under UV light. Chromatography on silica gel was carried out on Merck Kieselgel (230-240 mesh). IR spectra were determined on a BOMEM MB 104 spectrophotometer using KBr discs. NMR spectra were obtained on a Bruker Avance III 400 at an operating frequency of 400 MHz for ^{1}H and 100.6 MHz for ^{13}C using the solvent peak as internal reference at 25 ^{o}C.

All chemical shifts are given in ppm using δH Me_4Si = 0 ppm as reference. Assignments were supported by spin decoupling-double resonance and bidimensional heteronuclear correlation techniques. UV/Vis titration profiles were carried out with JASCO V-650 spectrophotometer (Easton, MD, USA). Fluorescence measurements were recorded with a JASCO FP-8500 spectrophotometer. Commercially available reagents 4-(dimethylamino) benzaldehyde (**1**), 1,2-di(furan-2-yl)ethane-1,2-dione (**2a**), 1,10-phenanthroline-5,6-dione (**2b**) and ammonium acetate were purchased from Sigma-Aldrich and Acros and used as received. TLC analyses were carried out on 0.25 mm thick pre-coated silica plates (Merck Fertigplatten Kieselgel $60F_{254}$) and spots were visualized under UV light. Chromatography on silica gel was carried out on Merck Kieselgel (230-240 mesh).

Synthesis of 4-(4,5-di(furan-2-yl)-1H-imidazol-2-yl)-N,N-dimethylbenzenamine (3a).

4-(dimethylamino) benzaldehyde (**1**, 0.15 g, 1 mmol), 1,2-di(furan-2-yl)ethane-1,2-dione (**2a**, 0.19 g, 1 mmol) and NH_4OAc (1.54 g, 20 mmol) were dissolved in glacial acetic acid (5 mL), followed by stirring and heating at reflux for 8 h. The reaction mixture was then cooled to room temperature, ethyl acetate was added (15 mL) and the mixture was washed with water (3 x 10 mL). After drying the

organic phase with anhydrous $MgSO_4$, the solution was filtered and the solvent was evaporated to dryness. The resulting crude product was purified by column chromatography (silica gel, DCM/MeOH 100:1 v/v); yield (64 mg, 60%) as grey solid. Mp = 240.2-240.9 ºC.

^{1}H NMR (400 MHz, DMSO-d_6): δ = 2.95 (s, 6H), 6.55 (s, 1H), 6.63 (br s, 1H), 6.71 (d, *J* = 2.0 Hz, 1H), 6.77 (dd, *J* = 8.8 and 2.0 Hz, 2H), 6.89 (d, *J* = 2.8 Hz, 1H), 7.68 (br s, 1H), 7.78 (br s, 1H), 7.90 (dd, *J* = 8.8 and 2.0 Hz, 2H), 12.47 (s, 1H, NH) ppm. ^{13}C NMR (100.6 MHz, DMSO-d_6): δ = 39.89, 106.56, 107.81, 111.33, 111.80, 117.50, 118.27, 126.68, 129.15, 141.61, 142.22, 144.79, 147.23, 149.59, 150.53 ppm. IR (Nujol): *v* = 3570, 1665, 1612, 1530, 1494, 1222, 1202, 1169, 1122, 1074, 1014, 986, 943, 911, 885, 815 cm^{-1}. HRMS-EI m/z: calcd for $C_{19}H_{17}N_3O_2$+H+: 320.1399; measured: 320.1394.

Synthesis of 4-(1H-imidazo[4,5-f][1,10]phenanthrolin-2-yl)-N,N-dimethylbenzenamine (3b).

4-(dimethylamino) benzaldehyde (**1**, 0.15 g, 1 mmol), 1,10-phenanthroline-5,6-dione (**2b**, 0.2 g, 1 mmol) and NH_4OAc (1.54 g, 20 mmol) were dissolved in glacial acetic acid (5 mL), followed by stirring and heating at reflux for 8 h. The reaction mixture was then cooled to room temperature, ethyl acetate was added (15 mL) and the mixture was washed with water (3 x 10 mL). After drying the organic phase with anhydrous $MgSO_4$, the solution was filtered and the solvent was evaporated to dryness. The resulting crude product was purified by column chromatography (silica gel, DCM/MeOH 98:2 v/v); yield (8 mg, 7%) as yellow oil.

^{1}H NMR (400 MHz, DMSO-d6): δ = 3.02 (s, 6H), 6.90 (d, *J* = 9.2 Hz, 2H), 7.81-7.84 (m, 2H,), 8.11 (dd, *J* = 8.8 and 2.0 Hz, 2H), 8.92 (dd, *J* = 8.0 and 1.6 Hz, 2H), 9.00 (dd, *J* = 4.0 and 2.0 Hz, 2H), 13.40 (s, 1H, NH) ppm. ^{13}C NMR (100.6 MHz, DMSO-d_6): δ = 40.13, 111.97, 117.29, 123.33, 127.45, 127.62, 129.77, 142.94, 147.34, 147.40, 151.21, 151.88 ppm. IR (liquid film): *v* = 3414, 2925, 1657, 1611, 1502, 1438, 1372, 1351, 1195, 1168, 1125, 1067, 1024, 946, 814, 739 cm^{-1}. HRMS-EI m/z: calcd for $C_{21}H_{17}N_5$+H+: 340.1562; measured: 340.1560.

UV-visible and emission measurements. Stock solutions of the cations (i.e., Cu(II), Pb(II), Mg(II), Ge(II), Ca(II), Zn(II), Co(II), Ni(II), Ba(II), Cd(II), Hg(II), Fe(III), In(III), As(III), Al(III), Cr(III), Ga(III), K(I), Li(I) and Na(I) as perchlorate salts) were prepared at (1.0×10^{-3} mol L^{-1}) in acetonitrile. The concentrations of probes used in spectroscopy measurements were ca. (5.0×10^{-5} mol L^{-1}) and (1.0×10^{-5} mol L^{-1}). We took care that the maximum addition of cations solutions did not exceed 10% of the volume of the receptor to avoid significant changes in the total solution concentration. In the experiments that required the addition of excess of ions (20 equiv.), corrections of the volume and concentration were made. The UV/Vis and fluorometric titrations were carried out at room temperature (25 ^{o}C).

6.4 Results and discussion

Synthesis and characterization of the probes.

Heteroaromatic commercially available diones **2a** and **2b** containing furyl and phenanthroline rings (see Scheme 1) were used as precursors for the synthesis of **3a** and **3b**. The synthesis of probes **3a** and **3b** was previously described.[45,46] The final probes were prepared through a condensation reaction between **2a** and **2b** diones and 4-(*N*,*N*-dimethylamino) benzaldehyde (**1**) in presence of ammonium acetate and glacial acetic acid at reflux under Debus-Radziszewski imidazole synthesis conditions (see also Scheme 1).[47]

Probes were synthesized in fair to moderate yields (Table 1) as a consequence of several factors such as the difficulty in the purification step due to the polarity of the compounds as well as their decomposition during the long reaction times under hard conditions (acetic acid reflux). The final probes **3a** and **3b** were characterized by ^{1}H and ^{13}C-NMR, and IR. The data obtained are in full agreement with the proposed formulations (see Experimental section).

Table 1. Yields and ^{1}H NMR data of imidazole probes **3a** and **3b** at 400 MHz in DMSO-D6.

Probe	Yield (%)	δH NH (ppm)
3a	60	12.45
3b	7	13.40

One of the most characteristic ^{1}H-NMR signals of probes **3a** and **3b** is that corresponding to the N-H proton in the imidazole ring (see Table 1). As could be seen, a clear correlation between the electronic nature of the rings (furan and phenanthroline) directly linked with imidazole and the shift of the N-H proton of this heterocycle was observed. At this respect, probe **3b** bearing the electron deficient phenanthroline system exhibited the highest chemical shift for the

nitrogen proton of the imidazole ring (13.40 ppm). On the other hand, probe **3a** functionalized with electron rich furan heterocycle exhibited lower chemical shifts for the nitrogen proton of the imidazole ring (12.45 ppm) when compared to **3b**.

UV/Vis and emission spectroscopic behaviour of probes in the presence of selected metal cations in acetonitrile.

In a first step, UV-visible changes of both probes in acetonitrile were studied. Acetonitrile solutions of **3a** and **3b** (1.0×10^{-5} mol L^{-1}) showed intense absorption bands in the UV zone (321 nm for **3a** and 341 nm for **3b**). The observed absorption bands are ascribed to charge-transfer transitions between the *N*,*N*-dimethylamino donor moiety and imidazole acceptor heterocycle. Besides, the wavelength of the charge-transfer band was affected by the aromatic units directly connected with the central imidazole heterocycle. At this respect, the presence of electron deficient phenanthroline unit in probe **3b** induced the larger charge-transfer character and the associated absorption appeared at the higher wavelength (341 nm). On the other hand, in probe **3a**, the imidazole core was linked to an electron donating heterocycle (furan) and, as a consequence, absorption bands are shifted to lower wavelengths (321 nm).

Besides, both probes were highly emissive in acetonitrile upon excitation at the maximum of the absorbance of the visible band. At this respect, excitation at 321 nm of acetonitrile solutions of probe **3a** (1.0×10^{-5} mol L^{-1}) induced the appearance of a marked emission band centred at 404 nm. Nearly the same results were obtained for probe **3b** with an intense emission centred at 437 nm. Besides, the quantum yield of the two probes (determined using pyrene as standard, see Supporting Information for details) was 0.41 and 0.31 for **3a** and **3b** respectively.

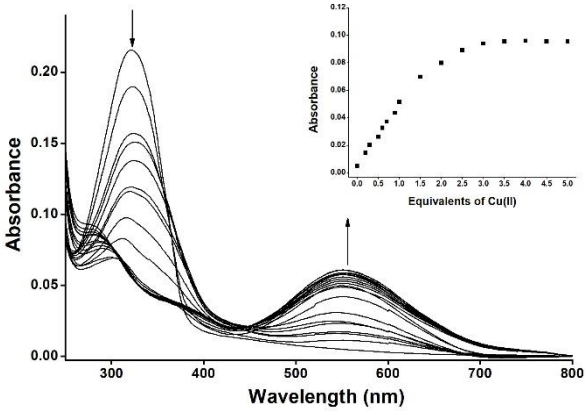

Figure 1. UV/Vis titration profile of probe **3a** in acetonitrile (1.0 x 10^{-5} mol L^{-1}) upon addition of increasing quantities of Cu(II) cation (0-10 eq.). Inset: Absorbance at 563 nm vs equivalents of Cu(II) added.

Then, UV-visible changes in acetonitrile solutions of both probes (1.0 x 10^{-5} mol L^{-1}) in the presence of increasing amounts (from 0.1 to 10 eq.) of selected metal cations (Cu(II), Pb(II), Mg(II), Ge(II), Ca(II), Zn(II), Co(II), Ni(II), Ba(II), Cd(II), Hg(II), Fe(III), In(III), As(III), Al(III), Cr(III), Ga(III), K(I), Li(I) and Na(I)) were tested. The two probes showed nearly the same behaviour and in all cases only Cu(II) induced the progressive appearance of a new red shifted absorption band. Figure 1 shows the set of spectra obtained upon addition of increasing quantities of Cu(II) cation to an acetonitrile solution of probe **3a**. As could be seen in Figure 1, addition of Cu(II) induced a progressive bathochromic shift together with a marked decrease of the band centred at 321 nm with the concomitant appearance of a red shifted absorption at 563 nm. Besides, a marked colour change from colourless to violet was observed.

Nearly the same behaviour was observed with probe **3b** in the presence of Cu(II) cation. Addition of Cu(II) to an acetonitrile solution of **3b** induced the appearance of a new absorbance at 466 nm with a marked colour change from colourless to yellow. Changes upon addition of Cu(II) to acetonitrile solutions of **3a** and **3b** was ascribed to the formation of complexes in which the cation interacts with the acceptor part of the probes (i.e. the imidazole heterocycle).

In a next step, the emission of probes **3a** and **3b** in acetonitrile (1.0 x 10^{-5} mol L^{-1}) was also studied upon addition of increasing amounts of selected cations. A marked selective response was obtained for Cu(II) that was the unique cation able to induce a remarkable emission quenching for both probes. Figure 2 shows the set of emission spectra obtained upon addition of increasing amounts of Cu(II) to probe **3a**. Addition of Cu(II) induced a progressive quenching of the emission band of **3a** at 404 nm (excitation at ca. 380 nm) together with a hypsochromic shift of ca. 10 nm. A similar quenching and hypsochromic shifts of the emission bands was observed upon addition of Cu(II) to acetonitrile solutions of probe **3b** (see Supporting Information). The obtained results are in accordance with the marked and well-known quenching behaviour of Cu(II) cation.

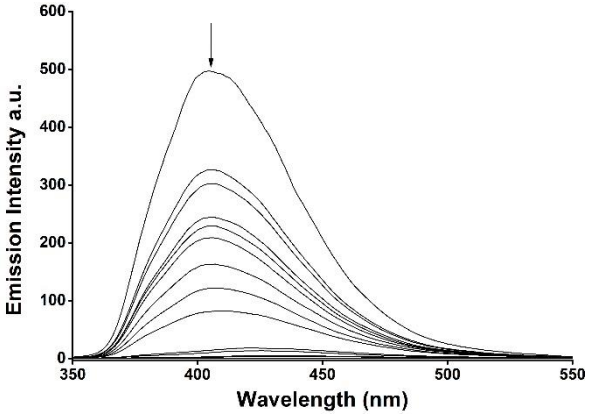

Figure 2. Fluorescence titration profile of probe **3a** in acetonitrile (1.0 x 10^{-5} mol L^{-1}) upon addition of increasing quantities of Cu(II) cation (0-10 equiv.).

From the UV-visible and emission titration profiles obtained for both probes, the limits of detection (LOD) for Cu(II) in acetonitrile were determined (see Table 2). LODs were assessed using the 3.3*(σ/s) equation, where σ is the standard error of the predicted Y-value vs. each X (i.e. Cu(II) concentration), and *s* is the slope for the linear relationship. Both probes presented similar Cu(II) LODs in the 0.9-2.0 μM range.

Table 2. Limits of detection of Cu(II) measured for **3a** and **3b** probes in acetonitrile.

Probe	UV/Vis [μM]	Emission [μM]
3a	0.9	1.0
3b	1.2	2.0

Determination of binding stoichiometries and stability constants of probe 3a and 3b with Cu(II) in acetonitrile.

In order to complete the characterization of the complex formed between probe **3a** and **3b** and Cu(II) cation we carried out UV-visible and emission studies to obtain Job's plots to assess the binding stoichiometry and to determine the stability constants.

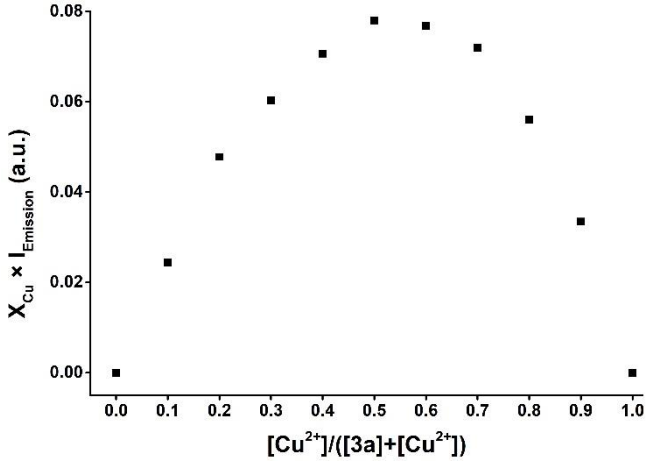

Figure 3. Job's plot for the binding of **3a** with Cu(II). Absorbance at 555 nm was plotted as a function of the molar ratio [Cu(II)]/([**3a**] + [Cu(II)]). The total concentration of Cu(II) and probe **3a** was (2.0×10^{-5} mol L^{-1}).

Job's plots, constructed using UV-visible measurements in acetonitrile, showed that **3a** and **3b** formed 1:1 complexes with Cu(II). As an example, Figure 3 showed the Job's plot obtained for probe **3a**. Besides, from the UV-visible and fluorescence titration profiles obtained for probes **3a** and **3b** in the presence of

Cu(II) cation, the stability constant for the formation of the corresponding 1:1 complexes were determined. The obtained values are shown in Table 3.

Table 3. Logarithms of binding constants measured for the interaction of probes **3a** and **3b** with Cu(II) in acetonitrile.

Probe	Log K	
	UV/Vis	Emission
3a	5.1 ± 0.1	6.4 ± 0.3
3b	5.8 ± 0.9	5.8 ± 0.1

UV/Vis and emission spectroscopic behaviour of probes 3a and 3b in the presence of selected metal cations in aqueous environments.

In order to assess the possible use of both probes for Cu(II) detection in real samples, the UV-visible and emission response toward Cu(II) was tested in aqueous environments. Probes **3a** and **3b** were fully solubilized in water (pH 7.4)-acetonitrile 1:1 v/v. In this medium, both probes showed charge-transfer absorption bands centred at 321 and 339 nm for **3a** and **3b** respectively. The maxima of the charge-transfer band in water-acetonitrile 1:1 v/v were very similar to those measured in pure acetonitrile, indicating that conformation and hydration of the probes did not change, to any remarkable extent, the energy of their electronic levels in the basal state.

Next, the UV-visible behaviour of aqueous solutions of both probes (5.0×10^{-5} mol L^{-1}) in the presence of selected metal cations was tested. None of the metal cations tested induced changes in the absorption bands of probe **3b**. In contrast, for probe **3a**, Cu(II) induced the appearance of a new redshifted absorption at 563 nm as could be seen in Figure 4 (similar to that found in acetonitrile) together with marked colour changes (Figure 5).

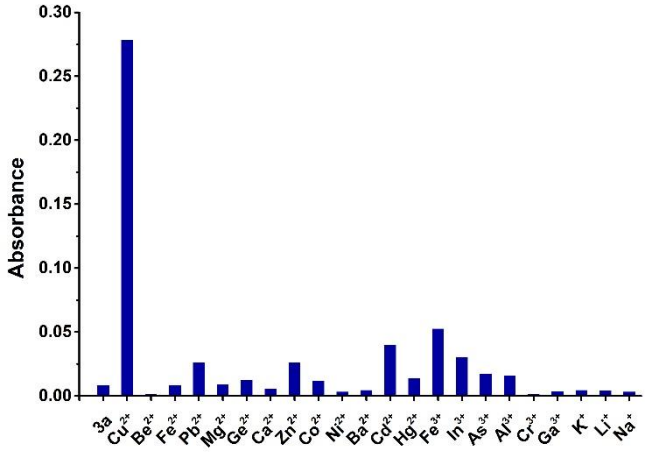

Figure 4. Absorption of probe **3a** at 563 nm (water (pH 7.4)-acetonitrile 1:1 v/v, 5.0×10^{-5} mol L^{-1}) in the presence of 10 eq. of selected metal cations.

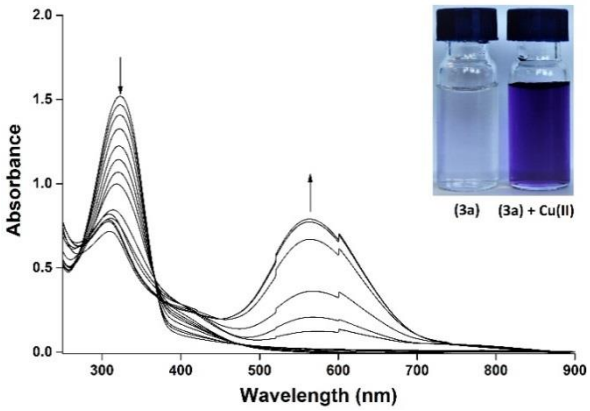

Figure 5. UV-Vis titration profile of probe **3a** in water (pH 7.4)-acetonitrile 1:1 v/v (5.0×10^{-5} mol L^{-1}) upon addition of increasing quantities of Cu(II) cation (0-10 eq.). Inset: colour change when Cu(II) cation was added to water (pH 7.4)-acetonitrile 1:1 v/v solutions of probe **3a**.

More in detail, addition of increasing quantities of Cu(II) cation to water (pH 7.4)-acetonitrile 1:1 v/v (5.0×10^{-5} mol L^{-1}) solutions of probe **3a** induced a moderate decrease of the absorption at 321 nm and the simultaneous appearance of a new band centred at 563 nm (see Figure 5). These spectral

changes were reflected in a clear colour change from colourless to violet (see inset in Figure 5). Besides, from the titration profile at 489 nm, a limit of detection for Cu(II) of 2.60 µM was determined.

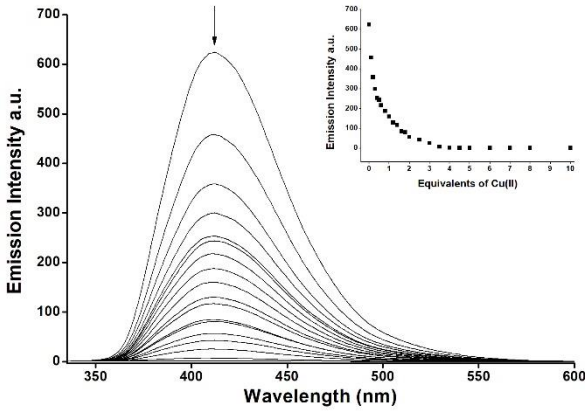

Figure 6. Fluorescence titration profile of probe **3a** in water (pH 7.4)-acetonitrile 1:1 v/v (5.0×10^{-5} mol L^{-1}) upon addition of increasing amounts of Cu(II) cation (from 0 to 10 eq.). Inset: Emission intensity at 420 vs equivalents of Cu(II) added.

On the other hand, **3a** was highly emissive in water (pH 7.4)-acetonitrile 1:1 v/v solutions showing a remarkable emission band at 420 nm (excitation at 321 nm). Moreover, fluorescence changes in the presence of selected metal cations was tested. For this purpose, solutions of probe **3a** were excited at the isosbestic point observed in the UV-visible titration profile (ca. 375 nm) and the emission recorded after the addition of different amounts of selected cations. From all cations tested, only Cu(II) was able to induce a response which consisted of a marked emission quenching of the emission band 420 nm (see Figure 6). The obtained results clearly resemble those obtained for probe **3a** in acetonitrile in the presence of Cu(II) cation. From the emission titration profile (see also Figure 6), a LOD for Cu(II) of 3.4 µM for **3a** was determined. This LOD is higher than that found in acetonitrile, most likely as consequence of a stronger solvation of Cu(II) cation in water.

Spectroscopic detection of biothiols.

In this section we studied the potential use of the **3a**·Cu complex for the recognition of biothiols.[48] Studies were carried out in the presence of selected amino acids (Ala, Arg, Asp, Cys, Gln, Glu, Gly, Hcy, His, Ile, Leu, Lys, Met, Phe, Pro, Ser, Thr, Trp, Tyr and Val) and small peptides (GSH).

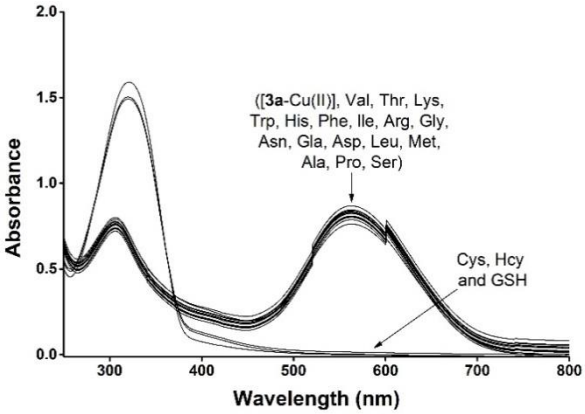

Figure 7. UV-visible changes of 3a·Cu (6.2 x 10-6 mol L-1) in water (pH 7.4)-acetonitrile 1:1 v/v in the presence of selected amino acids (0.2 eq.) and biothiols (0.2 eq.).

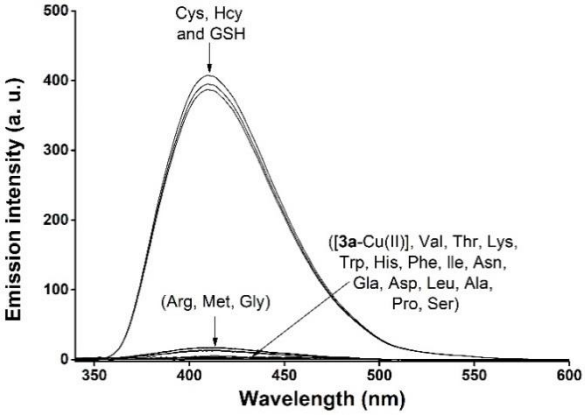

Figure 8. Changes in the emission band of **3a**·Cu complex (6.2 x 10^{-6} mol L^{-1}) in water (pH 7.4)-acetonitrile 1:1 v/v upon addition of biothiols (0.2 eq.) and selected amino acids (0.2 eq.).

Water (pH 7.4)-acetonitrile 1:1 v/v solution of complex **3a**·Cu (6.20 x 10^{-6} mol L^{-1}, formed *in situ* by the addition of equimolar quantities of probe and Cu(II)

cation) shows an intense absorption band at 563 nm which was the responsible of the strong violet colour observed. From all amino acids (0.2 eq.) and peptides (0.2 eq.) tested, only in the presence of thiol-containing molecules (Cys, Hcy and GSH) a bleaching of the solution was observed (see Figure 7).

Besides, water (pH 7.4)-acetonitrile 1:1 v/v solutions of the **3a**·Cu complex (6.2 x 10^{-6} mol L^{-1}) were weakly emissive and only addition of Cys, Hcy and GSH induced a marked emission enhancement at 420 nm (see Figure 8). The chromo-fluorogenic changes observed upon addition of biothiols to the aqueous solutions of **3a**·Cu complex are ascribed to a demetallation of the complex, that released the free probe **3a**. Finally, from UV-visible and fluorescence titration profiles obtained for **3a**·Cu, the LODs for biothiols were determined (Table 4).

Table 4. Limits of detection of biothiols measured for **3a**·Cu in aqueous environments.

	UV-visible (μM)			Fluorescence (μM)		
Complex	GSH	Cys	Hcy	GSH	Cys	Hcy
3a·Cu	0.6	1.3	0.8	0.6	0.9	0.7

6.4 Conclusions

In summary, we show herein the synthesis and chromo-fluorogenic behaviour toward metal cations and biothiols of easy to prepare imidazole-containing probes **3a** and **3b**. Acetonitrile solutions of both probes were characterized by the presence of a charge-transfer absorption band in the 320-350 range. Both probes were moderately emissive in acetonitrile. From all cations tested only Cu(II) induced the growth of new redshifted bands in the 450-570 nm interval. Besides, the emission bands of both receptors were quenched in the presence of Cu(II) cation. These spectral changes were ascribed to a preferential coordination of Cu(II) cation with the electron acceptor imidazole heterocycle. Only probe **3a** changed its UV-visible and emission spectra in the presence of Cu(II) in water-

acetonitrile mixtures. On the other hand, weakly emissive complex **3a**·Cu was used to detect biothiols (GSH, Cys and Hcy) in water-acetonitrile 1:1 v/v solution. In the presence of biothiols, the visible bands of the complex disappeared and the emission intensity of the free probe was fully restored. These changes were ascribed to a demetallation process.

6.5 Acknowledgments

We thank the Spanish Government (MAT2015-64139-C4-1-R) and Generalitat Valenciana (PROMETEO 2018/024). H. E. O. thanks Generalitat Valenciana for his Grisolia fellowship. Thanks are also due to Fundação para a Ciência e Tecnologia (Portugal) for financial support to the Portuguese NMR network (PTNMR, Bruker Avance III 400-Univ. Minho), FCT and FEDER (European Fund for Regional Development)-COMPETEQREN-EU for financial support to the research centre CQ/UM [PEst-C/QUI/UI0686/2013 (FCOMP-01-0124-FEDER-037302], and a post-doctoral grant to R.M.F. Batista (SFRH/BPD/79333/2011).

6.6 References

1. Udhayakumari D, Naha S, Velmathi S, Anal. Methods 2017; 9: 552-578.
2. Wu J, Kwon B, Liu W, Anslyn EV, Wang P, Kim JS, Chem. Rev. 2015; 115: 7893-7943.
3. Zhang J, Cheng F, Li J, Zhu JJ, Lu Y, Nano Today 2016; 11: 309-329.
4. Cheng J, Zhou X, Xiang H, Analyst 2015; 140: 7082-7115.
5. Swaminathan S, Gangadaran P, Venkatesh T, Ghosh M, J. Pharm. Biomed. Sci. 2011; 9: 1-15.
6. Kamble S, Utage B, Mogle P, Kamble R, Hese S, Dawane B, Gacche R, AAPS Pharm. Sci. Tech. 2016; 17: 1030-1041.
7. Jain AK, Singh RK, Jain S, Raisoni J, Transition Met. Chem. 2008; 33: 243-249.
8. Goswami S, Sen D, Das NK, Hazra G, Tetrahedron Lett. 2010; 51: 5563-5566.
9. Xie Q, Zhou T, Yen L, Shariff M, Nguyen T, Kami K, Gu P, Liang L, Rao J, Shi R, Nutr. Diet. Suppl. 2013; 5: 1-6.
10. Choo XY, Alukaidey L, White AR, Grubman A, Int. J. Alzheimer's Dis. 2013; 2013: 145345.
11. Sarkar B, Chem. Rev. 1999; 99: 2535-2544.
12. Barnham KJ, Masters CL, Bush AI, Nat. Rev. Drug Discov. 2004; 3: 205-214.

13. Ackerman CM, Lee S, Chang CJ, Anal. Chem. 2017; 89: 22-41.
14. Hotta H, Tsunoda K, Anal. Sci. 2015; 31: 7-14.
15. Townsend DM, Tew KD, Tapiero H, Biomed. Pharmacother. 2003; 57; 145−155.
16. Miller JW, Beresford SA, Neuhouser ML, Cheng TY, Song X, Brown EC, Zheng Y, Rodriguez B, Green R, Ulrich CM, Am. J. Clin. Nutr. 2013; 97: 827−834.
17. Dorszewska J, Prendecki M, Oczkowska A, Dezor M, Kozubski W, Curr. Alzheimer Res. 2016; 13: 952-963.
18. Rozycka A, Jagodzinski PP, Kozubski W, Lianeri M, Dorszewska J, Curr. Genomics 2013; 14: 534-542.
19. Santa T, Drug Discov. Ther. 2013; 7: 172-177.
20. Carlucci F, Tabucchi A, J. Chromatogr. B Analyt. Technol. Biomed. Life Sci. 2009; 877: 3347-3357.
21. Blair IA, Biomed. Chromatogr. 2010; 24: 29-38.
22. Isik M, Ozdemir T, Turan IS, Kolemen S, Akkaya EU, Org. Lett. 2013; 15: 216-219.
23. Liao YC, Venkatesan P, Wei LF, Wu SP, Sens. Actuators B Chem. 2016; 232: 732-737.
24. Lee KS, Park J, Park HJ, Chung YK, Park SB, Kim HJ, Shin IS, Hong JI, Sens. Actuators B Chem. 2016; 237: 256-261.
25. Kong F, Liu R, Chu R, Wang X, Xu K, Tang B, Chem. Commun. 2013; 49: 9176-9178.
26. Zhang J, Jiang XD, Shao X, Zhao J, Su Y, Xi D, Yu H, Yue S, Xiao LJ, Zhao W, RSC Adv. 2014; 4: 54080-54083.
27. Wang YW, Liu SB, Ling WJ, Peng Y, Chem. Commun. 2016; 52: 827-830.
28. Liu J, Sun YQ, Zhang H, Huo Y, Shi Y, Guo W, Chem. Sci. 2014; 5: 3183-3188.
29. Guan YS, Niu LY, Chen YZ, Wu LZ, Tung CH, Yang QZ, RSC Adv. 2014; 4: 8360-8364.
30. Fu ZH, Han X, Shao Y, Fang J, Zhang ZH, Wang YW, Peng Y, Anal. Chem. 2017; 89: 1937-1944.
31. Yang YL, Zhang FM, Wang YW, Zhang BX, Fang R, Fang JG, Peng Y, Chem. As. J. 2015; 10: 422-426.
32. Fu ZH, Yan LB, Zhang X, Zhu FF, Han XL, Fang J, Wang YW, Peng Y, Org. Biomol. Chem. 2017; 15: 4115-4121.
33. Singh Y, Arun S, Singh BK, Dutta PK, Ghosh T, RSC Adv. 2016; 6: 80268-80274.
34. Lee SH, Lee JJ, Shin JW, Min KS, Kim C, Dyes Pigm. 2015; 116: 131-138.
35. Maheshwaran D, Nagendraraj T, Manimaran P, Ashokkumar B, Kumar M, Mayilmurugan R, Eur. J. Inorg. Chem. 2017; 1007-1016.
36. Kim YS, Park GJ, Lee SA, Kim C, RSC Adv. 2015; 5: 31179-31188.
37. You GR, Lee JJ, Choi YW, Lee SY, Kim C, Tetrahedron 2016; 72: 875-881.
38. Santos-Figueroa LE, Llopis-Lorente A, Royo S, Sancenón F, Martínez-Máñez R, Costero AM, Gil S, Parra M, ChemPlusChem 2015; 80: 800-804.
39. Marín-Hernández C, Santos-Figueroa LE, El Sayed S, Pardo T, Raposo MMM, Batista RMF, Costa SPG, Sancenón F, Martínez-Máñez R, Dyes Pigm. 2015; 122: 50-58.

40. Lo Presti M, El Sayed S, Martínez-Máñez R, Costero AM, Gil S, Parra M, Sancenón F, New J. Chem. 2016; 40: 9042-9045.

41. El Sayed S, de la Torre C, Santos-Figueroa LE, Pérez-Paya E, Martínez-Máñez R, Sancenón F, Costero AM, Parra M, Gil S, RSC Adv. 2013; 3: 25690-25693.

42. El Sayed S, de la Torre C, Santos-Figueroa LE, Martínez-Máñez R, Sancenón F, Supramol. Chem. 2015; 4: 244-254.

43. Marín-Hernández C, Santos-Figueroa LE, Moragues ME, Raposo MMM, Batista RMF, Costa SPG, Pardo T, Martínez-Máñez R, Sancenón F, J. Org. Chem. 2014; 79: 10752-10761.

44. Okda HE, El Sayed S, Otri I, Ferreira RCM, Costa SPG, Raposo MMM, Martínez-Máñez R, Sancenón F, Dyes Pigm. 2019; 162: 303-308.

45. Nakashima K, Fukuzaki Y, Nomura R, Shimoda R, Nakamura Y, Kuroda N, Akiyama S, Irgum K, Dyes Pigm. 1998; 38: 127-136.

46. Bian, ZQ, Wang KZ, Jin LP, Polyhedron 2002; 21: 313-319.

47. Okda HE, El Sayed S, Ferreira RCM, Costa SPG, Raposo MMM, Martínez-Máñez R, Sancenón F, Dyes Pigm. 2018; 159: 45-48.

48. Mandal S, Das G, Singh R, Shukla R, Bharadwaj PK, Coord. Chem. Rev. 1997; 160: 191-235.

6.7 Supporting information

1. Fluorescence measurements in acetonitrile.

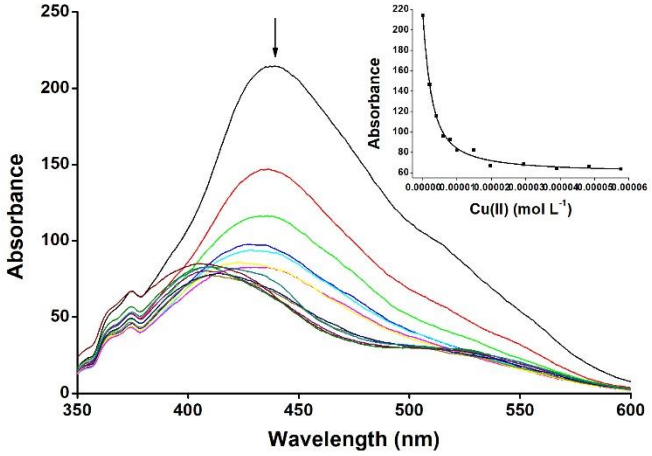

Figure SI-1. Changes in the emission intensity of probe **3b** in acetonitrile at 437 nm upon addition of increasing quantities of Cu(II) cation (0 -10 equiv.). Inset: Changes in the emission intensity of the emission band centred at 437 nm vs. Cu(II) concentration.

2. Fluorescence quantum yield measurements.

The fluorescence quantum yield of pyrene in cyclohexane (φ_f = 0.32) was used as a reference to determine fluorescence quantum yields of probes **3a** and **3b**. Equation 1 was used to calculate the fluorescence quantum yield:

$$\varphi_s = \varphi_f \frac{I_s A_f \eta_s^2}{I_f A_s \eta_r^2} \qquad (1)$$

Here φ_f is the fluorescence quantum yield of reference. I stand for the integrated area under the emission curves. The subscripts s and r stand for sample and reference, respectively. A is the absorbance at a particular excitation wavelength. η is the refractive index of the medium. The absorbance of the dye at

the excitation wavelength was always kept ~0.1. The steady state absorption and emission spectra were fitted by the log normal line shape function. Consequently the fluorescence quantum yield for probe **3a** is φ = 0.41 and for **3b** is φ = 0.31.

3. Stability constant determination.

The apparent binding constant for the formation of the respective complexes were evaluated using the Benesi−Hildebrand plot (equation 2):

$$1/(A - A_0) = 1/\{K(A_{max} - A_0)C\} + 1/(A_{max} - A_0) \quad (2)$$

Where A_0 is the absorbance of **3a** and **3b** at 321 and 339 nm, A is the observed absorbance at that particular wavelength in the presence of a certain concentration of Cu(II) (C), A_{max} is the maximum absorbance value that was obtained at 555 (for **3a**) and 466 nm (for **3b**) during titration with varying Cu(II) concentrations, K is the apparent binding constant, which was determined from the slope of the linear plot, and C is the concentration of the Cu(II) added during titration studies.

4. Limit of detection evaluation for Cu(II) and biothiols.

The limit of detection for Cu(II) and biothiols using probes **3a and 3b** was calculated using the spectrophotometric/spectrofluorometric titration profiles obtained. The limits of detection were calculated using equation 3:

$$LOD = 3.3\,\sigma/k \quad (3)$$

Where σ is the standard deviation of the blank measurement, and k is the slope between the ratios of UV−vis absorbance vs. Cu(II) or biothiols concentration.

Chapter 7: Conclusions and perspectives

Conclusions and perspectives

Based on the supramolecular chemistry principles, the development of design and synthesis of novel molecular chromo-fluorogenic chemosensors for detection of hazardous chemical species that have impact to the humankind has attracted great attention in the last years. In fact, progress on new approaches by using different recognition and sensing protocols to make more selective and sensitive chemosensors offer a new interdisciplinary area with wide horizons to the development of specific applications. In particular, organic and analytical chemistry are combined in order to synthesize molecular probes for the optical detection of cations and anions of environmental and biological significance.

The fundamental principles of the supramolecular chemistry, especially about molecular recognition chemistry, are addressed in the general introduction presented in chapter one.

The third chapter of this PhD thesis was devoted to the synthesis and characterization of a new chromo-fluorogenic chemosensors based in an imidazole derivative for selective detection of GSH in aqueous environment using a "displacement assay" approach. Among all cations tested, only Cu(II) was able to form a reddish-brown and weakly-emissive complex with the probe in water (pH 7.4)-acetonitrile 1:1 (V/V) solutions. Due to the high affinity of Cu(II) toward thiol moieties, the probe-Cu(II) complex was able to detect GSH detection in mixed aqueous solutions, while negligible changes were observed in the presence of other biothiols (Cys and Hcy). Upon addition of GSH to water (pH 7.4)-acetonitrile 1:1 (V/V) solutions of the probe-Cu(II) complex a marked bleaching of the colour and the appearance of an intense emission band was observed. The optical changes where ascribed to a GSH-induced demetallation of the Cu(II) complex which regenerated the free probe. Through complexation studies, the limit of detection was determined to be 2.0 μM.

On the fourth chapter, an imidazole-based probe containing two thiophene rings was synthesized and used as a selective chemosensor for chromo-fluorogenic detection of Cu(II) in competitive mixed aqueous solutions. Upon addition of Cu(II) to solutions of the probe (water-acetonitrile 90:10 v/v) a color change from colorless to deep blue was observed. Besides, Cu(II) was able to form a non-emissive complex with the imidazole probe. Moreover, the imidazole probe was used to detect Cu(II) in living cells by confocal microscopy.

The fifth chapter focused on the design, synthesis and characterization of three new chemosensors (containing *N*,*N*-diphenylanilino electron donor moiety and heterocyclic aldehydes) used for the chromo-fluorogenic detection of Cu(II). Of all the cations tested, only Cu(II) induced the appearance of strong absorption bands in the NIR zone together with remarkable colour changes for the three probes in acetonitrile. Besides, Cu(II) cation induced marked emission quenching for the three probes.

Finally, throughout the sixth chapter the synthesis and chromo-fluorogenic behaviour toward metal cations and biothiols of two more imidazole-based probes was studied. Acetonitrile solutions of both probes were characterized by the presence of a charge-transfer absorption band in the 320-350 range. From all cations tested only Cu(II) induced the growth of new redshifted bands in the 450-570 nm interval. Moreover, the colour of the solutions changed from colourless to deep blue and deep yellow for the ttwo probes developed. Besides, the emission bands of both receptors were quenched in the presence of Cu(II) cation. These spectral changes were ascribed to a preferential coordination of Cu(II) cation with the electron acceptor imidazole heterocycle in the probes. Only one of the probes changed its UV-visible and emission spectra in the presence of Cu(II) in water-acetonitrile mixtures. On the other hand, the weakly emissive probe-Cu(II) complex was used to detect biothiols (GSH, Cys and Hcy) in water-acetonitrile 1:1 v/v solution. In the presence of biothiols, the visible bands of the complex

disappeared and the emission intensity of the free probe was fully restored. These changes were ascribed to a demetallation process.

Gracias al Generalitat Valenciana por concederme una beca SANTIAGO GRISOLÍA.